

TABLE OF CONTENTS

	Page
INTRODUCTION	1
CHAPTER 1 PROPOSED DESIGN PROCESS FOR HIGH-PRESSURE GAS TURBINE HOUSING AND SHROUD SEGMENTS	5
CHAPTER 2 LITERATURE REVIEW: STATIC STRUCTURES DESIGN AND DATA ANALYSIS TECHNIQUES.....	11
2.1 Turbine Housing and Shroud Segment Geometry and Physic Mechanism.....	11
2.1.1 Principal HPT Components	11
2.1.2 Tip Clearance.....	12
2.1.3 Shroud Segment Cooling.....	13
2.2 Static Structures Design.....	15
2.2.1 Shape Parameterization.....	16
2.2.2 Introduction to Shape Optimization.....	17
2.3 Methodology of a Correlation Study	18
2.3.1 Introduction to Design of Experiments.....	19
2.3.2 Introduction to Regression Analysis.....	21
2.3.3 Model Selection in Linear Regression.....	25
2.3.4 Confidence Interval and Hypothesis Testing.....	27
CHAPTER 3 PARAMETERIZATION OF HIGH-PRESSURE TURBINE HOUSING AND SHROUD SEGMENTS	33
3.1 Current Turbine Housing and Shroud Segment Models.....	33
3.2 New Design Process Requirements	35
3.3 Parametric Models Limitations.....	38
3.4 Parametric Approaches	39
3.4.1 Skeleton Approach.....	40
3.4.2 Modular Approach.....	41
3.4.3 Fixed Modular Approach.....	42
3.5 New Turbine Housing and Shroud Segment Model.....	43
3.5.1 Turbine Housing and Shroud Segment Parameters	43
3.5.2 Turbine Housing and Shroud Segment Configurations	44
3.6 Static Structure User Interface.....	45
3.7 Evaluation of the New Design Process.....	47
3.8 Conclusion	50
CHAPTER 4 CORRELATION STUDY OF THE GEOMETRIC PARAMETERS	51
4.1 Context and Objective of the Correlation Study.....	51
4.2 Methodology in the Correlation Study	52
4.3 Risk Assessment	54

4.4	Relations of the Geometric Parameters.....	55
4.4.1	Standardized Dimensions.....	56
4.4.2	Geometric Correlations.....	59
4.4.3	Conclusion of the Geometric Correlations.....	68
4.5	Multiple Linear Regression of the Geometric Parameters.....	69
4.6	Geometry Accuracy.....	71
4.7	Conclusion.....	73
CHAPTER 5 CORRELATION STUDY ON SHROUD SEGMENT COOLING FLOW.....		75
5.1	Context of the Correlation Study.....	75
5.1.1	Current Design Process for Cooling Flow Predictions.....	75
5.1.2	Objectives of the Correlation Study.....	77
5.2	Creation of a Simplified Prediction Model.....	78
5.2.1	Methodology.....	79
5.2.2	Correlations with Cooling Flow.....	81
5.2.3	Selection of a Simplified Prediction Model.....	83
5.3	Accuracy of the Simplified Prediction Model.....	85
5.3.1	Prediction Interval of the Simplified Prediction Model.....	85
5.3.2	Comparison with the current design process.....	89
5.3.3	Conclusions on the Accuracy.....	93
5.4	Simplified Shroud Segment Selection Process.....	93
5.5	Conclusion.....	96
CONCLUSION AND RECOMMENDATION.....		97
APPENDIX I CORRELATIONS IN RISK ASSESSMENT.....		99
APPENDIX II VALIDITY ASSESSMENT IN COOLING FLOW CORRELATIONS AND REGRESSION EQUATIONS.....		101
LIST OF REFERENCES.....		103

LIST OF TABLES

		Page
Table 2.1:	Design of Experiment Example	20
Table 2.2:	Best Subset Summary Example	26
Table 2.3:	Hypothesis Testing Decision Table	28
Table 3.1:	Design Process Comparison	49
Table 4.1:	Trade-Off in Risk Assessment	54
Table 4.2:	Correlations with Static Structures Thermal Displacement.....	55
Table 4.3:	Standardized Dimensions Validation.....	58
Table 4.4:	Hook Correlations and Error Comparison	61
Table 4.5:	Small Sample Correlation Results	68
Table 4.6:	Correlation Table; n=19.....	69
Table 4.7:	Regression Models for H1	70
Table 4.8:	Accuracy of the Parameterized Turbine Housings and Shroud Segments.....	73
Table 5.1:	Shroud Segment Selection Process.....	77
Table 5.2:	Correlations with Cooling Flow.....	81
Table 5.3:	Correlation of $T_{hot}-T_{cold}$; n=8	83
Table 5.4:	Prediction Models with the Best Subset and $\alpha=5\%$; n=8	84
Table 5.5:	Prediction Models with the Best Subset and $\alpha=10\%$; n=8	84
Table 5.6:	Prediction Models with Hot Gas and Cooling Air Temperatures; n=8	85
Table 5.7:	Accuracy of the Predictions	88
Table 5.8:	Accuracy of Current and Simplified Predictions	92
Table 5.9:	Engine Parameters Comparison in Shroud Segment Selection	95

LIST OF FIGURES

	Page
Figure 0.1: Propulsion System Integration and Optimization Architecture	2
Figure 1.1: New Design Process for High-Pressure Turbine Housing and Shroud Segments	6
Figure 2.1 : Simplified View of a Turbine Stage Cross Section	12
Figure 2.2: Types of Cooling on a Shroud Segment, adapted from (Proctor et al., 1992)	14
Figure 2.3: Relation Between a Parametric Model and Shape Optimization.....	17
Figure 2.4: Interaction Plots	21
Figure 2.5: Fitted Value Y in Function of an Observed Value X.....	23
Figure 2.6: Fitted Line Plot for the Linear Model	31
Figure 3.1: Current Design Process for Tip Clearance Calculation	34
Figure 3.2: Simplified Turbine Housing and Shroud Segment	34
Figure 3.3: Cross Section Overlay.....	35
Figure 3.4: New Design Process for Tip Clearance Calculation.....	36
Figure 3.5: High-Pressure Turbine Components.....	37
Figure 3.6: Boundary Conditions Comparison.....	38
Figure 3.7: Skeleton Approach.....	40
Figure 3.8: Modular Approach	41
Figure 3.9: Fixed Modular Approach.....	42
Figure 3.10: Turbine Housing and Shroud Segment Parameterization.....	44
Figure 3.11: Baseline Configurations.....	45
Figure 3.12: Static Structure User Interface	47

Figure 4.1:	Correlation Study Objective	51
Figure 4.2:	Methodology for the Correlation Study of the Geometric Parameters	53
Figure 4.3:	Risk Assessment Parameters for Tip Clearance	55
Figure 4.4:	Standardized Dimensions.....	56
Figure 4.5:	Sample Observation for the Standardized Dimensions	57
Figure 4.6:	Hook Correlations Parameters	60
Figure 4.7:	Housing Leg Width Regression Model; n=13 & $R^2=13.1\%$	62
Figure 4.8:	Segment Feet Height Regression Model; n=18 & $R^2=62.7\%$	63
Figure 4.9:	Outlier Geometry – W3 & H8	64
Figure 4.10:	Housing Feet Height Regression Model; n=19 & $R^2=57.5\%$	65
Figure 4.11:	Outlier Geometry - H7	66
Figure 4.12:	Small Sample Correlated and Non-Correlated Parameters.....	67
Figure 4.13:	Multiple Correlation Parameters.....	70
Figure 4.14:	Accuracy of New Baseline Model 7	72
Figure 5.1:	Current Design Process for Cooling Flow Predictions	76
Figure 5.2 :	Assumption for the Cooling Correlations	78
Figure 5.3:	Methodology of the Correlation Study on Cooling Flow	80
Figure 5.4:	Parameters Correlated with Cooling Flow.....	82
Figure 5.5:	Simplified Prediction Model C2	86
Figure 5.6:	Overprediction for Reference Shroud Segment 7.....	87
Figure 5.7:	2D Representation of the Simplified Prediction Model.....	90
Figure 5.8:	Accuracy Comparison for Reference Shroud Segment 8	91
Figure 5.9:	Shroud Segment Selection with the Simplified Prediction Model	94

LIST OF ABBREVIATIONS

ACC	Active Clearance Control
CAD	Computer Aided Design
CI	Confidence Interval
CFPT	Cooling Flow Prediction Tool
CA	Cooling Arrangement
DOE	Design of Experiments
FEA	Finite Element Analysis
FEM	Finite Element Model
HTC's	Heat Transfer Coefficients
HPT	High-Pressure Turbine
LE	Leading Edge
MDO	Multi-Disciplinary Optimization
MLR	Multiple Linear Regression
NSERC/P&WC	Natural Sciences and Engineering Research Council of Canada/Pratt & Whitney Canada
OTDF	Overall Temperature Distribution Factor
PCC	Passive Clearance Control
PI	Prediction Interval
PSIO	Propulsion System Integration and Optimization
PMDO	Preliminary MDO
SLR	Simple Linear Regression
SS	Shroud Segment

SSM	Static Structure Module
SFC	Specific Fuel Consumption
TH	Turbine Housing
TCC	Tip Clearance Calculator
TE	Trailing Edge
TSO	Turbine System Optimizer

LIST OF SYMBOLS AND UNITS OF MEASUREMENTS

R_a^2	Adjusted coefficient of determination
r	Coefficient of correlation of the sample or Pearson's linear correlation
ρ	Coefficient of correlation of the population
R^2	Coefficient of determination
T_{cold}	Cooling air temperature in the turbine stage
ϵ	Cooling effectiveness
η	Cooling efficiency
T_{hot}	Hot gas temperature in the turbine stage
α	Level of significance
C_p	Mallow's C_p
R	Rankine
B_i	Regression coefficient
n	Sample size
VIF	Variance inflation factor

INTRODUCTION

Context

The gas turbine industry has evolved over the past decades. The increase in computer performance allowed the arrival of computerized analytical tools. These tools reduced drastically the time required to design a gas turbine. Therefore, in the search for an optimal solution for better engine performances, the number of design iterations increased with an acceptable overall design time.

In the search of an optimal design process, the complex task of gas turbine design was divided into multiple subtasks. Then each discipline was responsible for optimizing a sub-system of the engine. This methodology can be referred as Multi-Disciplinary Optimization (MDO). Gas turbine design is also divided in two phases named the preliminary and the detail design phase. At the detail design phase, efficient interactions between each discipline tools are crucial and it is extremely challenging to make significant changes to the design at this stage. To overcome this difficulty, the use of MDO at the preliminary design phase (Preliminary MDO or PMDO) allows making more design iterations where there is more freedom to make modifications. Brophy et al. (2009) and Panchenko et al. (2002) explain into more details the benefits of PMDO. To implement PMDO, the NSERC/P&WC chair aims to create a set of preliminary design tools. All the tools will be integrated into the Propulsion System Integration and Optimization (PSIO) that should be capable of finding a balanced design.

Two key characteristics in a balanced design are the calculation of the tip clearance and the shroud segment cooling flow in high-pressure turbines (HPT). To improve the engine overall efficiency, turbine tip clearance and shroud segment cooling flow must be minimized. The tip clearance has to be as small as possible but also large enough to avoid rubs between rotating and static components. In addition, the shroud segment cooling flow must be minimized but sufficient to maintain the temperature below the material limit. In order to

make accurate tip clearance and cooling flow predictions at the preliminary design phase, the turbine housing and shroud segment geometry are required. The PSIO architecture presented in Figure 0.1 highlight the modules necessary for the creation of a new design process for turbine housing and shroud segments. A data structure (1) is necessary for the integration of the static structures shape definition module (2) with the static structures analyses and optimization modules (3). In order to create the new design process, this research aims to create parametric models, new geometry correlations and new cooling flow correlations for the static structures design and cooling modules. The parametric models will be compatible with the analysis modules to automate tip clearance analysis. The new geometry and cooling correlations will minimize the number of parameters used in the design to reduce the turn-around time of the new design process.

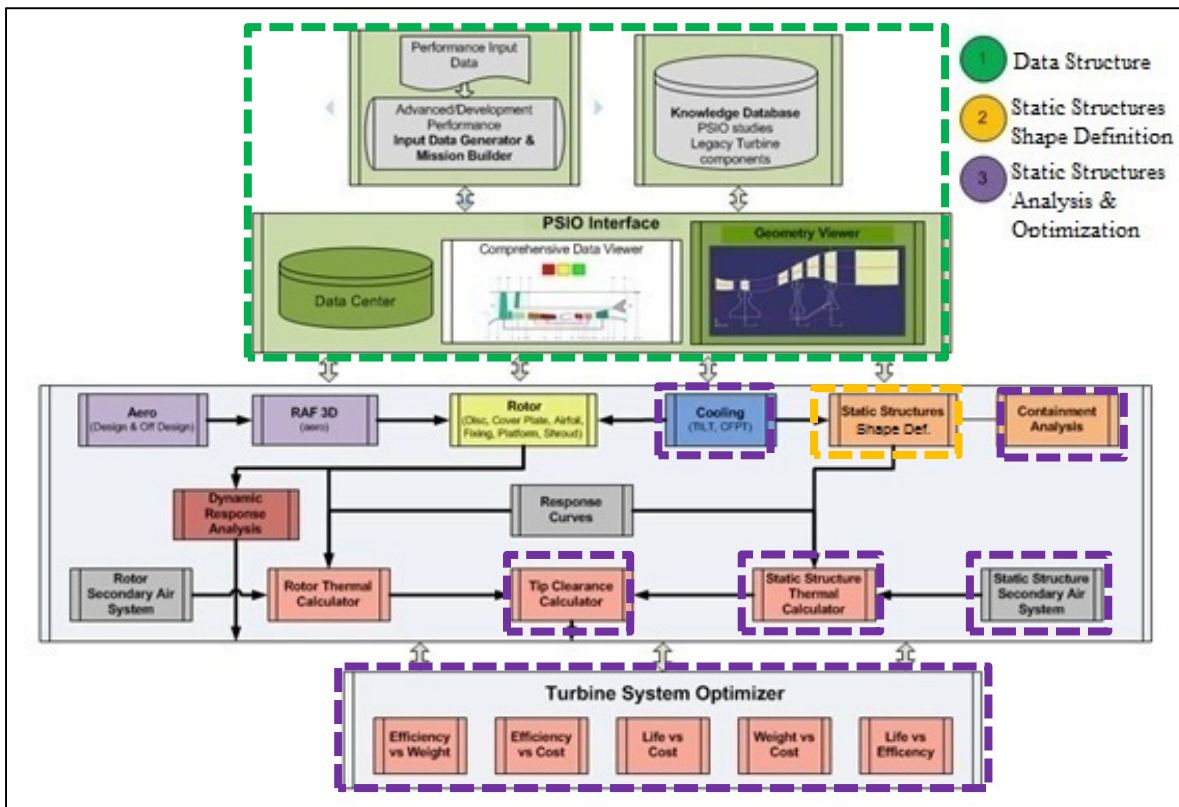


Figure 0.1: Propulsion System Integration and Optimization Architecture

Thesis Outline

The first chapter presents the new design process for turbine housing (TH) and shroud segment (SS), what the different modules of the design process consist of and how they interact with one another. The objectives of this research are also explained into more details. Finally, the contribution of this research to the new design process is estimated and the missing modules are mentioned.

The second chapter is a literature review on turbine housing and shroud segment geometry and physic mechanism that play a role in durability and engine efficiency. Then, a review of parameterization and optimization techniques is done to explain the benefit of a correlation study. Finally, a methodology to study geometry and cooling flow correlations is described.

The third chapter presents TH and SS parameterization and the creation of the baseline configurations. The different levels of flexibility that were studied to create the baseline configurations are presented. It is also explained why the flexibility was limited. Then, the new parametric models and the user interface created to modify them are presented. Finally, the benefits of the new parametric models are explained.

In the fourth chapter, the correlation study of the geometric parameters will be presented. It will be explained how care was taken not to oversimplify the parametric formulation. Then, the relations among the geometric parameters that were used to simplify the parametric formulation will be presented. Finally, the third section will present the additional studies that were conducted for the validation of the parametric models

The fifth and last chapter, before the conclusion and recommendation, presents a correlation study on shroud segments cooling flow. The current design process will be presented to explain the difficulty in choosing a reference shroud segment. Then, it will be explained how a simplified prediction model was created. The accuracy of this model will be compared with the current design process. Finally, an alternative SS selection process will be presented.

CHAPTER 1

PROPOSED DESIGN PROCESS FOR HIGH-PRESSURE GAS TURBINE HOUSING AND SHROUD SEGMENTS

It was explained in the introduction that the objective of this research is to create parametric models and new correlations for turbine housing (TH) and shroud segments (SS). In this section, the new design process for TH and SS will be presented. First, it will be explained in what consist the different modules of the new design process and how they interact with one another. Second, the objectives of this research will be explained into details. Then, it will be explained in which proportions the parametric models and the correlations contribute to the creation of the new design process. Finally, the recommendations to complete the design process will be presented

The proposed design process for high-pressure gas turbine housings and shroud segments is presented in Figure 1.1. TH and SS are also referred as the turbine static structures. In order to develop the new design process, a centralized data structure is necessary for the integration of the shape definition, analysis and optimization modules. At each step of the design, the data is stored in the data structure and the engine parameters are modified through the design. The shape definition module consists in a CAD system and a user interface. The CAD system is a vault for the parametric models which is the heart of the design process. In other words, the design process cannot be automated without the parametric models. On the other hand, the user interface is used to modify the parametric models before the initial geometry is analyzed. The design process also requires several analysis modules and an optimization module. Regarding the analysis modules, the design process requires a tip clearance, a cooling flow, and a containment module since it was developed for the purpose of PMDO. In addition, the tip clearance module requires an air system and a thermal module. Finally, the new design process requires an optimization module because a trade-off between optimal tip clearance, cooling flow and containment has to be made to obtain a balanced design. Next, the objectives will explain why parametric models and new correlations were created.

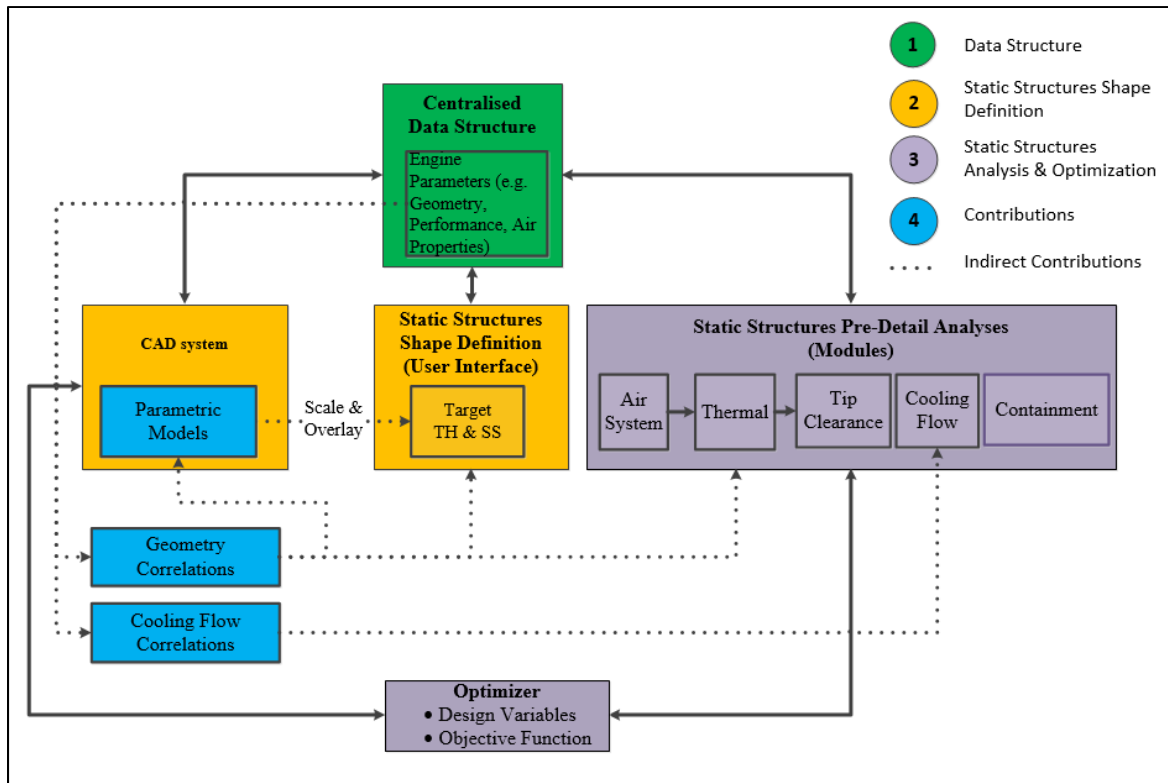


Figure 1.1: New Design Process for High-Pressure Turbine Housing and Shroud Segments

Objectives

The current tip clearance calculator (TCC) tool in use today allows the calculation of thermal displacements and tip clearance by generating a 2D mesh of rotor, turbine housing (TH) and shroud segment (SS) geometry. The tip clearance is the result of rotor, TH and SS radial displacements. The geometry in this tool is not parameterized and a limited number of engine configurations can be analyzed. In addition, the user has to manually collect and enter the dimensions of legacy engines to generate the geometry. Finally, the geometry is not integrated with the analysis and optimization modules.

In addition, a Cooling Flow Prediction Tool (CFPT) also currently in use predicts the amount of cooling flow of new SS designs using a reference SS. The selection of the appropriate reference SS and the cooling flow predictions require the comparison of many engine parameters. As a result, a choice has to be made as to which parameters are more important

for SS cooling flow predictions. In order to overcome the limitations of the tip clearance calculator and the cooling flow prediction tool, three objectives that will be developed in chapters 3 to 5 were identified in this research.

1. The first objective, addressed in chapter 3, is to create baseline configurations to mimic legacy TH and SS geometry. Thus, a repository of Computer Aided Design (CAD) geometry parametric models will be created using the baseline configurations. A user interface will be developed to allow modifications of the parametric models. In addition, the parametric models will be compatible with other modules of PSIO to automate tip clearance optimization studies. With the parametric models and the user interface, the new design process should have:

- An increased flexibility that will be estimated using the number of engine models that can be analyzed with the new TH and SS parametric models that will include new components.
- A reduced design time that will be calculated with the time it takes to perform shape definition in the new and the current design process.
- An acceptable tip clearance, cooling flow and containment accuracy that should be calculated when the new design system is completed. In the new design process, the accuracy of the tip clearance, cooling flow and containment pre-detail calculations will be reduced compared to the predictions made at detail design phase. The accuracy of the pre-detail calculations will be acceptable if it results in time saved at the detail design phase.
- An increased geometry accuracy that will be estimated with an increase in flexibility. Since the flexibility can be estimated with the number of engine models that can be analyzed, an increase in geometry accuracy should improve tip clearance, cooling flow and containment accuracy compared to the non-parameterized TH and SS models. The geometry accuracy should be revisited as well when the new design system is completed.

2. The second objective, addressed in chapter 4, is to create relations among TH and SS dimensions so as to minimize the number of geometry parameters that can be used for the modification of TH and SS geometry. In the parametric models, the parameters are dimensions that are either dependent or independent. The independent dimensions are used to modify the geometry and the dependent dimensions have a relation with the independent dimensions. The new relations should not affect the accuracy of tip clearance, cooling flow and containment predictions. This will be estimated with:
 - Correlations between thermal displacement for tip clearance and the geometry parameters to verify which parameter can be used to create new relations.
 - Geometry accuracy where the shape of detailed and pre-detailed geometry will be compared. Geometry accuracy in chapter 4 will not be sufficient to validate that the accuracy of tip clearance, cooling flow and containment calculations is acceptable. Only when the new design system is completed will an acceptable accuracy of the tip clearance, cooling flow and containment predictions be confirmed.
3. The third objective, addressed in chapter 5, is to minimize the number of engine parameters used to predict SS cooling flow and to create a simplified SS selection process. With a correlation study, the relations between the engine parameters and shroud segment cooling flow will be studied. Then highly correlated parameters will be used to create a simplified prediction model and a simplified SS selection process. Finally, the accuracy of the cooling flow predictions of the simplified prediction model and the current design process will be compared. The accuracy of the cooling flow predictions can be calculated with the difference between the cooling flow obtained from detail design analyses and the cooling flow predicted using the simplified prediction model or the current design process. The simplified prediction model and the current design process should have similar cooling flow accuracy.

In conclusion, the contributions of this research to the new design process are the parametric models, the new geometry and the cooling correlations. In order to obtain a new design

process, several modules in progress must be completed. In addition, other modules that were not started must be developed. More details on the contributions and the remaining work necessary to obtain a new design process will be presented in the conclusion and recommendations of the thesis. The next chapter is a literature review that sets the basis for the creation of the parametric models and the new correlations.

CHAPTER 2

LITERATURE REVIEW: STATIC STRUCTURES DESIGN AND DATA ANALYSIS TECHNIQUES

As explained in the introduction, the focus of the present work is the creation of a static structure module. In this chapter, the static structures components will be presented. A review of tip clearance control and static structures cooling techniques will be done to explain how they affect turbine efficiency and component durability. The second part of this chapter will explain the relation between shape parameterization and shape optimization. The third and last part of this chapter will explain how to conduct a correlation study in the context of TH and SS design.

2.1 Turbine Housing and Shroud Segment Geometry and Physic Mechanism

2.1.1 Principal HPT Components

The static structure components in this research are presented in Figure 2.1. They comprise the turbine housing (TH) and the shroud segment (SS) above the blade, which is a rotating structure component. The radial gap between the blade tip and the SS is named the tip clearance. In the evolution of static structures geometry, double wall static structures were widely adopted for tip clearance control (Hennecke, 1985). In that case, the inner wall is named the shroud segment (SS), facing the main gas path and the outer wall is named the housing. These two components are assembled with hooks. The housing and the shroud may be cooled using a different configuration. An example of a cooling configuration is presented in the section Shroud Segment cooling.

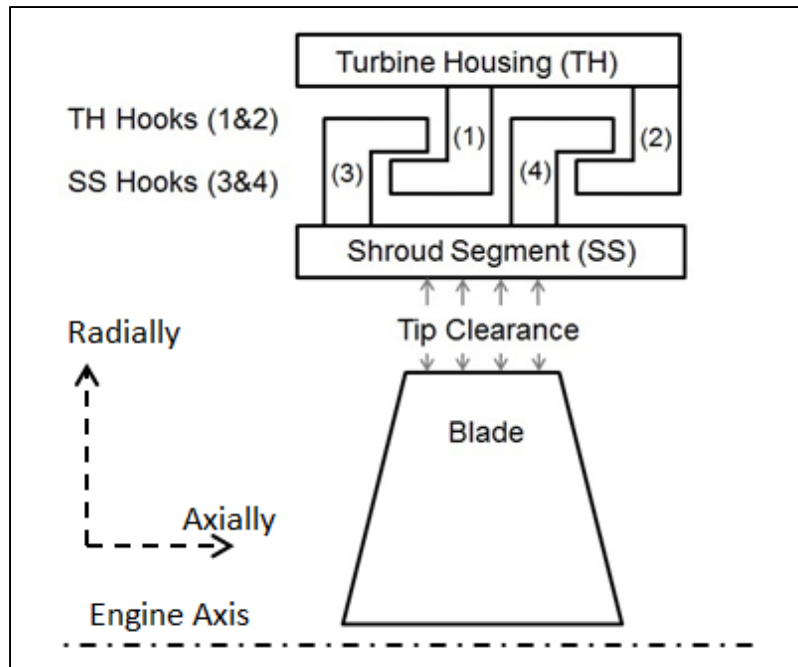


Figure 2.1: Simplified View of a Turbine Stage Cross Section

2.1.2 Tip Clearance

During a mission, an aircraft will undergo various cycles of temperature, pressure and altitude (Lattime et Steinetz, 2004). Therefore, the rotational speed and the turbine inlet temperature will increase and decrease with time. The rotating and static structures of a turbine will expand and contract due to centrifugal and thermal forces. Since the rotating and static structures have different masses and materials, their radial displacement varies at a different rate in response to the centrifugal and thermal forces. Consequently, the tip clearance can be large enough at certain times to reduce turbine overall efficiency. The build clearance is the tip clearance of a new engine before engine start (as built). The tip clearances can also greatly reduce during the mission at a condition commonly called the pinch point when the blade may rub on the shroud segment. As a result, the life of both rotating and static structures is reduced, as well as decreased engine performance

In essence, the tip clearance has to be balanced to achieve the desired turbine overall efficiency and both static and rotating structures durability. As a matter of fact, Hennecke

(1985) explains that at a tip clearance larger than 1% of blade height, for every 1% increase in tip clearance, engine overall efficiency will be reduced by 1%. Concerning the pinch point, Melcher et Kypuros (2003) explain that with blade and SS wear, material particles can partially block cooling channels, therefore, reducing cooling efficiency. For this reason, passive clearance control (PCC) and active clearance control (ACC) designs were developed and studied. Hennecke (1985) explains that PCC uses mass and material properties to achieve a faster thermal response of the rotating structures and a slower thermal response of the static structures. This author also explains that in ACC designs, a system that can be actively turned on and off controls tip clearance by heating and cooling the rotor or the casing.

First, an example of PCC that Hennecke (1985) gives is the use of a double wall casing where the outer wall supports the inner wall with hooks. The inner wall is circumferentially segmented and surrounds the rotor. The outer wall is protected by the inner wall and the radial movement of the casing is determined by the outer wall. Specific to the current research, the inner wall is a ring made of shroud segments and the outer wall is the housing. In another example, Hennecke (1985) explain that small amounts of air can be used to adjust the thermal response of the casing.

Second, for ACC designs to be viable in commercial or military gas-turbine engine, technical and economical requirements have to be met (Lattime et Steinetz, 2004). For this reason, passive clearance control designs using cooling air ducted from the compressor and a double wall casing seem to be more widely used than active clearance control designs. In any tip clearance control design, the static structures cooling efficiency will play a major role in its thermal response. The next section describes different types of cooling that are commonly used to cool gas turbine shroud segments.

2.1.3 Shroud Segment Cooling

Proctor et al. (1992) explain that, in the history of gas turbine, turbine inlet temperature has increased over material limits to achieve better engine performance. Therefore, the shroud segment comprised in hot sections has to be maintained below the material limit to allow the

engine to work properly and increase the service life. To address this problem, many designs were developed and studied using various cooling techniques to maintain components' temperature within the material limits. Such a design was developed by Proctor et al. They refer to impingement, convective and film cooling interactions in shroud segments. These three types of cooling have limitations when used separately in shroud cooling designs. Figure 2.2 shows the three cooling types on a simplified shroud.

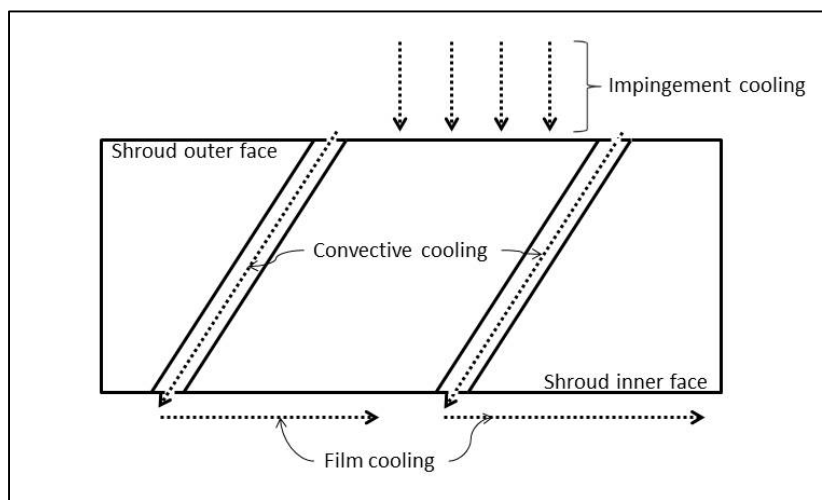


Figure 2.2: Types of Cooling on a Shroud Segment, adapted from (Proctor et al., 1992)

The first cooling type, film cooling, consists of a film of cooling air surrounding a surface to protect it from hot gas. In SS cooling, the film of cooling air is directed through the SS inner face. Since the inner face of SS is facing the main air stream, the cooling air is being constantly removed by hot gas leaking at the blade tip. Therefore, film cooling has a limited cooling efficiency.

The second cooling type, convective cooling, can be referred to a surface cooled by a moving fluid. Cooling air on the shroud outer face can be used to produce a film of cooling air on the shroud inner face. This way, the cooling air passing through SS is a convective cooling flow. However, a different configuration of cooling passages can result in a reduced cooling efficiency. There is no specific guideline in optimizing convective cooling for SS.

The third cooling type, impingement cooling, uses a liquid or a gaseous flow directed against a surface with a nozzle (Zuckerman et Lior, 2006). The nozzle has to be within a specific range from the cooled surface determined by nozzle height to nozzle diameter ratio (H/D). In other words, the cooling air passes through holes before it impacts a surface. In addition, the exit of the hole is named the nozzle. Authors agree that impingement cooling can require a large amount of air to be efficient. Since a common practice is to extract pressurized air from the compressor section for cooling purposes, impingement cooling can reduce significantly turbine overall efficiency. Therefore, a design that minimizes the amount of cooling air is required for impingement cooling to be a viable solution in the field of SS cooling.

Finally, other designs were developed to cool gas turbine shrouds trying to reach optimal cooling efficiency by minimizing the amount of cooling air ducted from compressor sections. In each design, the cooling efficiency depends on the cooling arrangement and the geometry. In other words, defining the cooling arrangement and the geometry are part of the tip clearance optimization process. The next section of this chapter will review the parameterization technique used in this research. Then an introduction to shape optimization will be made. Finally, a methodology of a correlation study will give insights on how to improve a parameterization.

2.2 Static Structures Design

In the context of PMDO, the final shape of the static structures results from the requirements of many disciplines. The requirements in preliminary optimization of the static structures are optimal tip clearance, cooling flow, and containment thickness. To meet those requirements, the shape of the static structures is modified several times. This is the field of shape optimization which can be manual or automated. Before shape optimization can be performed the shape has to be parameterized. This section will present the parameterization technique that was used and why it is suitable to this research. Then an introduction to shape optimization will be made. It will explain the relation between shape parameterization and shape optimization.

2.2.1 Shape Parameterization

There are many approaches suitable for shape parameterization in the context of PMDO. Samareh (1999) describes and compares several approaches with criteria that can be grouped in two categories: the geometry and the optimization. A criterion that was used for the geometry is the consistency in the parameterization between the disciplines. Static and rotating structure designs are two disciplines where the parametric models have to be consistent (i.e. same approach). On the other hand, a criterion for the optimization is CAD Connection. In other words, the choice affects the relation between the shape parameterization and shape optimization. Further to that, Ouellet (2013) explains that the choice of the parametric approach has a great impact on integration and optimization. Nevertheless, the approaches described by Samareh were not extensively studied in this research. Only the CAD-based approach was considered for the parameterization of the TH and SS.

The CAD approach was considered for two reasons. First, the previous work of Ouellet that focused on shape parameterization of HPT rotor components used the CAD parametric approach. For consistency between the disciplines, TH and SS parametric models were also created using the CAD approach. Second, tip clearance optimization requires both static and rotating structures parametric models. With consistency between the disciplines, it becomes easier to have a fully integrated tip clearance optimizer. However, the CAD approach has advantages and limitations that will guide the shape parameterization of TH and SS.

The CAD-based approach is known for its simplicity and efficiency to create parametric models because it uses various types of parameters (Length, Boolean, Real, etc.). Most CAD systems use sketches to create a 2D or 3D parameterized shape. As Hardee et al. (1999) explain, assigning a parameter to a dimension is more intuitive since sketches are used to create the model. Another advantage of the CAD approach is that the initial shape of the model is automatically modified once parameters are changed. On the other hand, the parametric model is limited by its complexity that can be estimated by the number of angles, radii and geometric constraints. As a result, the more complex the shape is, the more

parameter variation has to be conducted in a specific order to keep the integrity of the initial design.

2.2.2 Introduction to Shape Optimization

A review of the parameterization techniques that are suitable in the context of MDO was done. It was explained that the CAD approach was chosen for the parameterization of the static structures. In shape optimization, a parametric model is required. For this reason, there is a relation between shape parameterization and optimization. Bin, Nan et Huajun (2010) proposed a process flow of integrated optimization. A simplified process flow will be presented to explain the relation between a parametric model and shape optimization.

A process flow of shape parameterization and optimization is presented in Figure 2.3. A parametric model can have independent and dependent parameters as variables. The independent parameters can be used to modify the shape of the model and the dependent parameters are function of one or many independent parameters. Additional parameters are fixed with a constant value. In the context of this research, one of the objectives is to create an interface that allows the manual modification of a baseline parametric model. The baseline parametric model is modified with its independent parameters to create a shape that is similar to the baseline. The new shape is the geometry to be optimized.

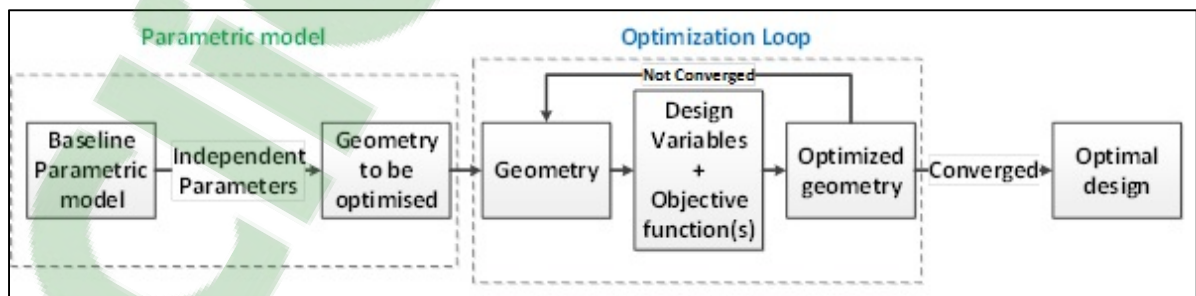


Figure 2.3: Relation Between a Parametric Model and Shape Optimization

In shape optimization, all the independent parameters of a parametric model can be considered as a design variable. One or many objective functions are defined. The design

variables are modified until the objective function reaches its maximum or minimum. When the objective function reaches a maximum or a minimum, the shape is considered to be optimized. The loop continues until the model converges. Then, in shape optimization, the more design variables there are, the longer it takes to reach the optimal shape. In addition, the independent parameters of a parametric model are not necessarily all used as design variables for shape optimization. A proportion of the independent parameters can be fixed. However, choosing a different set of parameters as design variables will result in a different optimal shape. Therefore, the design variables cannot be randomly chosen. Only the parameters that have no influence on the objective function can be neglected. A solution to determine whether or not a parameter has an influence on the objective function is to assess the strength of the relation. Consequently, the relations between the geometric parameters and the static structures objective functions (i.e. optimal tip clearance, cooling flow and containment thickness) have to be defined. In addition, if two or more geometric parameters affect simultaneously one or more objective function, it is possible that they are correlated with one another. The next section will give the guidelines to study the relations between the geometric parameters and the static structures objective functions.

2.3 Methodology of a Correlation Study

The geometry of the static structure is defined by various dimensions possibly dependent on one another. For example, it is possible to affect the thermal response of the static structures if TH and SS dimensions are modified. In other words, dimensions of TH and SS can affect simultaneously the thermal response of the static structures. In that situation, the dimensions are dependent to one another. As explained previously, TH and SS parametric models are defined with parameters corresponding to dimensions. This section will review how to study relations and create correlations among those dimensions. First, an introduction to design of experiments will be made. It will also be explained how it can be used to study the relation between geometric parameters. Second, multiple linear regression will be described into details. Measures of association will be defined, and an automated variable selection technique will be explained. Finally, it will be explained how hypothesis testing, confidence interval (CI) and prediction interval (PI) are used to assess the validity of the relation

between variables. It will be explained what is required in hypothesis testing and which tests are used in linear regression. Then it will be explained how confidence intervals are used for linear regression.

2.3.1 Introduction to Design of Experiments

In research, two common approaches to study the relations between variables are the true experiment and the ex-post-facto research. Hicks et Turner (1999) explain that true experiment is an experimental research procedure while the ex-post-facto research is not. A true experiment is a study in which independent variables are manipulated to observe their effect on one or more dependent variables. A true experiment can be conducted with a design of experiments. On the other hand, in the ex-post-facto research, the experimenter does not manipulate the independent variables. Instead, the researcher studies the relation between the variables based upon existing data. An application of the ex-post-facto research is multiple regression that will be covered in the next section.

In SAS Institute Inc. (2013) it is explained that designs of experiments are centered around factors, responses, a model and runs. Design of experiments, also named experimental design is divided into three major steps by Hicks et Turner (1999) which is the experiment, the design and the analysis. During the first step, the experimenter chooses the dependent variable named response, the independent variables named factors and the levels. The levels are the values that will take the factors during the experiment. There is always at least two levels which are the extreme values of the factors. The levels must be chosen such that the variation in the response is maximized. Then, in the design, the number of observations and the mathematical model must be defined. The number of observations is the number of runs or experiments. Each run has a different combination of levels for each factor. The mathematical model is an equation that will present the response variable as a function of all factors. Finally, in the analysis step, the data is collected and analyzed with appropriate statistical measures. Next, there are several types of DOE and not all of them are suitable to study the interactions between factors.

Experimental design can be divided into two categories of DOE, single factor experiments and factorial experiments. In a single factor experiment, the experimenter is interested in the effects that one factor has on the response. On the other hand, in a factorial experiment, the experimenter is interested in the effects that several factors have on the response. A factorial experiment can be conducted one factor at a time or in a factorial arrangement. With a factorial arrangement, it is possible to study the interaction between the factors because the levels of the factors are varied simultaneously. For the same reasons, a factorial arrangement requires less experimentation. In a DOE in a factorial arrangement, with three factors and two levels in each factor, there are 2^3 runs. Next, it will be explained how DOE relates to the geometric parameters, tip clearance, cooling flow and containment thickness.

As explained previously, TH and SS geometric parameters can have a simultaneous effect on tip clearance, cooling flow and containment thickness. Consequently, in a DOE where the interactions between the geometric parameters are studied, the responses are the tip clearance, the cooling flow and the containment thickness. The factors are the geometric parameters, and the levels are the values of those parameters. To study the effect that two geometric parameters have on tip clearance, the design of experiment has two levels and two factors, therefore, $2^2=4$ runs. Figure 2.4a and b presents the interaction plots of a hypothetical experiment. It presents the response for two possible outcomes of the four-run experiment in Table 2.1. Parallel lines indicate that there is no interaction between the factors. The more the lines depart from being parallel, the greater the interaction is.

Table 2.1: Design of Experiment Example

Run	Factors		Response	
	Geom. Param. 1	Geom. Param. 2	Tip Clearance (a)	Tip Clearance (b)
1	2	1.5	2	2
2	6	1.5	3	1
3	2	5	3.5	3.5
4	6	5	4.5	6

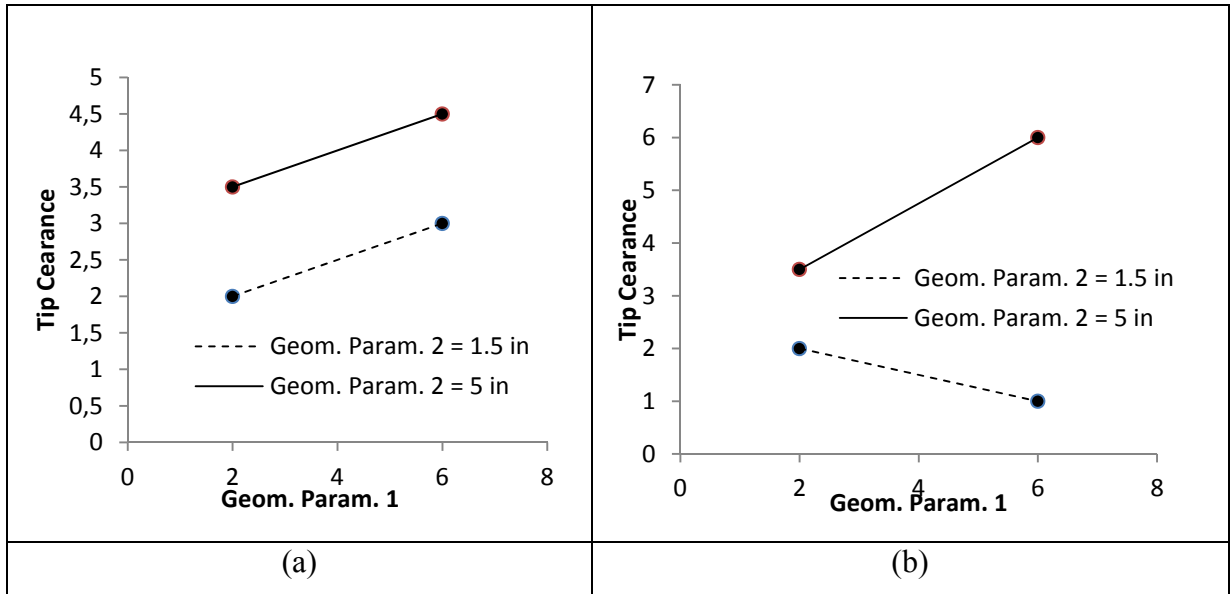


Figure 2.4: Interaction Plots

Finally, in an experiment, each run can represent a simulation using a Finite Element Model (FEM) or a test cell. Simulation using FEM or a test cell is time-consuming therefore impossible to conduct in the context of this research. In addition, simulations were already made with different TH and SS configurations resulting in different tip clearance, cooling flow and containment thickness. In other words, in this research, the factors are not manipulated. Consequently, this research cannot be conducted with a true experiment or DOE. Instead, it has to be conducted in ex-post facto mode with regression analysis which will be explained in the next section.

2.3.2 Introduction to Regression Analysis

Regression analysis can be used to study the relations between two or more geometric parameters and between the geometric parameters and tip clearance, cooling flow or containment thickness. Chatterjee et Simonoff (2013a) explain that regression analysis is used for modeling the relationship between an independent and a dependent variable. The dependent variable is usually identified with y and is named target variable or response. The independent variable is identified with x and is named predicting variable or predictor. A

regression model with only one predictor is a simple regression model. When there are at least two predictors, the model is a multiple regression model. Linear and non-linear regression models can be used to study the relationship between a response variable and one or more predictors. However, in Minitab documentation V15 it is explained that non-linear regression models are used when the ordinary least square (OLS) criterion fails to fit the data. Then, linear regression models must be studied first. The OLS criterion is used to study simple and multiple linear regression models. In this section, the simple and the multiple linear regression models will be presented. It will be explained what is the least square criterion. It will be explained:

1. What is the OLS criterion;
2. How to compute the strength of the relationship in a regression model;
3. How to select a model based on the number of predicting variables.

First, in a linear regression model, Chatterjee et Simonoff (2013b) explain that data consist of n set of observations $\{x_{1i}, x_{2i}, \dots, x_{pi}, y_i\}$ where n is the sample size, p is the number of predictors in the model and i represents the i^{th} observation. When there is one predictor, the model is represented by a line. When there are 2 predictors, the model is represented by a plane. For more than 2 predictors, there is no geometric representation for the model. Each observation satisfies a linear relationship with an error term ϵ_i also named the residual and unknown coefficients $\{\beta_0, \beta_1, \dots, \beta_p\}$. The residual is the difference between the observed and the fitted value. The fitted value is the estimated expected response for one observation of the predicting variables. The coefficients of the fitted response $\{\hat{\beta}_0, \hat{\beta}_1, \dots, \hat{\beta}_p\}$ are estimated as well. The best estimation is found with the OLS criterion where the sum of the squared residuals is minimized.

Linear relation for one observation

$$y_i = \beta_0 + \beta_1 x_{1i} + \dots + \beta_p x_{pi} + \epsilon_i \quad (2.1)$$

Linear relation for the fitted value

$$\hat{y}_i = \hat{\beta}_0 + \hat{\beta}_1 x_{1i} + \dots + \hat{\beta}_p x_{pi} \quad (2.2)$$

OLS

$$\sum_{i=1}^n [y_i - (\beta_0 + \beta_1 x_{1i} + \dots + \beta_p x_{pi})]^2 = \sum_{i=1}^n \epsilon_i^2 \quad (2.3)$$

For example, in the linear regression model with one predictor, in Figure 2.5, the residual is the vertical distance from the line to the observed value (x_i, y_i) . The fitted value is the value of y on the line for an observed value of x .

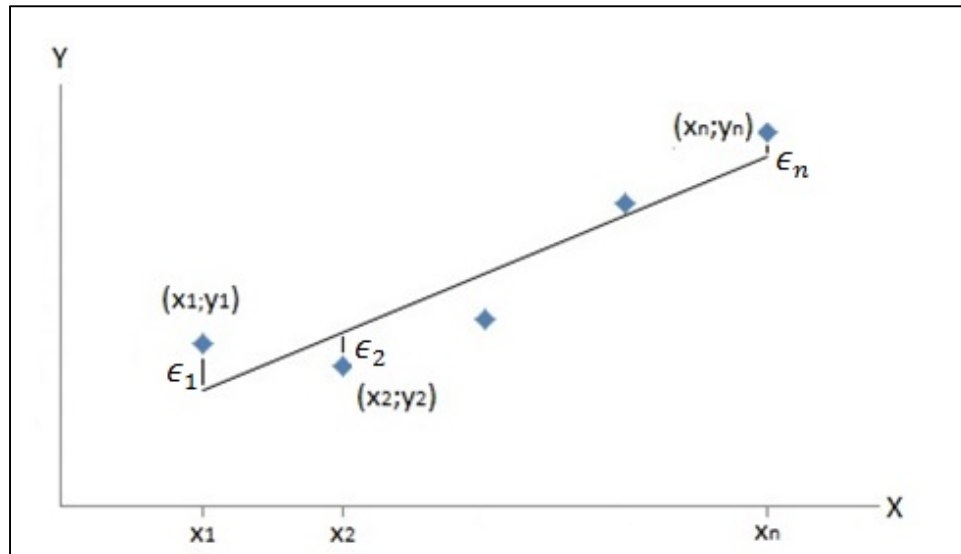


Figure 2.5: Fitted Value Y in Function of an Observed Value X

Assumptions of the ordinary least square:

1. The expected value of the errors is zero for all i ($E(\epsilon_i) = 0$);
2. The variance of the errors is constant for all i ($V(\epsilon_i) = \sigma^2$);
3. The errors are uncorrelated with each other;
4. The errors are normally distributed.

Further to that, the OLS does not guarantee the validity of the resulting model unless certain assumptions are met. As a matter of fact, when violating the first assumption, that is when the expected value of the errors is not zero for all i , estimating the regression coefficient β_0

can be difficult. In addition, it indicates that a predictor is possibly missing in the model. When the variance of the errors is not constant, confidence intervals and predictions intervals are poorly calibrated. Therefore, it is difficult to give reliable conclusions on the model. When the errors are correlated with each other, the strength of the regression can be misleading. Finally, when the errors are not normally distributed, hypothesis test, confidence interval and prediction interval can be misleading. Those assumptions can be verified with various plots, tests and diagnostic.

In addition, the OLS defines what the best estimation to fit observed data is. However, OLS does not measure the strength of the relationship. In regression analysis, the coefficient of determination R^2 and the adjusted coefficient of determination R_a^2 are used to measure the strength of the relation. Both coefficients can take any value between 0 and 1. When R^2 is close to 1, the model has a good predictive power. On the other hand, when R^2 is closer to 0, the model has a low predictive power. There is not a fixed R^2 value where a model should be rejected. Instead, it depends on the level of risk or the application for which the model is meant. In addition, R^2 can measure the strength of the relation for any number of predictors. In comparison, the coefficient of correlation r or Pearson's linear correlation, often confused with R^2 , measures the strength of the relation between two variables only. Nevertheless, the correlation coefficient is useful in hypothesis testing, especially when there is co-linearity among the predictors. Co-linearity and hypothesis testing will be explained later in this chapter. Finally, R_a^2 is especially useful in model selection because it takes into account the number of predictors p . Model selection will be explained into details next.

Measures of the strength in linear regression:

$$r = \frac{\sum_{i=1}^n (x_i - \bar{x})(y_i - \bar{y})}{\sqrt{\sum_{i=1}^n (x_i - \bar{x})^2} \sqrt{\sum_{i=1}^n (y_i - \bar{y})^2}}; \quad \bar{x} = \frac{1}{n} \sum_{i=1}^n x_i; \quad \bar{y} = \frac{1}{n} \sum_{i=1}^n y_i \quad (2.4)$$

$$R^2 = \frac{\sum_{i=1}^n (\hat{y}_i - \bar{y})^2}{\sum_{i=1}^n (y_i - \bar{y})^2} = r^2 \quad (2.5)$$

$$R_a^2 = R^2 - \frac{p}{n - p - 1} (1 - R^2) \quad (2.6)$$

2.3.3 Model Selection in Linear Regression

As explained previously, in regression analysis, certain assumptions should be validated so the OLS is justified. If the assumptions are not validated, additional models should be studied. However, studying only one model is not a good approach, whether the assumptions of the OLS are validated or not. In regression, there are the concepts of over-fitting and under-fitting. There is over-fitting when unnecessary predictors are in the model. There is under-fitting when important effects are missed by omitting predictors. Choosing between different models to avoid overfitting and underfitting is called model selection. Studying different models with various numbers of predictors can be time-consuming. Statistical software usually has an algorithm capable of producing a summary of all possible regression models. Such algorithms are often called best subset. Although using software automates model selection, it is recommended that the potential models are based on theoretical grounds before analyzing data. In addition, in model selection, an important concept is collinearity. That is when 2 or more predictors are highly correlated. In this section, the strategy to choose the best model within a best subset summary will be explained. Then, it will be explained why collinearity is an issue in model selection and how to address it.

First, in model selection, the statistical software produces a summary of models. The number of models for each number of predictors and the number of predictors must be defined. In Table 2.2, there are two models for each number of predictors and four predictors. The predictors suggested for each model are marked with an 'X'. The best model has to be studied with residual plots and hypothesis testing to confirm the validity of the model. To choose the best model within the best subset summary, several criteria are proposed. Usually, R^2 , R_a^2 and Mallows Cp are available to choose the best model. Then, R^2 and R_a^2 allow to avoid underfitting and Mallows Cp allows to avoid over-fitting. Since R^2 generally increases with additional predictors, the best subset summary will propose models with additional predictors until R^2 decreases.

Table 2.2: Best Subset Summary Example

Variable Qty.	R^2	R_a^2	Mallows C_p	Predictor 1	Predictor 2	Predictor 3	Predictor 4
1					X		
1							X
2					X	X	
2					X		X
3				X	X		X
3				X	X	X	
4				X	X	X	X

In addition, after generation of the best subset summary, choosing the best model can be simplified in three steps. Each model with the same number of predictors is compared, and the model with the highest R^2 is kept. Then, the remaining models are eliminated such that R_a^2 is maximized and C_p is minimized.

Model Selection Criteria:

1. Maximize R^2 for models with the same number of predictors;
2. Maximize R_a^2 for models with different number of predictors;
3. Minimize C_p where; $C_p \leq p + 1$.

Second, the model selection criteria do not address collinearity because the best subset algorithm does not take it into account. As explained earlier, there is collinearity when 2 or more predicting variables are highly correlated. The best model of the summary has to be studied with residual plots and hypothesis testing to confirm the validity of the model. At this step, statistical software proposes to calculate the variance inflation factor or VIF. It is calculated for each j predicting variable where R_j^2 is the coefficient of determination of the variable x_j with the other predicting variables in the model.

$$VIF_j = \frac{1}{1 - R_j^2} \quad (2.7)$$

Collinearity is not a problem when the following relation is satisfied where R_{model}^2 is the coefficient of determination for the regression of the response and the predictors.

$$VIF < \max\left(10, \frac{1}{1 - R_{model}^2}\right) \quad (2.8)$$

In presence of collinearity, the regression model should be simplified with a smaller number of predictors. For example, if there are 2 highly correlated variables in a three predictor regression model, 1 of the two correlated variables is removed, and the new model is studied. However, this guideline does not guarantee underfitting and important effects might be missed by removing correlated variables. Then, for the same regression model with three predictors, two models should be studied. Each model has one of the two correlated variables. In addition, in model selection, the VIF addresses collinearity only once the best subset has been used. An alternative would be to compute r or R^2 between all the possible combinations of 2 predictors. In other words, collinearity can be addressed before and after the best subset summary is produced. Finally, once the assumptions of the OLS are validated, another important step in validating a regression model is the interpretation of the regression coefficients β_0 and β_1 . Hypothesis testing is used to interpret the regression coefficients and the correlation coefficient. In the next section, an introduction to hypothesis testing will be made. It will also be explained how hypothesis testing can be used to interpret the regression coefficients and the correlation coefficient.

2.3.4 Confidence Interval and Hypothesis Testing

First, Taeger et Kuhnt (2014) explain that hypothesis testing can be used to decide whether or not the statistic (e.g. correlation coefficient, regression coefficient) of a sample is valid for the population. Hypothesis testing is composed of: a null hypothesis H_0 , an alternative

hypothesis H_1 , the level of significance α , and a decision to reject or not the null hypothesis. The null hypothesis can be true or false. This is why there are four different cases with specific probability in hypothesis testing. The level of significance is the probability that the null hypothesis is rejected when it is true and is referred as the type I error. On the other hand, when the null hypothesis is false but failed to be rejected, it is referred as a type II error with a probability of β which should not be confused with the regression coefficient β_i . Generally, β cannot be computed therefore the probability for type II error is unknown. Furthermore, common levels of significance are 5%, 1% or 0.1% but α can take any other value. «The choice of α depends on the nature of the problem. (Kreyszig, 2010)» Table 2.3 is an example for a test on the population correlation coefficient ρ . The level of significance for the correlation coefficient is the probability to conclude there is a correlation between two variables when the correlation does not exist.

Table 2.3: Hypothesis Testing Decision Table

	Test decision for the correlation coefficient	
	Do not reject H_0	Reject H_0
H_0 true $\rho=0$	Correct decision $\rho=0$ Probability : $1-\alpha$	Type I error $\rho\neq 0$ Probability α
H_0 false $\rho\neq 0$	Type II error Probability: β	Correct decision $\rho\neq 0$ Probability $1-\beta$

Second, in the context of this research, the correlation coefficient and the regression coefficients are tested. The null hypothesis, the alternative hypothesis and the level of significance for these tests are:

Correlation Coefficient

$$H_0: \rho=0 ; H_1: \rho\neq 0$$

α : Probability to conclude $\rho\neq 0$ when $\rho=0$

Regression Coefficient

$$H_0: \beta_i=0 ; H_1: \beta_i\neq 0$$

α : Probability to conclude $\beta_i\neq 0$ when $\beta_i=0$

Further to that, tests on the correlation and the regression coefficients can tell whether or not there is a linear relationship between 2 variables. For example, in equation 2.9, the test of the correlation coefficient between Z and X and the test of the regression coefficients for the linear relation where Z is function of X are referred to as $\rho(Z, X) \neq 0$ and $(\beta_1 \neq 0; \beta_2 \neq 0)$. We can conclude there is a linear relation between Z and X by computing only of the tests (i.e. correlation or regression).

Linear Relation between Z and X

$$Z = \beta_1 + \beta_2 * X; \quad (2.9)$$

$$\rho(Z, X) \neq 0 \text{ or } (\beta_1 \neq 0; \beta_2 \neq 0).$$

When a relation between more than 2 variables is studied, the test on the regression coefficient is necessary to assess the validity of more complex relations. For example, in equation 2.10, the linear relation between Z and Y can be verified with the test of the correlation or regression coefficients. However, finding that Z is correlated with X and Y, in equation 2.9 and 2.10, does not tell whether or not the linear relation in equation 2.11 is valid. Then, the test of the regression coefficients (β_5, β_6 and β_7) is used. Finally, the linear relation between Z, X and Y is valid because the three regression coefficients are different than 0. Next, it will be explained what confidence interval (CI) and prediction interval (PI) is and how they can be used to assess the accuracy of a valid regression model.

Linear Relation between Z and X

$$Z = \beta_3 + \beta_4 * Y; \quad (2.10)$$

$$\rho(Z, Y) \neq 0 \text{ or } (\beta_3 \neq 0; \beta_4 \neq 0).$$

Linear Relation between Z, X and Y

$$Z = \beta_5 + \beta_6 * X + \beta_7 * Y; \quad (2.11)$$

$$(\beta_5 \neq 0; \beta_6 \neq 0; \beta_7 \neq 0).$$

Third, Lesik (2009) and Chatterjee et Simonoff (2013b) explain that CI can be used to calculate a margin of error for the regression coefficients β_i . This means that the regression

line is the average expected response between upper and lower limits calculated with a margin of error. The margin of error is function of the confidence level. The standard confidence level is $1-\alpha=95\%$. With a confidence level of 95%, the regression line of samples of the same population would fall 95 times out of 100 between the upper and the lower limits. Further to that, PI can be used to predict the fitted value y_i with a specific value of the predicting variable x_i . The prediction interval also gives upper and lower limits calculated with the margin of error. As a result, the PI gives the accuracy of the fitted value y_i for a specific value X_i of the predicting variables. When $PI=95\%$, there are 95/100 of the new predicted valued that will fall between the PI limits.

Regression Equation

$$Y=\beta_1+\beta_2*X \quad (2.12)$$

Model Value

$$y_i=\beta_1+\beta_2*X= Y(X_i) \quad (2.13)$$

Confidence Interval for β_i

$$(\beta_i-\text{margin of error} \leq \beta_i \leq \beta_i+\text{margin of error}) \quad (2.14)$$

Prediction Interval of the Fitted Value

$$(y_i-\text{margin of error} \leq y_i \leq y_i+\text{margin of error}) \quad (2.15)$$

Figure 2.6, presents the regression equation with confidence and prediction intervals for the regression equation with one predictor X . The regression line is centered with CI and PI upper and lower limits. The CI gives the limits where the regression line will lie 95 times out of 100 when the confidence level is 95%. For example, a random regression line was drawn to show that it can lie anywhere between the CI limits. In addition, the PI is always wider than the CI because there is more uncertainty predicting a single response than the mean response or fitted line. Finally, the true value of Y for a given value of X will fall anywhere between PI upper and lower limits 95 times out of 100.

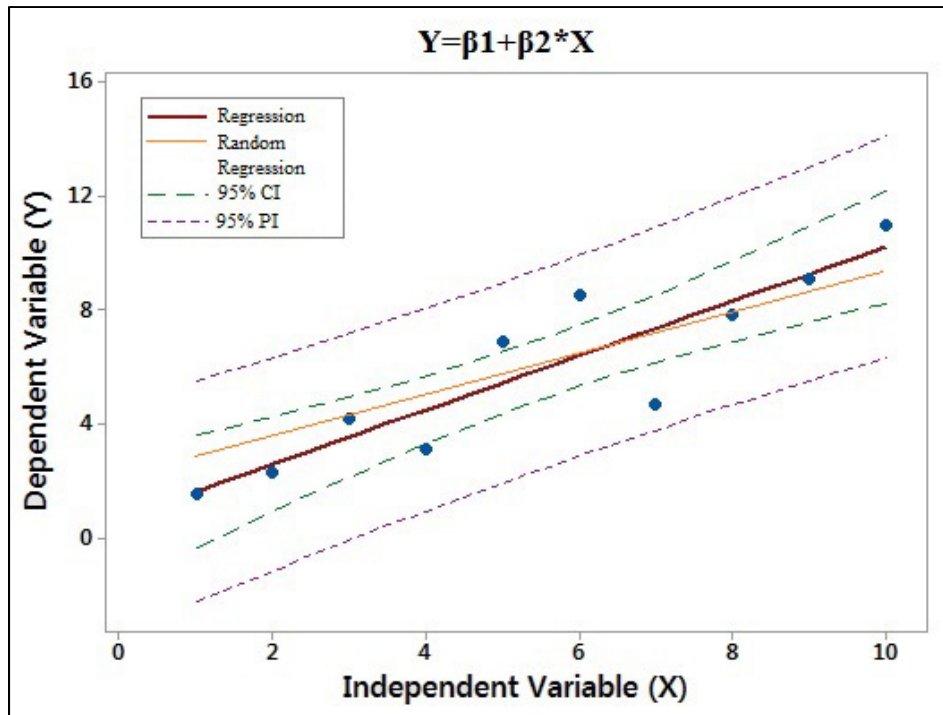


Figure 2.6: Fitted Line Plot for the Linear Model

In this section, it was explained that the test of the correlation coefficient and the regression coefficient are used to assess the validity of a linear relation. It was also explained that CI and PI can be used to assess the accuracy of the predicted response given a specific value of the predicting variable. The next chapter will explain how the parametric models were developed and how they interact with the static structures user interface. It will also be explained what are the benefits of the new design process regarding the parametric models, the user interface and the geometry correlations.

CHAPTER 3

PARAMETERIZATION OF HIGH-PRESSURE TURBINE HOUSING AND SHROUD SEGMENTS

This chapter will address the first objective which is the creation of the parametric models and a user interface. The current design process for tip clearance calculation will be presented to explain the context of the creation of the parametric models. The limitations and the new components required in the parametric models will be explained. Then, the levels of flexibility that were studied to create the parametric models will be described. In addition, it will be explained how the user interface works. Finally, the current and new design processes will be compared to estimate the benefits of the parametric models, the user interface and the geometry correlations. The geometry correlation will be developed in the next chapter.

3.1 Current Turbine Housing and Shroud Segment Models

As introduced in the previous chapter, the tip clearance is the radial gap between the shroud segment and the blade tip. The tip clearance varies through an engine mission because the thermal responses of the static and rotating structures are different. A key step in preliminary tip clearance predictions is to create 2D models that will be used for finite element analysis. This research focuses on the 2D turbine housing and shroud segment models. This is explained into more details with the current design process presented in Figure 3.1. It consists of a simplified geometry (i.e. rotating and static structures) that is drawn on a pre-detail design cross-section. The dimensions of the simplified geometry are measured and copied into a spreadsheet. Then, the spreadsheet has macros that convert the geometry to create a finite element model. The spreadsheet is also responsible to calculate heat transfer coefficients (HTC's). The geometry and HTC's are transferred to Finite Element Analysis (FEA) software where the transient thermal displacement of the static and rotating structures is computed. Finally, the tip clearance is calculated from thermal and centrifugal displacements. The Tip Clearance Calculator (TCC) comprises a spreadsheet and FEA. Further to that, TCC was developed to do quick transient analyses which would take months

with a 3D geometry. The simplified geometry was validated with test results, therefore, the differences between the simplified and the pre-detail geometry are considered acceptable. The simplified TH and SS geometry is presented in Figure 3.2. It will be explained next.

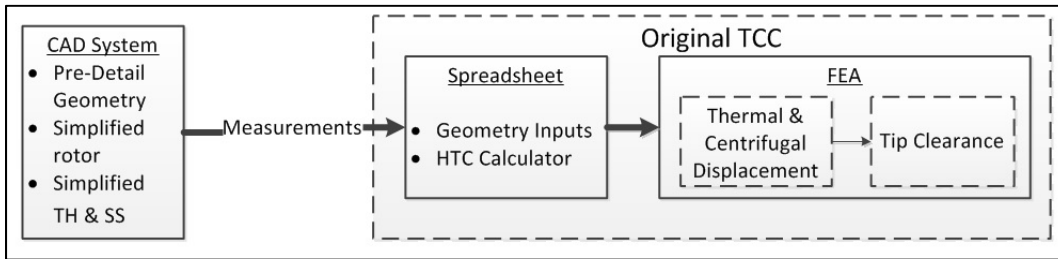


Figure 3.1: Current Design Process for Tip Clearance Calculation

The simplified geometry consists of the TH, the SS and an optional impingement baffle. All three components are made of rectangles. Details such as fillet and chamfers are not represented. Other details such as varying thicknesses are approximated with a constant thickness. Figure 3.2 depicts the rectangles that have to be drawn over a pre-detail geometry. Once the overlay is complete, the lines have to be measured to define the axial and radial locations of TH and SS in TCC. Four measures are presented as an example in Figure 3.2. The result of the overlay is presented in Figure 3.3.

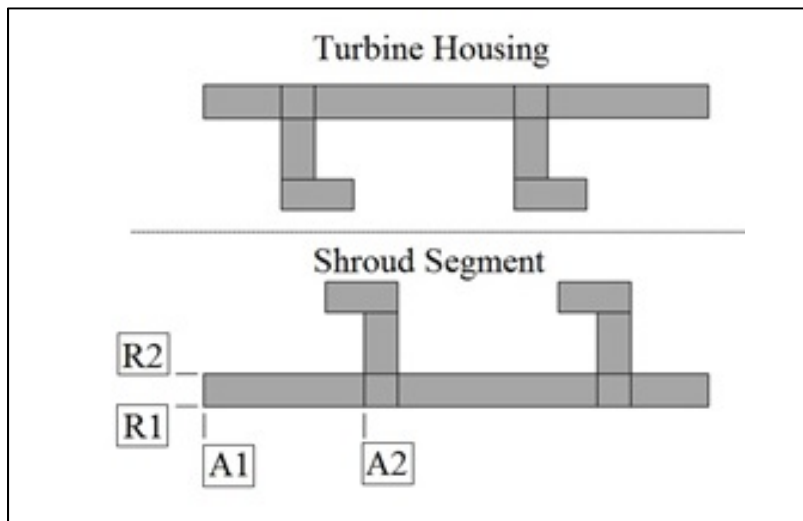


Figure 3.2: Simplified Turbine Housing and Shroud Segment

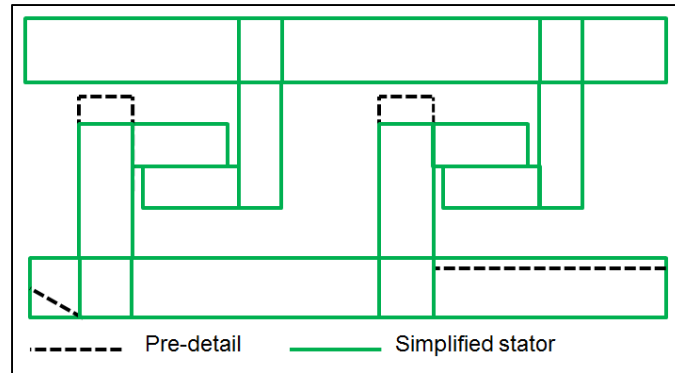


Figure 3.3: Cross Section Overlay

Further to that, there are limitations in the current design process that justify the creation of a new design process. First, the current design process is limited by the number of engine models that can be analyzed because the simplified geometry does not capture all the details of the different engine configurations. Second, the simplified geometry is not parameterized and a new geometry has to be created if a dimension changes after the FEA. For example, the FEM would not be updated if a dimension was changed in the spreadsheet. Third, the simplified geometry is not user-friendly. Figure 3.2 is only a guideline to draw lines over the detailed geometry. The simplified model is not displayed until FEA. Then, inconsistencies in the geometry due to manual manipulation of the data are visible only in the FEA software. In the next section, the requirements of the new design process will be described.

3.2 New Design Process Requirements

The new design process for tip clearance calculations is presented in Figure 3.4. The new design process comprises CAD parametric models, a user interface, a stator thermal calculator (STC), a rotor thermal calculator (RTC), a tip clearance calculator (TCC+) and an optimizer. However, it is not in the scope of this research to create STC, RTC, TCC+ and the optimizer. To overcome the difficulties of the current design process for tip clearance calculations, the new design process has 5 requirements.

1. An increased flexibility that will be estimated with the number of engine models that can be analyzed compared to the non-parameterized TH and SS models. With a repository of CAD parametric models that include new components, additional engine configurations can be analyzed.
2. A reduced design time that will be calculated in a test case where shape definition using the parametric models and the user interface is compared to shape definition in the current design process using the non-parameterized TH and SS.
3. An increased user friendliness that can be defined as the creation of a model viewer and the implementation of automated data transfer.
4. An increased geometry accuracy that will be estimated with the increased flexibility.
5. An increase in results consistency that can be defined as the differences in the same design made by two different people.

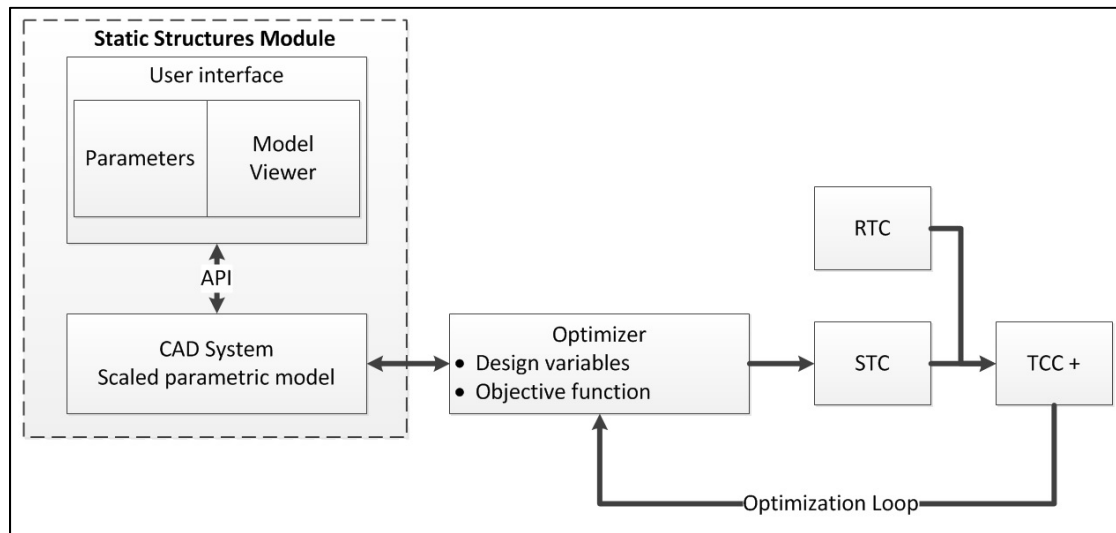


Figure 3.4: New Design Process for Tip Clearance Calculation

Next, the CAD parametric models in the new design process must include additional components not available in the simplified TH and SS models presented in Figure 3.2. Those components are the groove, the rails and a shroud segment impingement baffle. The groove should be movable at the leading edge, at the trailing edge or centered with the stacking line.

In addition, the hooks must be orientable to the right as well. In Figure 3.5, the hooks of the shroud segment are pointing to the left, towards the leading edge. The groove and the rails are first required because they add stiffness to the housing. Second, the groove and the segment baffle create additional boundary conditions. Third, the hook orientation, already available but not user-friendly in the current design process allows the user to study tip clearance for older and more recent engine designs as well as cooled and uncooled turbine stages. The new components are necessary to compute accurate tip clearance results. Next, it will be explained that some limitations must be considered in the creation of the parametric models.

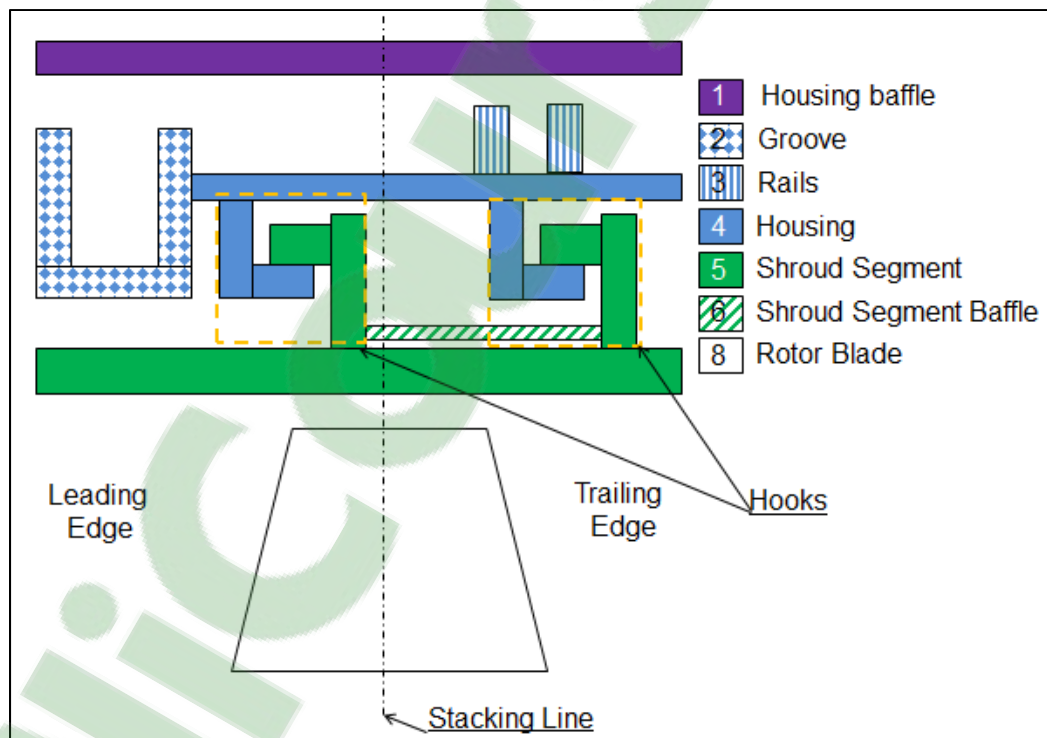


Figure 3.5: High-Pressure Turbine Components

3.3 Parametric Models Limitations

The parametric models are required to create a user-friendly user interface and to automate the communication between the parametric model and the static structure thermal calculator. In the user interface, every parameter has to be programmed such that the behavior of each parameter is the same in the CAD and the user interface. Consequently, the user interface imposes no limitations to how the parametric models are created. It only takes additional time to create a user interface with more parameters. Instead, the parametric models are limited by the complexity in defining the boundary conditions of the finite element model. That is the difficulty in automating the communication with the stator thermal calculator. The thermal boundary conditions automated calculation consists in using the appropriated correlation depending on the surface's topography and the air system distribution. It is thus mandatory to have a limited number of possible configurations in order to program logic for each surface. This is to allow an inexperienced user to perform a tip clearance study. In order to have predefined boundary conditions, the location of the feature relative to one another must be known. For example, if the segment baffle is deactivated or left hook is at the left of the groove, the boundary conditions will be different. Those differences are depicted by Figure 3.6. To respect this limitation, a set of baseline parametric models have to be created in order to assign a set of boundary to each surface. The next section presents three parametric approaches that were studied to increase the flexibility while respecting the limitations.

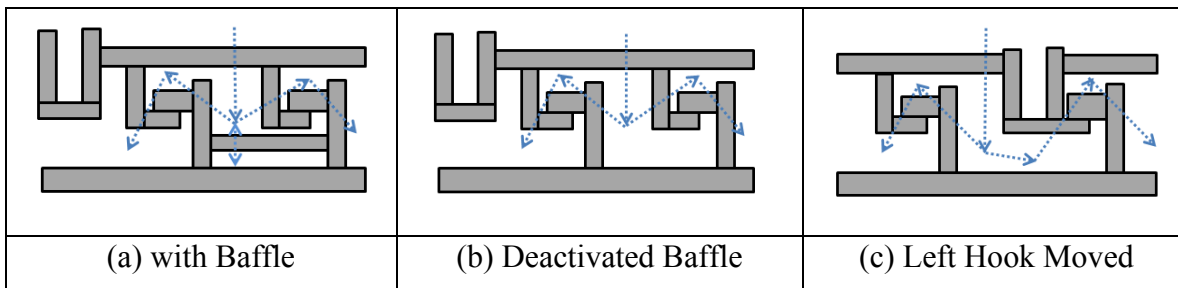


Figure 3.6: Boundary Conditions Comparison

3.4 Parametric Approaches

The methodology to increase the flexibility of the current model with a repository of CAD parametric models can be divided in several steps. Since the current rectangle based model was validated with tests, the CAD parametric models can be created with rectangles disregarding radii and chamfers. However, with variable thicknesses and steps in the geometry, it is not a simple task to observe a large number of drawings and organize them by their similarities.

The first step in defining the parametric models was to simplify shapes using a skeleton approach. Only the variations in the geometry of housings were studied since shroud segments present little variation. The second step was to study various levels of flexibility in order to increase the number of possible variations a parametric model can have. The modular approach was created. The third step was to study the limitations of each approach and verify that the boundary conditions of the thermal calculator are manageable. Finally, the fixed modular approach that compromises flexibility of the geometry and complexity in managing the boundary conditions was developed. A model for the shroud segment was created with the final approach to have fully parameterized TH and SSs. A description of the skeleton, the modular and the fixed modular approach will be created. The limitations in the skeleton and the modular approach will justify the compromises that were made to develop the fixed modular approach.

3.4.1 Skeleton Approach

The skeleton approach consists of a skeleton and an outer shape. The skeleton is represented by dashed lines and the outer shape is represented by continuous lines as shown in Figure 3.7. Only one horizontal and one vertical line of the skeleton must be fixed with a radial and a horizontal parameter. The rest of the skeleton is fixed with the thickness of the outer shape around each line of the skeleton. A new parameter is required to control the thickness around each line of the skeleton. This approach is useful to study a large quantity of different TH and SS configurations and to simplify them. Steps and variable thicknesses are disregarded while a skeleton is drawn in the averaged center of more detailed TH and SSs. The downside of the skeleton approach is that the number of variations a parametric model can have is limited. For example, Figure 3.7a and b represent 2 different baseline models. It is not possible to reproduce one baseline with the other even if the skeleton is modified with the acceptable parameters, otherwise, the outer shape will fail to regenerate. Next, the modular approach will be presented.

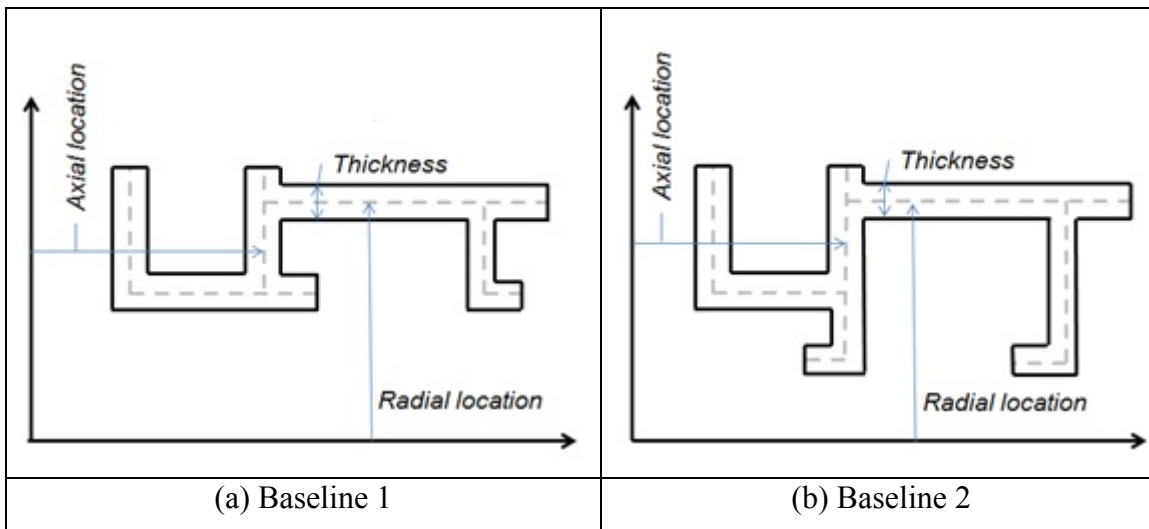


Figure 3.7: Skeleton Approach

3.4.2 Modular Approach

The modular approach was developed to address the limited flexibility of the skeleton approach. This approach is defined by components that are fixed by their local axis system, represented by a red cross as shown in Figure 3.8. Each closed shape can be deactivated. The two baselines of the skeleton approach in Figure 3.7 can be reproduced with a baseline modular model. As a result, the modular approach is limited in flexibility only by the component it has. The downside of the modular approach is also its high flexibility. Each possible arrangement of the components has to be studied such that a different set of boundary conditions is available for each arrangement. In other words, this approach creates additional complexity in the development of a fully automated thermal calculator. If an unexpected arrangement is created by the modular model, the thermal calculator will fail. Another downside of the modular approach is that the parameters are referenced to the local axis system of the components. It then becomes difficult for a designer to use those parameters that are not related to the dimensions used in the final design of TH and SSs.

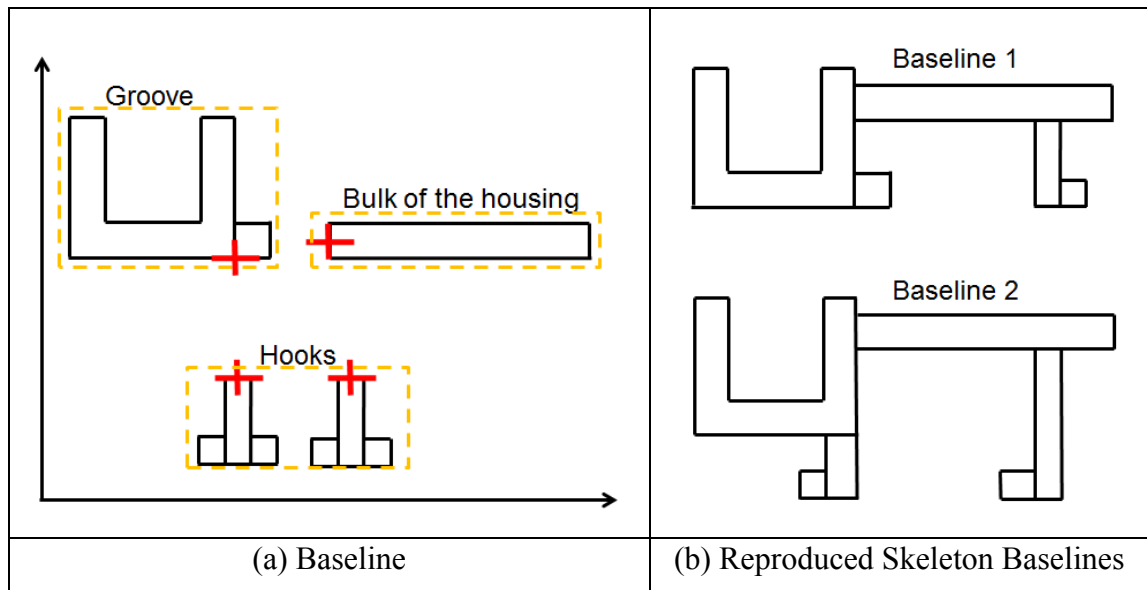


Figure 3.8: Modular Approach

3.4.3 Fixed Modular Approach

The fixed modular approach is the final approach. It is similar to the modular approach because there are components that can be moved independently from one another. Compared to the modular approach, the flexibility of the fixed modular approach was limited such that a stack-up assembles the components together. Then, each baseline configuration is similar to a baseline of the skeleton approach except that the flexibility is increased. For example, the configuration presented in Figure 3.9a has the same shape as the baseline configuration no. 2 of the skeleton approach. The robustness, i.e. number of variations where the integrity of the initial shape is maintained, brought by the independent components of the fixed modular approach allows the creation of a similar shape with a different hook orientation as shown in Figure 3.9b. In addition, the fixed modular approach is faster than the skeleton approach in creating a new baseline since it is feature-based. A new baseline with the skeleton approach would require to be created from scratch. In addition, in the fixed modular approach, the parameters can be easily chosen such that they are similar to the dimensions of detail design TH and SSs. Finally, the fixed modular approach is manageable in terms of defining a set of boundary conditions for each baseline configuration. In the next section, the new design process and TH and SS models, developed with the fixed modular approach are presented.

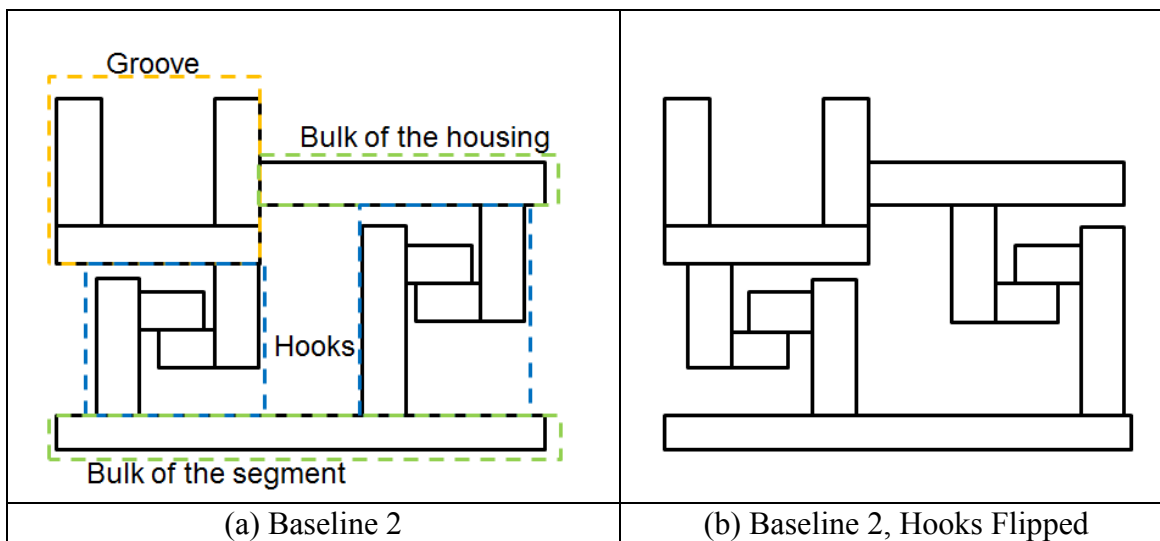


Figure 3.9: Fixed Modular Approach

3.5 New Turbine Housing and Shroud Segment Model

The new TH and SS models use some dimensions of the current TH and SS models. With the new components, additional parameters had to be created. In this section, the new parameterization is summarized. The parameters are also divided by first and second order of importance. Then, the baseline configurations that were created to meet the requirements of the new design process are presented.

3.5.1 Turbine Housing and Shroud Segment Parameters

Turbine housing and shroud segments are sized with the shroud inner radius (R1) of the turbine stage and the locations from the stacking line also named axial center of the turbine stage (A0, A1 & A2). Then, the radius, the hooks (R2 & R3) and the housing (R4 to R6) are fixed. The second step is to fix the right hook axially with respect to the stacking line and the left hook with respect to the right hook. Those parameters are presented in Figure 3.10a. Other parameters that are of the second order of importance are the height and width of the rectangles. Those parameters are not presented in Figure 3.10a. The parameters presented in Figure 3.10b are also of the second order of importance but are still necessary to have a fully parameterized model. Those are radial and axial offsets that are necessary to capture the design intents of the TH and SSs. For example, an impingement baffle is fixed with its distance from the cooled surface instead of the radius from the axis of the engine. Finally, a total of 50 geometry parameters were necessary to fully constrain the TH and SS parametric models.

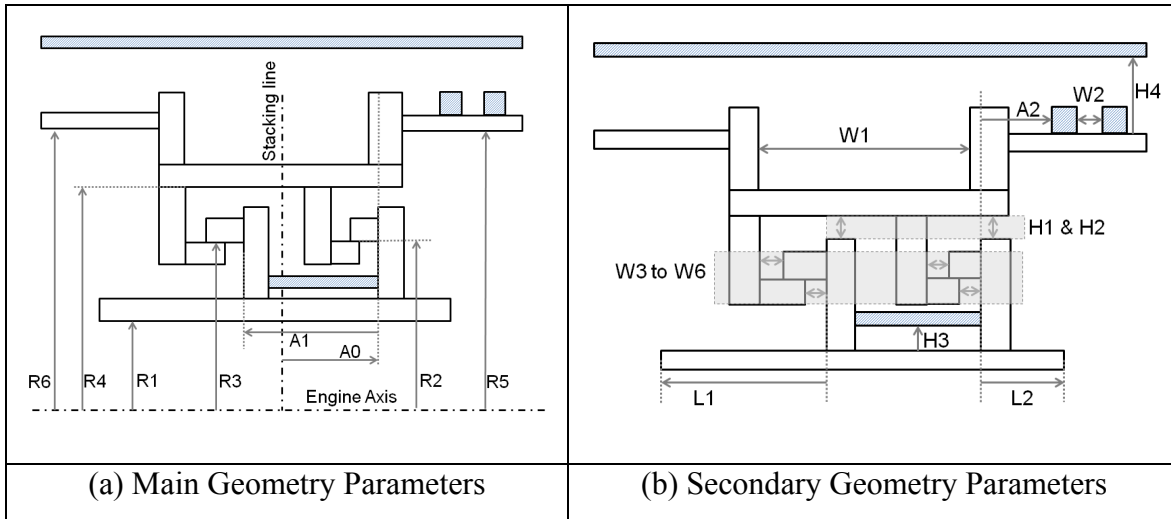


Figure 3.10: Turbine Housing and Shroud Segment Parameterization

3.5.2 Turbine Housing and Shroud Segment Configurations

To meet the requirements of the geometry described in Section 2.2, seven different baseline configurations were created. With the fixed modular approach, the configurations were defined by the groove location with respect to the stacking line and hook location. The stacking line is the center of the blade in the axial dimension and it is usually located between the shroud segment hooks. The stacking line can be closer to one hook or another. The hooks can be located under the bulk of the housing, under the groove or attached to the groove. Every configuration has a housing baffle, a shroud segment baffle and 2 rails that can be activated or deactivated. The hook orientation can be modified where both hooks can be flipped, considering that the groove cannot be flipped. The seven configurations are presented in Figure 3.11 without the rails and the baffles. Next, the user interface that was developed to overlay a parametric model on detail TH and SS will be presented.

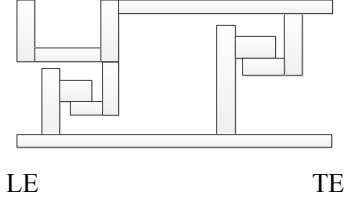
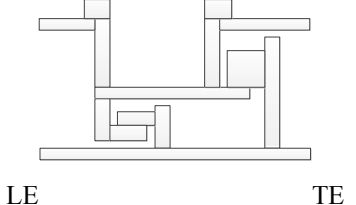
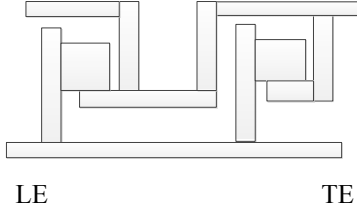
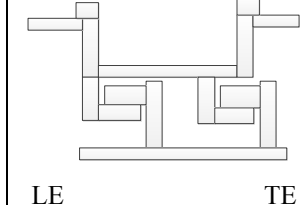
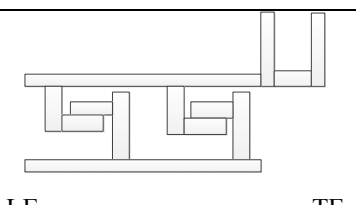
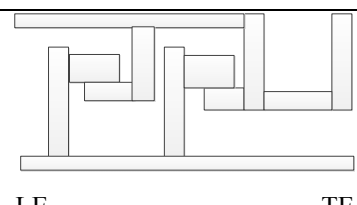
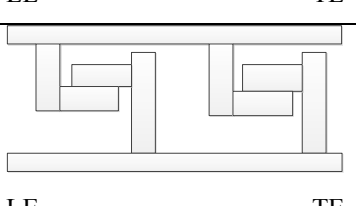
LE Groove	 LE TE		
Middle Groove	 LE TE	 LE TE	 LE TE
TE Groove	 LE TE	 LE TE	
No Groove	 LE TE		

Figure 3.11: Baseline Configurations

3.6 Static Structure User Interface

The second and third requirements of the new design process are that it must be user-friendly and that the manual operations must be minimized. To meet those requirements, the requirements for a user interface were defined and it was developed. It was not within the scope of this research to develop the user interface so the job was assigned to a software engineer intern named Valentin Debris, from ETS. Nevertheless, the functionalities of the interface highlight the contributions of the parametric models to the new design process. The three steps required to use the interface will be described. Then, the guidelines to overlay a parametric model on detailed TH and SSs will be explained.

The design of TH and SSs using the user interface is completed in three steps. First, there are 7 different baseline parametric models. Each parametric model was associated with legacy engine models. If new engine architectures are created, new baseline parametric models should be created as well. The designer that uses the interface has to determine which engine model is the closest to the target TH and SS. Then, the designer chooses additional options such as the hook orientation, to display the rails or not and to display the baffles or not. The baseline model is configured and the geometry appears in the model viewer. The baseline models are the TH and SS represented by the green lines in Figure 3.12.

The second step consists in preparing the detailed TH and SS for the display in the model viewer. The detailed TH and SSs are also named the target TH and SSs because the purpose of the user interface is to overlay the baseline model on the detailed TH and SS. It was found that the orientation and the location of the TH and SS were not standardized in the drawings. Then, the key information in the source drawing is collected and entered. The user interface displays the target TH and SS from the source drawing in the appropriate orientation and automatically attaches the anchor point of the baseline model to the anchor point of the target TH and SS. The target TH and SS are represented by the dotted black lines and the anchor point is represented by the red dot in Figure 3.12.

The third and final step consists in modifying the geometric parameters to overlay the lines of the baseline configuration on the target TH and SS one by one. It was found that modifying the parameters randomly is not efficient. A standardized order was defined and parameter groups were created. The standardized order of modification keeps the user from modifying a parameter twice. In other words, once a line is moved with a parameter, modifying other parameters will not move this line. In addition, parameter groups helped improving the friendliness of the user interface and facilitated defining the standardized order. Finally, with the simplifications of the baseline configurations, it is not possible, to overlay each line on the target TH and SS. The detailed documentation provided with the user interface brings consistency in the results. For example, if two different people were to

overlay a baseline configuration on the same target TH and SS, the result would be the same. The benefits of the new design process will be presented in the next section.

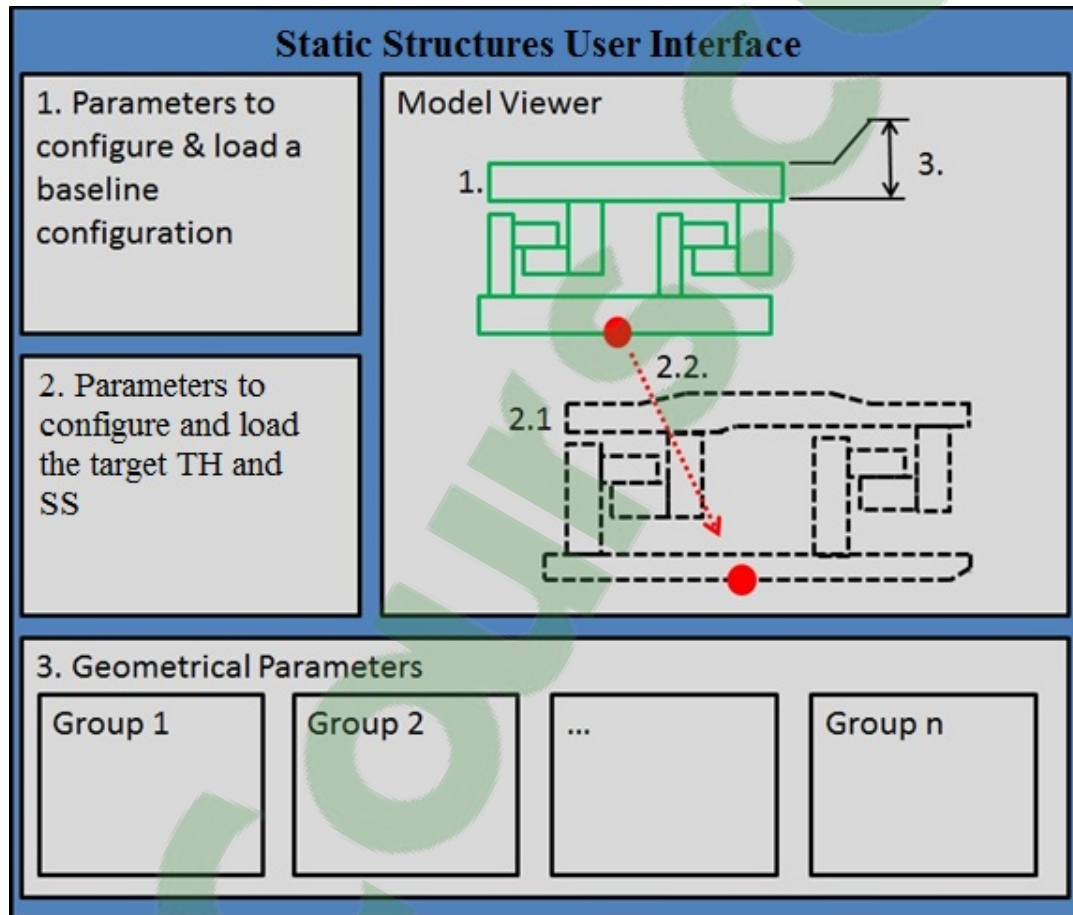


Figure 3.12: Static Structure User Interface

3.7 Evaluation of the New Design Process

The new design process and the current design process can be compared in terms of flexibility, time, user-friendliness, accuracy and results consistency. The flexibility of the current and the new design process is calculated in terms of the quantity of different engines that each baseline configuration can reproduce. The current TH and SS models have the same geometry that is parameterized with configuration 7. The flexibility of configuration 7 is 36%. With the new baseline configurations, the flexibility of the new design process

increases to 92%. Those statistics include recent engine models in production. The detailed drawings were compared to the parametric models. When a drawing is not available, the engine model is obsolete, non-certified or no-longer sealable therefore not considered in the statistics.

The time required to scale a new TH and SS was calculated. The reference time in the current design process is the time to do a manual overlay and copy the dimensions into the TCC spreadsheet. Minor to major modifications would require starting from scratch. The current design process is also subjective since the result depends on the user. On the other hand, with an integrated user interface, it was calculated in a test case that importing target TH and SS, overlay a baseline configuration and scale it to the dimensions of the target takes $\frac{1}{2}$ reference time. It is more robust and consistent in the results because a template is provided. Different users can obtain the same results. In addition, data transfer is managed by the user interface, therefore, the new design process is more time efficient. Finally, the reduced time of the new design process allows performing more design iterations. That results in a more optimized shape.

Next, it was explained that the flexibility of the new design process is 92% compared to 36% for the current design process. Extensive work was realized to increase the flexibility such that the most important configurations and components are covered. However, for the remaining 8%, additional configurations would be required. Even for configurations not covered, it was estimated that the new design process reduces the time to re-program. The current design process was not created for more than one TH and SS configuration. With the current design process, new macros would be required. As a result, time to re-program was also used as a reference to calculate the improvement of the new design process which would take $\frac{3}{5}$ reference time. It is much faster to create a baseline parametric model with the fixed modular approach than to create new macros. However, the time to re-program does not include the time required to define new components and parameters.

The user-friendliness and results consistency are difficult to quantify. Instead, the comparison is qualitative. An integrated user interface has the ability to have an interactive model viewer and automated data transfer. As a result, it is considered more user- friendly.

The accuracy of the current design process was validated with tests. The new design process has more configurations with similar rectangle based shapes. The accuracy should be similar. However, it remains unknown for 6/7 baseline configurations. It should be validated as well. Nevertheless, considering an increase in flexibility of 56%, i.e. 92-36, it is estimated that there is equivalent increase accuracy.

Finally, results consistency is a comparison between simplified TH and SS designed by two different people. With the current design process, a figure is provided as the guideline of what should be the simplified shape. Two different people can choose to draw a simplified shape differently on detailed TH and SS. With the new design process, the user variability has been greatly reduced. Each engine has been associated with a baseline configuration. In addition, a standard procedure, based on experience, has been developed to overlay a baseline configuration on detailed TH and SS. In other words, a turbine generalist could do the job of turbine specialist.

Table 3.1: Design Process Comparison

	Current	New
Flexibility	1 hard coded geometry	7 parameterized configurations
	36%	92%
Time (Use/Re-Program)	Ref. (approximated)	1/2 Ref. (test case)
	Ref.	3/5 Ref.
User Friendliness	-	Increased
	No model Viewer	Interactive model viewer
	Manual data transfer	Automated data transfer
Accuracy	Validated with test	Current +56%
Results consistency	Based on experience	Hardcoded

3.8 Conclusion

A new design process was developed. The requirements were that it should be more flexible, more user-friendly, automated and faster to use. In addition, it should remain accurate. The creation of a repository of seven baseline parametric models increased the flexibility from the current to the new design process by a factor of 2.6 (92% divided by 36%). The time of the new design process was reduced by 50% compared to the current design process because it takes 1/2 reference time to overlay a baseline parametric model to the dimensions of target TH and SS. A user interface was developed and the procedure to use it was standardized. As a result, the user friendliness and results consistency have increased in the new design process. However, those improvements cannot be calculated. An increase accuracy of 60% was also estimated but the accuracy assessment with a static structure thermal calculator is recommended. However, the static structure thermal calculator was not developed because it requires the creation of parametric models first. An alternative methodology to assess the accuracy of the parametric models, not based on flexibility, is presented in the next chapter. Finally, a standard list of parameters was created to fully constraint the 7 baseline configurations. Most of the parameters were presented in Figure 3.10. In the next chapter, the correlation study of the geometric parameters will explain how the parameterization can be simplified. The methodology of the correlation study and the benefits will also be presented.

An aspect that was not covered by this chapter are the improvement in time and accuracy at the detail design phase. The new design process was developed for pre-detail analyses. It was explained that the optimization of the static structures becomes possible with parametric models. With optimization at the pre-detail phase, time and accuracy improvements should be observed at the detail design phase which is a benefit for the overall design process.

CHAPTER 4

CORRELATION STUDY OF THE GEOMETRIC PARAMETERS

4.1 Context and Objective of the Correlation Study

In this chapter, the second objective of this research will be addressed. In the previous chapter, 7 different parametric models were created for the new design process. The flexibility of the parametric models can be estimated with the number of components they have (i.e. groove, hooks, etc.). The number of components will determine the number of parameters that are required. The number of parameters is also an indicator of the flexibility of a parametric model. In the previous chapter, it was explained that the flexibility of the parametric models was limited using the fixed modular approach. Nevertheless, the relations between the geometric parameters were not studied. The second objective of this research is to study those relations and to reduce the number of parameters that are available for static structures design and optimization. As depicted by Figure 4.1, the number of independent parameters n is reduced to $n-m$ with the correlation study. That results in fewer independent parameters. In addition, in static structures optimization, a fraction $p/(n-m)$ of the independent parameters can be used as design variables. The simplified parameterization should result in improved design and shape optimization time for the static structures. Next, it will be explained how the correlation study was conducted.

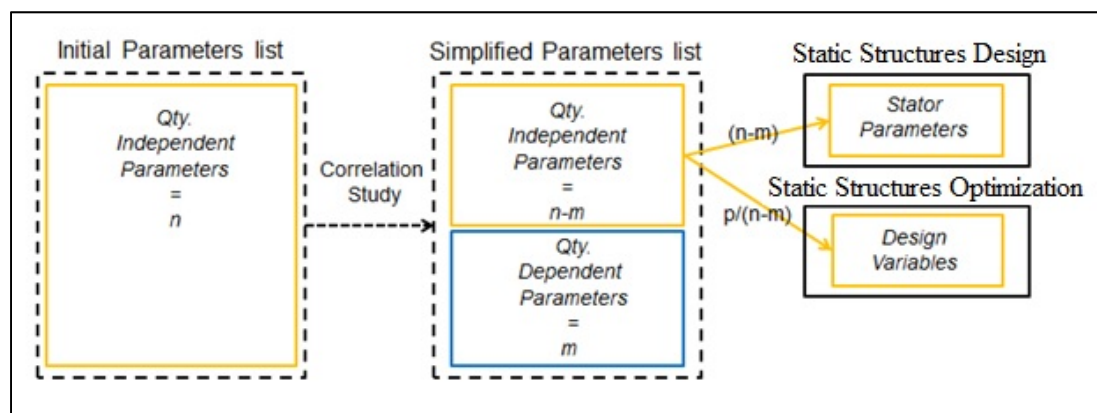


Figure 4.1: Correlation Study Objective

4.2 Methodology in the Correlation Study

The methodology of the correlation study is presented in Figure 4.2. The correlation study of the geometric parameters was divided in three steps: risk assessment, the relations of the geometric parameters and parametric model validation. The first step, risk assessment consists in verifying that the parametric formulation is not oversimplified. Since many geometric parameters are important in tip clearance, cooling flow and containment predictions, there is a risk to affect the accuracy of the predictions if those parameters are simplified. The purpose of risk assessment is to find those parameters. However, the correlations with cooling flow and containment were not calculated. Instead, only the correlations between the geometric parameters and tip clearance were calculated due to the resources available. Finally, a total of 9 correlations with tip clearance were found for the 7 baseline configurations and a level of risk, from low to high, was assigned.

In the second step, the relations of the geometric parameters were studied to simplify the TH and SS parametric formulation taking into account that the parameters correlated with tip clearance should remain independent. Standardized dimensions and geometric correlations were created. In the standardized dimensions, four constants were created. On the other hand, in the geometric correlations, hook and small sample correlations were studied. The hook correlations outliers were studied to assess the validity of the hook correlations. A total of six geometric correlations were created. Finally, it was verified by P&WC specialists that the standardized dimensions and the geometric correlations are acceptable for the design of TH and SSs.

The third and last step of the correlation study is named the parametric model validation. Relations between more than 2 parameters were studied with multiple linear regressions to prove that the parametric formulation cannot be simplified further. Then, the accuracy of the geometry was estimated to prove that the parametric models are not oversimplified.

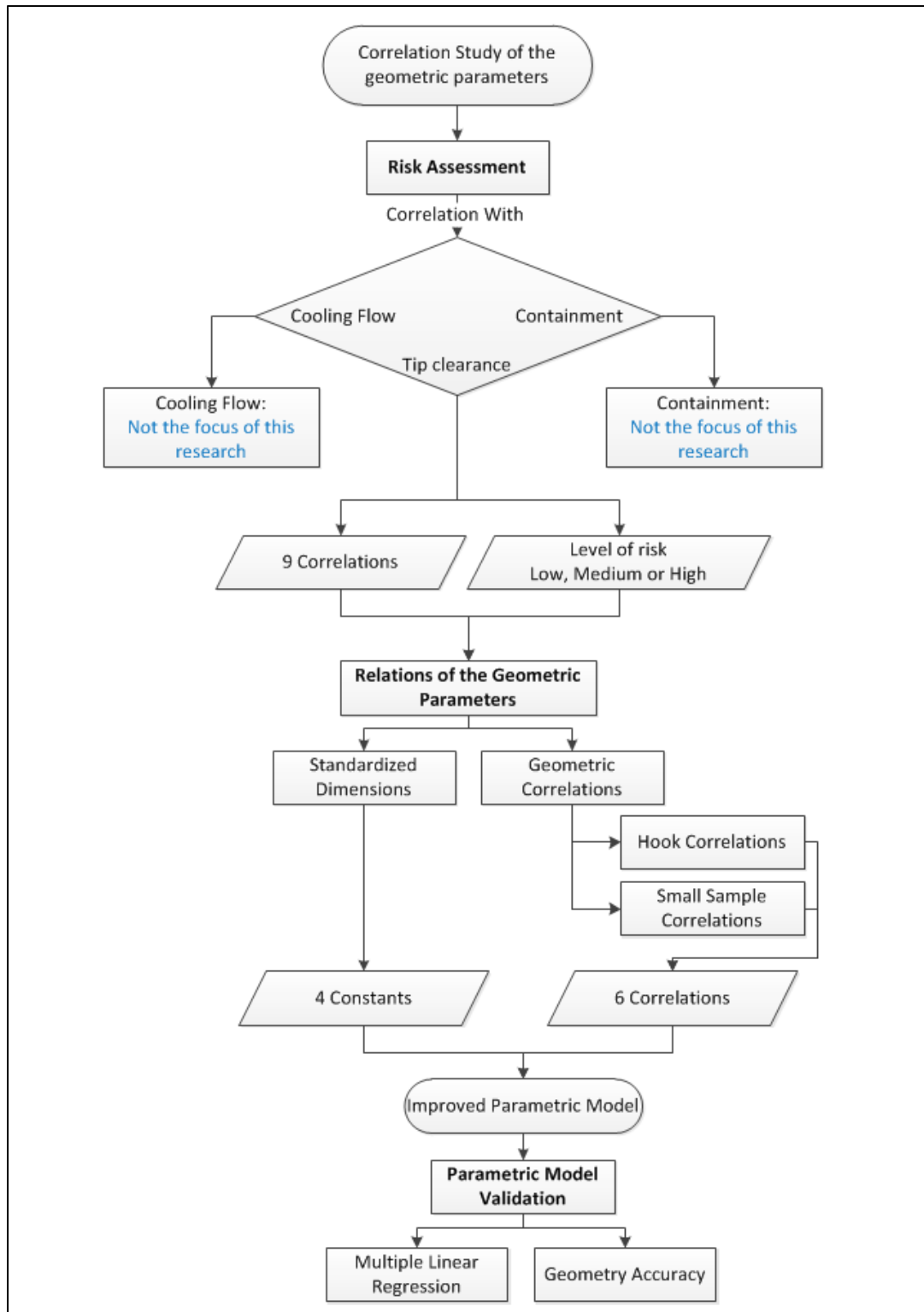


Figure 4.2: Methodology for the Correlation Study of the Geometric Parameters

4.3 Risk Assessment

Risk assessment consists in finding which geometry parameters affect tip clearance calculations the most. Since tip clearance is function of the displacement of the rotating and static structures, the static structure thermal displacement is used to calculate the correlation of the geometric parameters with tip clearance. In order to find the parameters correlated with the thermal displacement and estimate the level of risk, a trade-off was made between the sample size n , the level of significance α and the strength of the relation R^2 . The trade-off is presented in Table 4.1. For additional validity of the correlation, a level of risk was assigned only to the parameters that were correlated at two engine conditions. The results for the two engine conditions are presented in appendix I.

Table 4.2: Trade-off in Risk Assessment

Sample Size n	Level of Significance α	Strength R^2 %	Level of Risk
10	10	70-100	High
5	10	50-100	Medium
3-10	20	0-100	Low

The parameters correlated with static structures thermal displacement are presented in Table 4.2. For R1, R2, R3 and R5, $n=10$ and $\alpha=10\%$ and R^2 is relatively high and varies from 68.75% to 75.5%. As a result, the level of risk is high. For the parameters R4 and W12, $n=5$, $\alpha=10\%$ and R^2 is very high and varies from 91.45 to 93.85. It was decided that the sample size has more impact than the strength of the relation on the level of risk. This is why R4 as a medium to high risk. On the other hand, W12 has a low to medium risk because W13 is a similar parameter that has a low risk. For the parameters, H1 and H8, R^2 is low and $\alpha=20\%$. As a result, the level of risk is low. The fact that $n=10$ does not increase the level of risk. Finally, for W13, even though $R^2=97.35$ the risk is low because $n=3$ and $\alpha=20\%$. The parameters correlated with the thermal displacement are presented on two TH and SS configurations in Figure 4.3. The geometric correlations will be presented in the next section.

Table 4.2: Correlations with Static Structures Thermal Displacement

Thermal Displacement VS	Sample Size n; Level of Significance α	Strength R^2 %	Level of Risk
R1	n=10; α =10%	68.75	High
R2		75.15	High
R3		75.5	High
R5		74.85	High
R4	n=5; α =10%	93.85	Medium - High
W12		91.45	Low - Medium
H1	n=10; α =20%	32.4	Low
H8		19.05	Low
W13	n=3; α =20%	97.35	Low

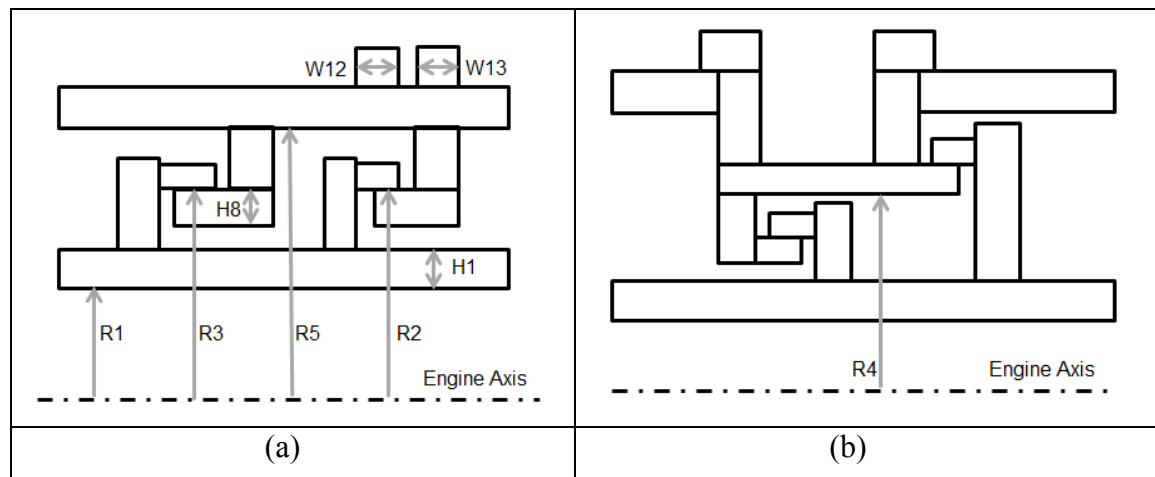


Figure 4.3: Risk Assessment Parameters for Tip Clearance

4.4 Relations of the Geometric Parameters

The relations of the geometric parameters are divided into two sections. First, the standardized dimensions are parameters that were replaced by a constant value. It will be explained which parameters were used in the standardized dimensions and how the constant values were determined. Second, the geometric correlations will be presented. The parameters that are highly correlated will be presented. It will also be explained how the parameters were simplified.

4.4.1 Standardized Dimensions

The simplifications in this section were made because TH and SS were over-parameterized. As a result, constant values were assigned to TH and SS dimensions that don't need to be modified when they showed a very small variation among existing engine models. In addition, those parameters are not correlated with static structures thermal displacement. The purpose of this section is to explain how the constants were assigned. The standardized dimensions are the radial clearance between the hook and the housing, the axial clearance between the hooks and the segment and housing baffle thicknesses. The four standardized dimensions that were created with eight parameters are presented in Figure 4.4. The radial clearance S1 replaced 2 parameters by 1 constant value. The axial clearance S4 replaced 4 parameters by 1 constant value. Finally, the segment and housing baffle thicknesses S2 and S3 replaced 2 parameters by 2 constant values.

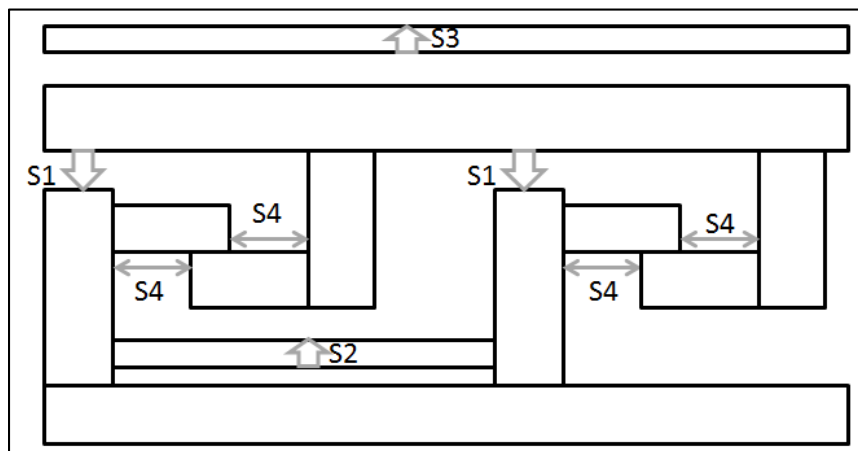


Figure 4.4: Standardized Dimensions

Further to that, to create the standardized dimensions, the mean of the sample and the standard deviation were calculated. The mean of the sample is the value assigned to the constant and the parameter values at ± 1 standard deviation are the limits observed to prove whether there is little variation or not. In addition, it was verified that a majority (i.e. more than 50%) of TH and SS were within a region of ± 1 standard deviation. An example is presented in Figure 4.5. There is 12/13 or 92 % of the observed engines within ± 1 standard

deviation, therefore, a majority of the parameter values are close to the mean. As a result, the mean of the sample is an appropriate constant value for a standardized dimension.

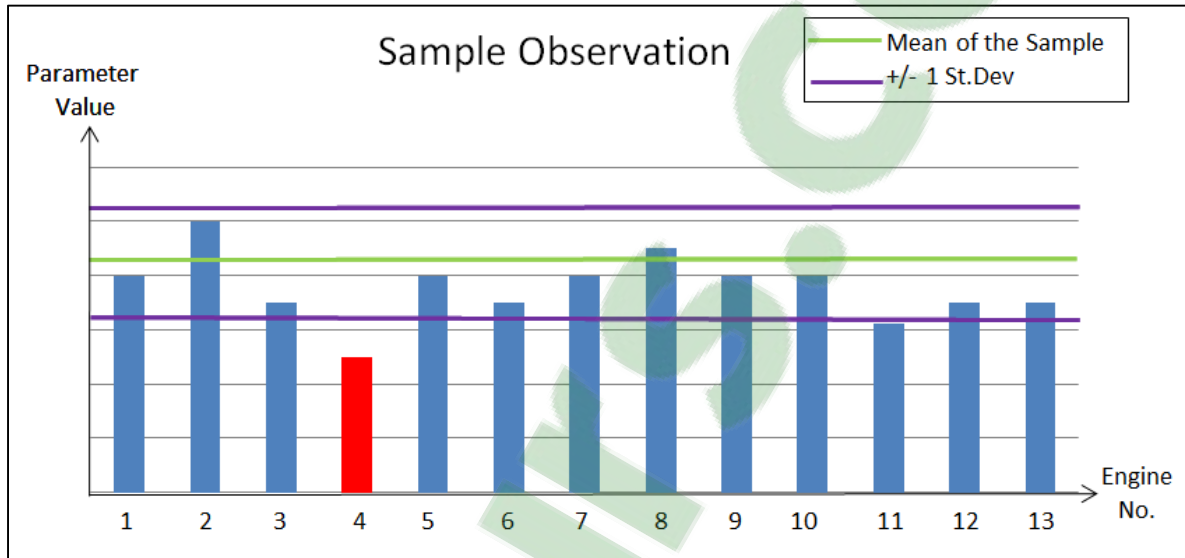


Figure 4.5: Sample Observation for the Standardized Dimensions

The statistics that were observed in the creation of the standardized dimensions are presented in Table 4.3. The standard deviation is divided by the average of S4 to obtain the dimensionless standard deviation. For S1, 73.1% of the data is within ± 1 standard deviation. In addition, there is 2% in dimensionless standard deviation. As a result, S1 is almost constant compared to S4. As a result, it is appropriate to use the mean of the sample to assign a constant.

For S2 and S3, 100% and 71.4% of the data is within ± 1 standard deviation. In addition, there is 1.3% and 23.3% in dimensionless standard deviation for S2 and S3. In addition, the standard deviation for S3 is larger but the baffle thicknesses are not correlated with static structures thermal displacement. As a result, it is appropriate to use the mean of the sample to assign the constants.

For S4, 66% of the data is within ± 1 standard deviation. In addition, there is 66.6% dimensionless standard deviation. Assigning a constant to for S4 does not seem appropriate

considering the large dimensionless standard deviation. However, S4 is not correlated with static structures thermal displacement based on P&WC experience. As a result, the mean of the sample was used to assign a constant to S4. The accuracy of the geometry was also verified to see how the geometry is affected by S4. This will be explained in the last section of this chapter.

Table 4.3: Standardized Dimensions Validation

Dimension	n	Engine Qty.	Engine Qty. (%)	Dimensionless St. Dev. (%)
S1	26	19/26	73	2.0
S2	2	2/2	100	1.3
S3	7	5/7	71	23.3
S4	47	31/44	66	66.6

In conclusion, four standardized dimensions were created to simplify the parametric formulation. The mean of the sample was calculated to assign a constant value to those dimensions. It was concluded that the mean of the sample is acceptable for S1 to S4 because there is more than 50% of the parameter values within +/- 1 standard deviation. In addition, the small standard deviation of S1 and S2 confirmed that there is little variation in the parameter values. The standard deviation of S3 and S4 was larger but still showed a relatively small variation in the parameter values. The discrepancy resulting from the simplifications will be presented in the last section of this chapter, the geometry. Finally, it is recommended to revise the majority to 66% and use S4 as a reference in the future. As a matter of fact, having fewer engine models above and below +/-1 standard deviation is preferable.

4.4.2 Geometric Correlations

In the geometric correlations, the symmetry of TH and SS was used to simplify the parametric formulation. The relations among the parameters were studied when two parameters appeared redundant. The correlations are divided three sections: the hook correlations, the hook correlations outliers and the small sample correlations. It will be explained why the parameters in those correlations are considered redundant and how the parametric formulation was simplified using the average of the parameters, two parameters at a time.

4.4.2.1 Hook Correlations

The hook correlations are correlations between leading edge (LE) and trailing edge (TE) dimensions of the hooks. When a strong correlation was observed between the LE and TE dimensions, dependent parameters list were created. In order to verify that the correlations were valid, the test of the correlation coefficient was used with $\alpha=5\%$. Then, to properly define dependent and independent parameters, the linear relation between those parameters was established using linear regression. For example, the relation between LE and TE foot width (W1.LE and W1.TE) is presented in equation 4.1. The LE and TE foot width are the independent and dependent parameters. As a result, W1.LE' is function of W1.TE and the W1.LE is no longer available for static structure design and optimization. Since there is no evidence that either of TE or LE is more important to design TH and SS, the assumption that the average is more appropriate was made. This approach was verified by P&WC. The average of LE and TE foot width is presented in equation 4.2. A new independent parameter W1 is created and W1.LE and W1.TE become dependent parameters. The average was used to create the five parameters presented in Figure 4.6. There is the feet width W1, the segment and housing leg width W2 and W3 and the segment and housing feet height H7 and H8.

$$W1.LE' = \beta_1 + \beta_2 \times W1.TE \quad (4.1)$$

$$W1 = (W1.LE + W1.TE)/2 \quad (4.2)$$

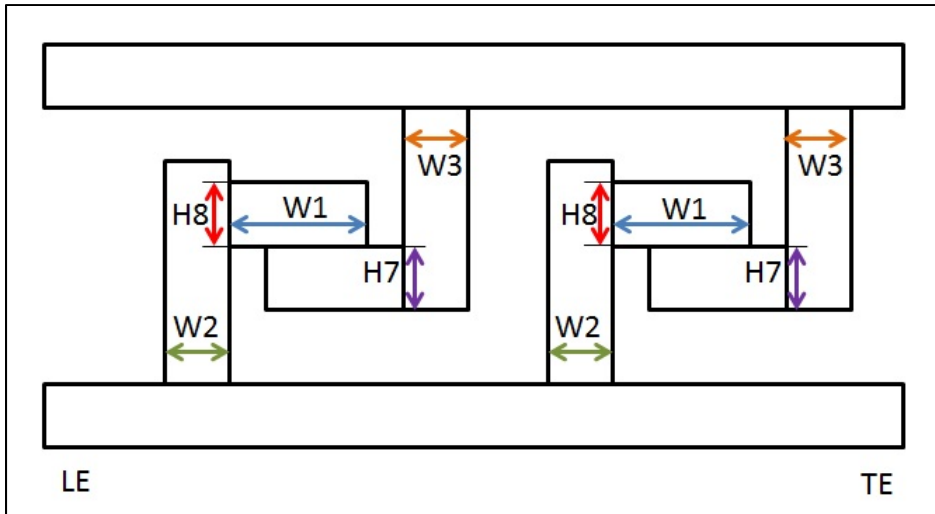


Figure 4.6: Hook Correlations Parameters

Next, in order to verify that defining LE and TE dimensions as the average of the two was appropriate, the regression error and the error of the average were compared. An example of those errors is presented in equations 3.3 and 3.4. The regression error consists in the difference between $W1.LE'$ and $W1.LE$. On the other hand, the error of the average consists in the difference between the average of LE and TE feet width $W1$ and $W1.LE$.

$$\text{Regression Error(\%)} = (W1.LE' - W1.LE)/W1.LE \quad (4.3)$$

$$\text{Error of the average (\%)} = (W1 - W1.LE)/W1.LE \quad (4.4)$$

The results of the correlations and error comparisons are presented in Table 4.4. The strength of the relation in the correlations varies from $R^2=71.1\%$ to 91.9% . With the value of R^2 , there was enough evidence to suggest that dependent parameters should be created to simplify the hooks. The regression error varies from 4% to 10% and is always bigger than the error of the average that varies from 2% to 9.1%. As a result, defining LE and TE dimensions as the average of the two is more appropriate than using the regression equation. Further to that, the samples that were used in the hook correlations are different because several TH and SSs were considered outliers. For $W3$, $H7$ and $H8$, weak correlations were observed for larger

samples that included outliers. It will be explained why it was considered acceptable to remove those outliers from the correlations and consider higher R^2 values.

Table 4.4: Hook Correlations and Error Comparison

Correlation	n *Without outlier	R^2 (%)	Regression Error (%)	Error of the average (%)
W1 – Housing Feet Width	19	77.2	7.0	3.5
W2 – Segment Leg Width	18	82.9	8.8	3.7
W3 – Housing Leg Width	12*	71.1	10.0	9.1
H7 – Housing Feet Height	14*	87.8	8.0	4.0
H8 – Segment Feet Height	17*	91.9	4.0	2.0

4.4.2.2 Hook Correlations Outliers

The correlation between LE and TE dimensions was calculated for five parameters. When there is a correlation, a regression model is created to show the variation of the LE dimension in function of the TE dimension. To be consistent with the test of the test of the correlation coefficient, there is a 95% CI associated with the regression models. In order to identify the outliers in the correlations, the regression models and their CI will be used to show which TH and SS are far from the bulk of the data. Finally, the geometry of the outliers will be presented to explain why correlations with smaller sample size were accepted.

W3 & H7 Outliers

The regression model of W3.LE in function W3.TE is presented in Figure 4.7. The outlier, identified by a red circle, is far from the bulk of the data. The slope of the regression model is affected by the outlier. As a matter of fact, there is a larger variation in W3.TE (90%) than there is in W3.LE (20%) for the outlier. In comparison, there is approximately 29%

variation in W3.TE for 27% variation in W3.LE for the regression without outlier. In addition, the CI does not add additional information to prove there is an outlier in this regression model. Finally, a small $R^2=13.1\%$ in this model compared to a larger $R^2=71.1\%$ computed with $n=12$ in the previous section is explained by the presence of the outlier. Next, it will be explained why it was concluded there is an outlier in the correlation between H8.LE and H8.TE.

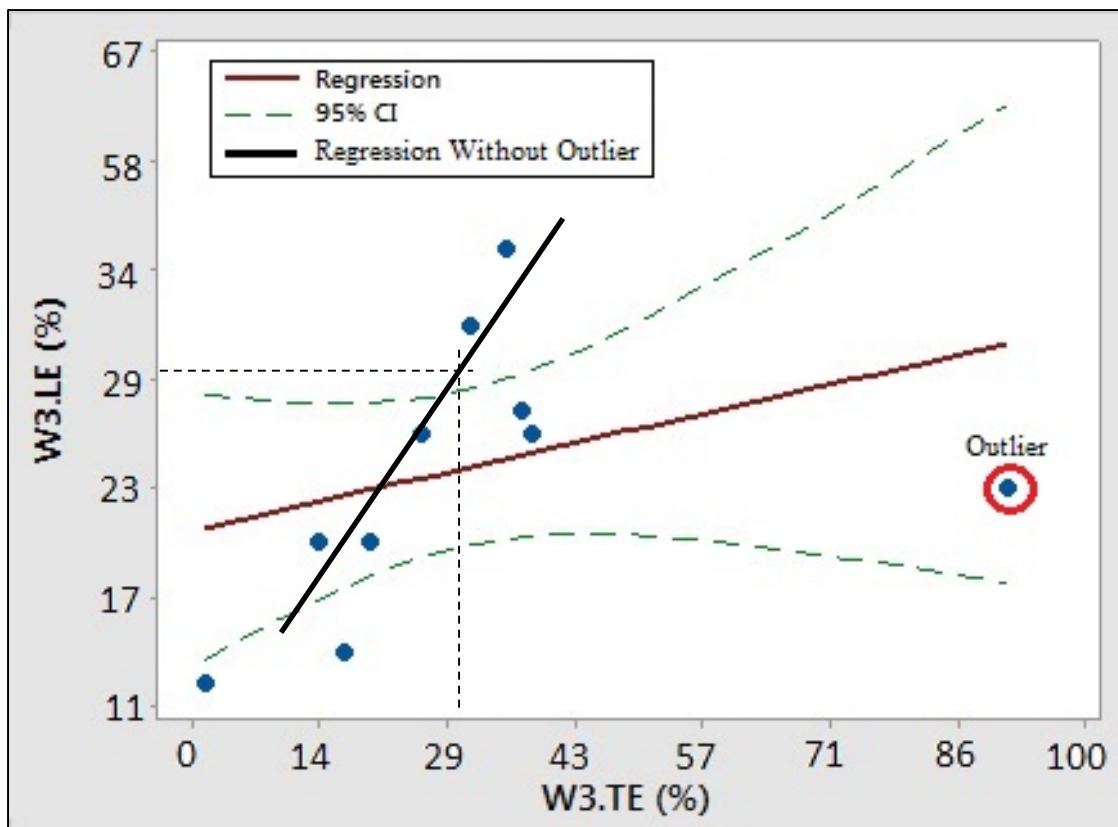


Figure 4.7: Housing Leg Width Regression Model; $n=13$ & $R^2=13.1\%$

The regression model of H8.LE in function H8.TE is presented in Figure 4.8. The outlier, identified by a red circle, is far from the bulk of the data. The slope of the regression model is clearly not affected by the outlier. However, there is a larger variation in H8.LE (100%) than there is in H8.TE (7%) for the outlier compared to the regression model that shows 31% variation in H8.LE for 40% variation in H8.TE. In addition, the CI clearly identifies the outlier since the bulk of the data is within CI upper and lower limits and the outlier is not.

Finally, a smaller $R^2=62.7\%$ in this model compared to the higher $R^2=91.9\%$ computed with $n=17$ in the previous section shows that even with the outlier, H8.LE is correlated with H8.TE. However, that does not explain why it is acceptable to remove the outliers in W3 and H8 correlations. It will be explained by presenting the geometry of unusual turbine housing and shroud segments.

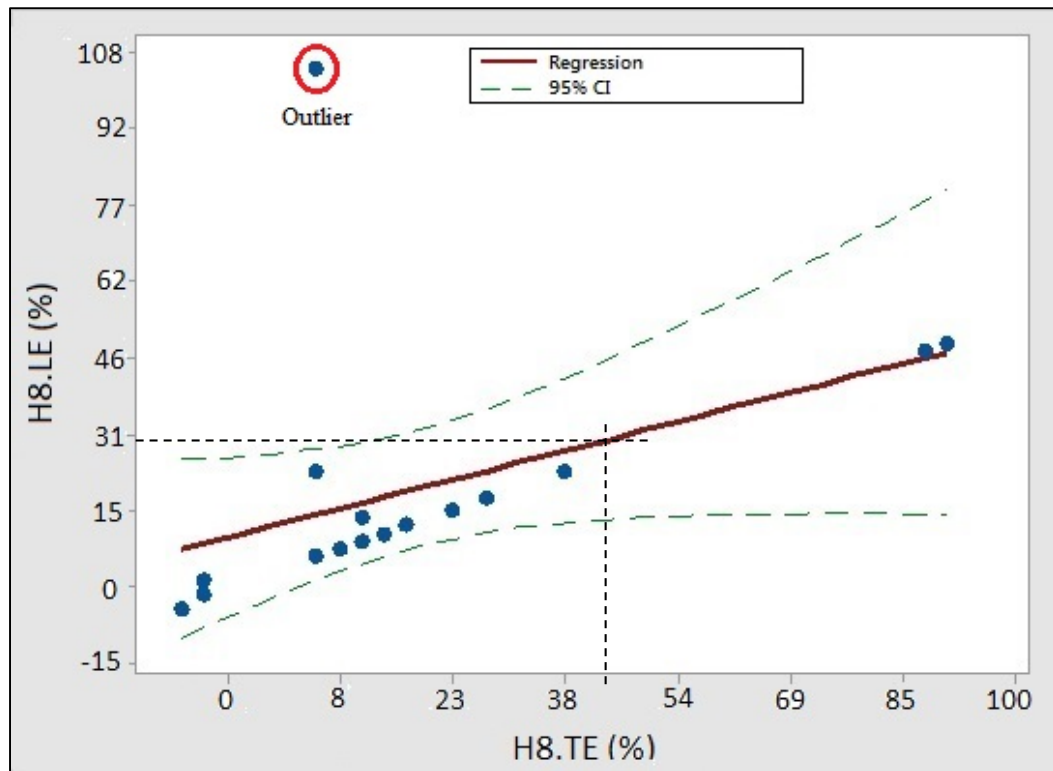


Figure 4.8: Segment Feet Height Regression Model; $n=18$ & $R^2=62.7\%$

The geometry for W3 and H8 outliers is presented in Figure 4.9a and b. The outlier for W3 is represented by the wider turbine housing TE hook. Standard turbine housings support only the shroud segments. A wider TE hook is required to support additional component with the right portion of the TE hook. On the other hand, the outlier for H8 is represented by a shroud segment with a thicker LE hook. It is thicker because it assembles with non-standard turbine housings. Both W3 and H8 outliers are non-standard designs used in old engine models. Since the correlations were calculated to simplify the design of currently used and future

engine models, a simplification that does not take into account the geometry of non-standard designs is acceptable.

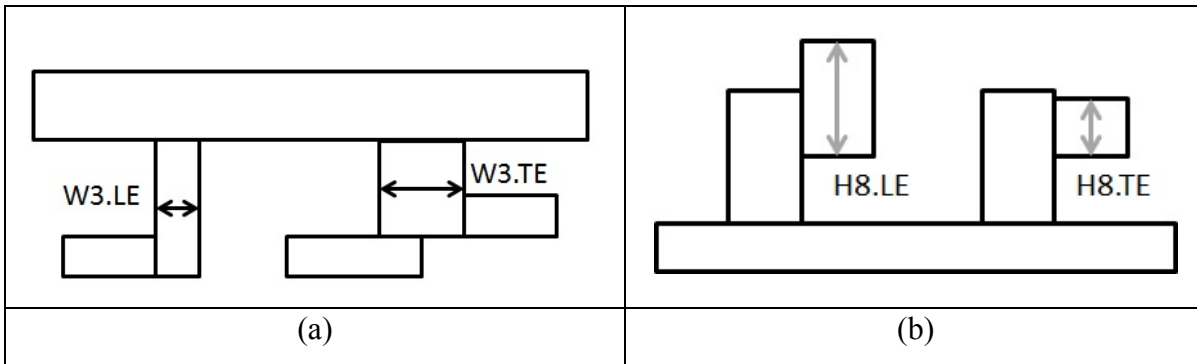


Figure 4.9: Outlier Geometry – W3 & H8

H7 Outlier

The regression model in Figure 4.10 presents the variation of H7.LE in function H7.TE. The five points identified by a red circle are assumed to be outliers because they follow a different relation. The outliers do clearly not affect the slope of the regression model. However, the outliers affected the strength of the relation since a lower $R^2=57.5\%$ was computed instead of $R^2=87.8\%$ with $n=14$ in the previous section. In addition, the configuration numbers from 1 to 7 were added to the model to explain the relation of the outliers. It appears that configuration 1 and 4 do not fit well to the regression model and follow a different relation. In order to explain why configurations 1 and 4 follow a different regression model, configuration 4 initial and modified parameterization will be presented. Configuration 1 will not be presented because it is similar to configuration 4.

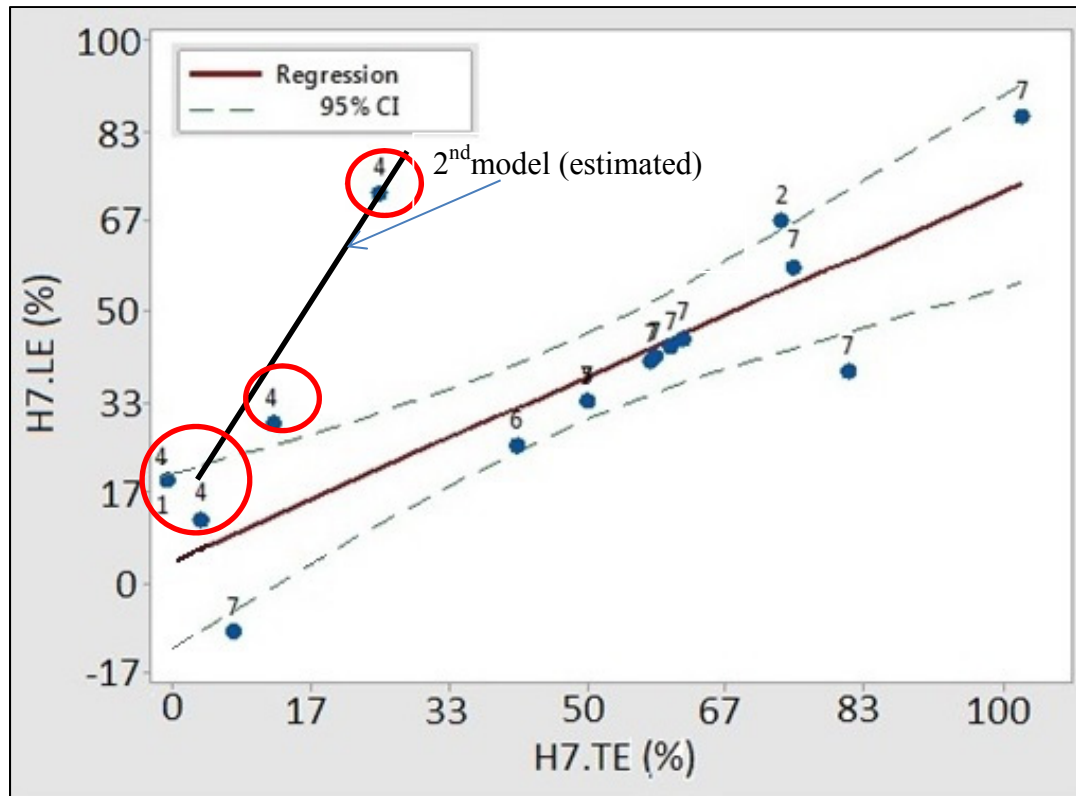


Figure 4.10: Housing Feet Height Regression Model; $n=19$ & $R^2=57.5\%$

Configuration 4 initial and modified parameterization are presented in Figure 4.11 a and b. In the initial parameterization, H7.LE was an independent parameter and R4 was not available. It was found in risk assessment that R4 is correlated with thermal displacement. For this reason, the initial parameterization was not acceptable for configuration 1 and 4. The parameter R4 should have been used instead of H7.LE to constrain the model. In the modified parameterization, H7.LE is function of R3 and R4 ($H7.LE=R3-R4$). In addition, with the modified parameterization, the relation between H7.TE and H7.LE will not affect configuration 1 and 4. Finally, it is acceptable to conclude that there is a strong correlation between H7.LE and H7.TE for configurations 2, 3, 5, 6 and 7.

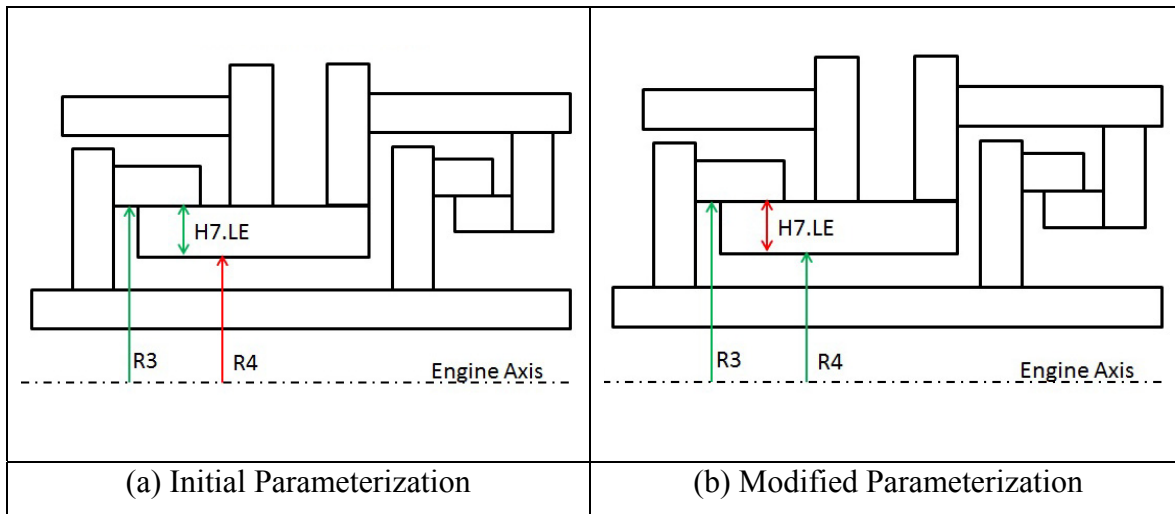


Figure 4.11: Outlier Geometry - H7

In conclusion, the relation between LE and TE hook dimensions was studied. Five correlations were created with high R^2 values that varied from 71.1% to 91.9%. Then, a regression model was created for each correlation. The regression error was compared the error of the average to determine if it is adequate to design the TH and SSs with the LE dimension function of the TE dimension or with a third parameters, the average of LE and TE. The error of the average was smaller in each correlation and varied from 2% to 9%. In comparison, the regression error varied from 4% to 10%. In order to conclude the LE is highly correlated with the TE dimensions, the outliers were observed in three correlations W3, H7 and H8. For W3 and H8, the outliers were old engine models. For H7, the outliers were following a different relation. As a result, it was acceptable to remove the outliers to conclude the LE and TE hook dimensions are highly correlated.

4.4.2.1 Small Sample Correlations

In the small sample correlation study, the relation between the LE and TE dimensions was studied for additional components, the rails and the groove walls. The groove and the rails are not necessarily located at the LE and the TE but there are two groove walls and two rails that are similar. For this reason, the right and left are equivalent to LE and TE to be

consistent with the hook correlations. The parameters used in the correlations are presented in Figure 4.12a and b.

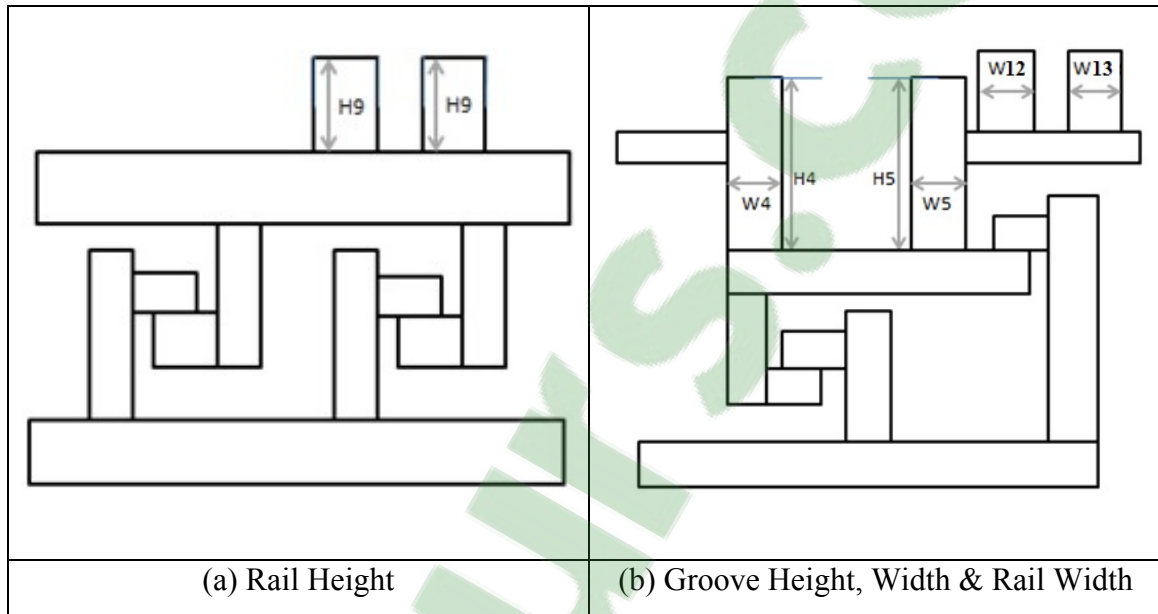


Figure 4.12: Small Sample Correlated and Non-Correlated Parameters

The results for the small sample correlations are presented in Table 4.5. For the rail height correlations, the number of rails with the same height and the same width was the observed. A correlation of 100% was validated with $\alpha=5\%$ for the rail height (H9). This was expected since there are 3 rails with the same height. In that situation, the regression error and the error of the average are equal to 0. Since there is no evidence that the height of one rail should be dependent of the other, a new parameter named the average rail height (H9) was created. Finally, the rail height was not correlated with the thermal displacement. However, the correlation is based on a small sample size. Therefore, this correlation should be updated when more data becomes available.

The inconclusive correlations are the groove wall width (W4 & W5) and height (H4 & H5) and the rail width (W12 & W13). For both the groove and the rail widths, the correlation was not validated with $\alpha=5\%$. In addition, there is only one out of eight of the TH and SSs where

W4=W5 and only 1/5 of the TH and SSs where W12=W13. There is no doubt that the groove wall and rail width should remain non-simplified parameters. On the other hand, for the groove wall height, there are 4/8 of the TH and SSs where H4=H8. However, the parameters W4 and W5 are weakly correlated with $R^2=9.7\%$, also validated with $\alpha=5\%$. As a result, the groove wall width correlation was rejected.

Table 4.5: Small Sample Correlation Results

Correlation	n	α (%)	R^2 (%)	Equal Value
H9 – Rails Height	3	5	100	3/3
W4 & W5 Groove Wall Width	8	>5	-	1/8
H4 & H5 Groove Wall Height	8	5	9.7	4/8
W12 & W13 Rails Width	3	>5	-	1/3

4.4.3 Conclusion of the Geometric Correlations

In the geometric correlations, the relation between LE and TE dimensions were studied to reduce the number of redundant parameters. A total of 5 hook and 1 rail correlations were created. Several statistics were presented to confirm that it is better to define the LE and TE as the average of the two than the LE dependent of the TE. In order to justify that all the LE and TE dimensions were highly correlated in the hook correlations, the outliers were observed to determine whether they can be disregarded or not. The outliers were old engine models and an inappropriate parameterization. The rail correlation was created because the TE and LE rails have the same height. Finally, three correlations were inconclusive. In the last section of this chapter, it will be explained how the accuracy of the geometry is affected by the geometric correlations.

Further to that, the relations between groups of two parameters were studied assuming that the parameters are redundant. It is the simplest way to study the correlations among the geometric parameters. On the other hand, the relations between groups of three or more parameters were not studied. That is also named multiple linear regression (MLR). The approach that was used to study correlations between more than 2 parameters will be presented in the next section.

4.5 Multiple Linear Regression of the Geometric Parameters

The correlations between groups of two parameters were studied to create the correlations in the previous sections. The relations between 3 parameters or more is the next logical step in a correlation study. A group of parameters correlated with one another is presented in Table 4.6. The parameter H1 is correlated with R1, R2, R3 and R5. In risk assessment, it was explained that H1 has a low level of risk and R1 to R5 have a high level of risk. As a result, H1 is the only parameter that can be defined as function of the others. If a correlation between 2 parameters was created, H1 would be function of R3 because the value of R^2 is the highest. In order to find an alternative relation with a higher R^2 , MLR was used to see if H1 can be a function of R1 to R5.

Table 4.6: Correlation Table; n=19

Correlation		R^2
H1 VS	R1	50.5 %
	R2	52.6 %
	R3	53.6 %
	R5	52.5 %

Next, it was explained in the first chapter that a standard approach to study MLR models is the model selection technique named best subset. The results of the best subset are presented in Table 4.7. In order to verify that the models are valid, the test of the regression coefficients was used with $\alpha=5\%$. In the first valid model, H1 is function of R5 and the parameters are moderately correlated with $R_a^2=53\%$. In the second valid model, H1 is function of R1 and R3 and the parameters are highly correlated with $R_a^2=77\%$. This proves that the second model is

more promising than the first. The other models with more than 3 parameters were not valid because α was greater than 5%. For this reason, they are not presented. Finally the third equation is not a regression model but it shows that there is a logical explanation for the second model. The radial clearance is function of is function of R1, R3 and H1. That is explained in the next figure.

Table 4.7: Regression Models for H1; n=19

Regression model	R_a^2 (%)
1- $H1 = \beta_1 + \beta_2 * R5$	53
2- $H1 = \beta_1 + \beta_2 * R1 + \beta_3 * R3$	77
3- Radial clearance = $R3 - (R1 + H1)$	-

The radial clearance and the parameters correlated with H1 are presented in Figure 4.13. The radial clearance is represented by a green arrow. The second regression model shows that if H1 was function of R1 and R3, the radial clearance would be standardized. In addition, the logical explanation to second regression model is that the parameters are related by the stack-up. The second model was not used to simplify the parametric formulation because H1 is required in the early design phase. Even though there is a low level of risk for H1, the second model oversimplified the parametric formulation.

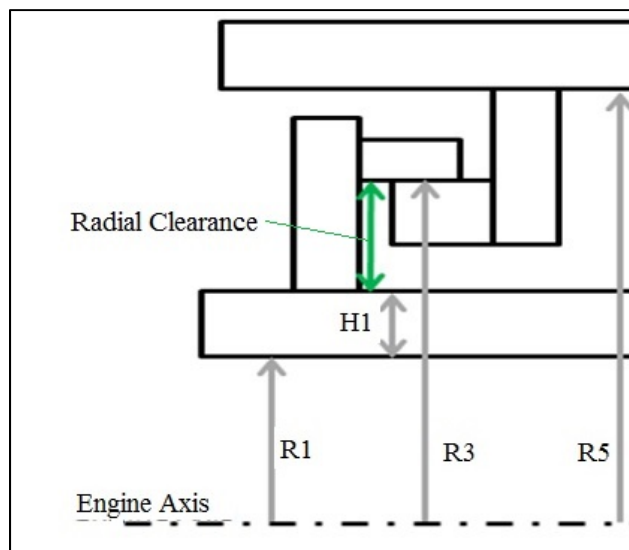


Figure 4.13: Multiple Correlation Parameters

In conclusion, a group of parameters correlated with one another was used to study a MLR model. It was found that the strength of the relation ($R_a^2=77\%$) is higher for a regression model with three parameters than a model with two parameters ($R_a^2=53\%$). The regression model was not used to simplify the parametric formulation, but it showed that the logical explanation for a relation between more than 3 geometric parameters is the stack-up of the parameters. The study of MLR models shows that the parametric formulation cannot be simplified further. It also confirms that the standardized dimensions and the geometric correlations cover the majority of the relations in the TH and SS parametric models.

4.6 Geometry Accuracy

In the previous sections of this chapter, a total of 4 standardized dimensions and 6 geometric correlations were created. In the risk assessment, care was taken to make sure the standardized dimensions and the geometric correlations do not affect the accuracy of the static structures thermal displacement. However, the static structure thermal displacements used to compute the correlations in risk assessment were not obtained with simplified TH and SSs. As a result, the effect of the standardized dimensions and the geometric correlations on thermal displacement accuracy should be studied to properly assess the accuracy of the geometry.

In this section, geometry accuracy is a comparison of detailed and simplified TH and SSs. In order to compare the simplified TH and SSs with the detailed geometry, a test case for each TH and SS configuration was conducted. The simplified TH and SSs were overlaid on the detailed geometry and the number of lines that overlay one another was counted. For example, in Figure 4.14, there are 27/39 or 69% lines of the simplified TH and SSs overlapping the detailed geometry for the new configuration 7. The lines in red are the lines that do not overlay the detailed geometry. Most of the lines that are not overlapping one another are the lines of the hooks and the housing baffle. This proves that the standardized dimensions and the geometric correlations affect geometry accuracy. Since the configurations have different levels of flexibility the total number of lines in each

configuration is different. This methodology is only a preliminary assessment of geometry accuracy. The effect of shape simplifications on tip clearance, cooling flow and containment calculations must be calculated as well when the new design process is completed.

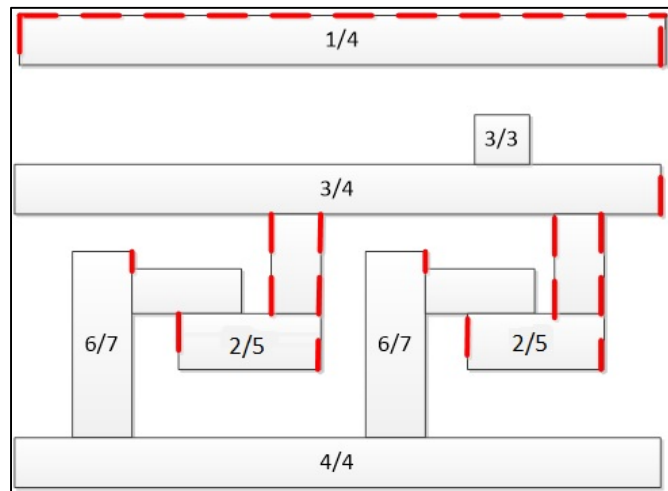


Figure 4.14: Accuracy of New Baseline Model 7

The results of the test cases are presented in Table 4.8. The geometry accuracy of the 7 new configurations varies from 67% to 86% and is higher than the geometry accuracy of the old TH and SS models (59%). Since none of the parameters with a medium to high level of risk were used in the correlations, the geometry accuracy is acceptable. In addition, the results in Table 4.8 show that geometry accuracy is a function of the configuration number. This could be used to verify whether or not the parametric formulation was oversimplified. For example, if the effect of shape simplifications on tip clearance, cooling flow and containment calculations is estimated, tip clearance, cooling flow and containment accuracy should be a function of the configuration number. Otherwise, the effect of the standardized dimensions and the geometry correlations would be negligible and it would confirm that the parametric formulation was not oversimplified.

Table 4.8: Accuracy of the Parameterized Turbine Housings and Shroud Segments

Config. No.	1(new)	2(new)	3(new)	4(new)	5(new)	6(new)	7(new)	7(old)
Lines that match	25/36	38/48	31/36	32/39	31/46	26/37	27/39	23/39
Accuracy %	69	79	86	82	67	70	69	59

4.7 Conclusion

In conclusion, the risk to oversimplify the parametric formulation was assessed and 5 parameters with a level of risk from medium to high were not used to create the standardized dimensions, the hook and the small sample correlations. In the standardized dimensions, 4 constant values were assigned to 8 parameters. Since the standardized dimensions remain constant through the design, the parametric formulation was simplified by 8 parameters. On the other hand, the 5 hook correlations simplified the parametric formulation by 5 parameters. Finally, the small sample correlations simplified the parametric formulation by 1 parameter. As a result, the simplified parametric formulation has 36 parameters which consist in an improvement of 1.4 (i.e. 50/36) compared to the non-simplified parametric formulation. It was verified by P&WC that the simplified parametric formulation is acceptable for TH and SS design. Further to that, the simplification of the parametric formulation contributed to the new design process. However, the time improvement in the new design process compared to the current design process cannot be computed for the geometry correlations on their own.

Further to that, geometry accuracy and multiple linear regression were conducted as additional studies. The geometry accuracy was estimated to prove whether or not the parametric formulation was oversimplified. It was found that the standardized dimensions and the geometry correlations affect geometry accuracy with 67% to 86% accuracy. As a result, geometry accuracy is a function of the configuration number. The results should be used to verify whether or not thermal displacement accuracy is a function of the configuration number to confirm that the parametric formulation was not oversimplified. Regarding multiple linear regression, a model showed that the parametric formulation cannot

be simplified further. In the next chapter, the relations between the engine parameters and shroud segment cooling flow will be studied.

CHAPTER 5

CORRELATION STUDY ON SHROUD SEGMENT COOLING FLOW

It was explained that historically, in gas turbines, the turbine inlet temperature has increased over the material limits to achieve better engine performance. With the increase of turbine inlet temperature, the shroud segment is a component at risk not meeting minimum life required without cooling. Several cooling technologies exist to maintain the shroud segment temperature below the materials limit. A cooling arrangement with a higher cooling efficiency is used when the turbine inlet temperature is higher. However, cooling technologies with a higher cooling efficiency require more cooling air from compressor sections. Since the amount of cooling air ducted from compressor sections directly affects the specific fuel consumption (SFC), shroud segment cooling is a trade-off between life and SFC. In this chapter, the third objective that was identified will be addressed (i.e. reduce the number of engine parameters to predict SS cooling flow). The current design process for cooling flow predictions will be presented. It will also be explained why it should be simplified. Second, it will be explained how the simplified prediction model was created. The parameters correlated with cooling flow and the prediction models that were studied will be presented. Third, it will be explained how the accuracy of the simplified prediction model was estimated. In this chapter, the accuracy refers to the difference between the cooling flow predictions and the detail design calculations. Fourth, the cooling flow predictions with the current design process and the simplified prediction model will be compared. Finally, it will be explained how the current design process could be simplified.

5.1 Context of the Correlation Study

5.1.1 Current Design Process for Cooling Flow Predictions

The current design process for cooling flow prediction is presented in Figure 5.1. It consists of a cooling flow prediction tool (CFPT), a reference and a new SS design. In order to predict the total segment cooling flow, CFPT requires the selection of a reference SS that is similar

in cooling arrangement (CA) to the new SS. The cooling flow prediction tool also requires the engine parameters (i.e. geometry, performance and air properties) and the cooling effectiveness of the new SS. The cooling effectiveness (ϵ) is necessary to adjust the predicted cooling flow to the maximum metal temperature of the new SS. Finally, CFPT requires the cooling efficiency of the reference SS to predict the cooling flow of the new SS.

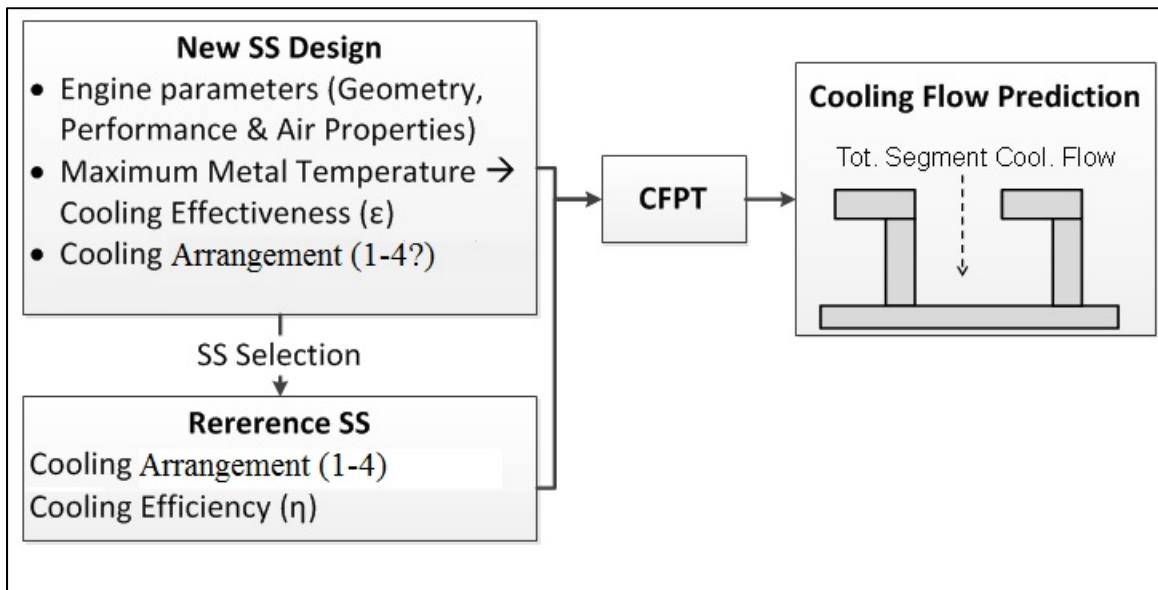


Figure 5.1: Current Design Process for Cooling Flow Predictions

Furthermore, when two reference SSs are similar in cooling arrangement to the new SS, the SS selection process requires the comparison of many engine parameters. An example with fictitious values is presented in Table 5.1. The first step in the selection of a reference SS is the comparison of reference and the new SS cooling technologies. The third reference SS is not considered because the cooling arrangement is different. The cooling arrangement of reference SS 1 and 2, is the same as the new SS. As a result, both SSs could be used as a reference. However, the reference SSs 1 and 2 have a different cooling efficiency η_1 and η_2 . Since the cooling efficiency affects the cooling flow prediction, the difference between the engine parameters of the reference and the new SS are compared. For example, the reference SS 1 is closer in performance because $(2-1.5) < (3-2)$. On the other hand, reference SS 1 is farther in geometry and air property because $(3-1) > (3-2)$ and $(3-2) > (3-2.5)$. Then,

reference SS 2 is more appropriate to predict the cooling flow of the new SS. However, there are many other engine parameters and the parameters that affect cooling flow the most are more important in the selection of the reference SS. As a result, care is taken in the choice of the reference SS. The objectives of the correlation study will be explained in the next section.

Table 5.1: Shroud Segment Selection Process

		Ref. SS 1	Ref. SS 2	Ref. SS 3	New SS Design
1	Cooling arrangement	CA 1	CA 1	CA 2	CA 1
2	Geometric Parameter 1	1	2		3
	...	-	-		-
	Performance Parameter 1	1.5	3		2
	...	-	-		-
	Air Property 1	2	2.5		3
...	-	-		-	
3	Cooling Efficiency, η	η_1	η_2		η_1 or η_2
	Total Segment Cooling Flow	-	-		?

5.1.2 Objectives of the Correlation Study

It was explained that the current design process requires many engine parameters and a reference SS for the cooling flow predictions. It was also explained that the selection of a reference SS requires the comparison of the engine parameters. Collecting all the engine parameters and selecting the most appropriate reference SS can be complex and time-consuming. In order to improve the time in the current design process, a correlation study was conducted to minimize the number of engine parameters. Since the prediction of shroud segment cooling flow is a heat transfer problem, an assumption was made. In a heat transfer problem, when a solid has a surface exposed to cold air and another surface exposed to hot air, cold and hot air temperatures are required to calculate the temperature of the hot surface. In Figure 5.2, it is explained that hot gas (T_{hot}) and cooling air (T_{cold}) temperatures are required to predict shroud segment cooling flow.

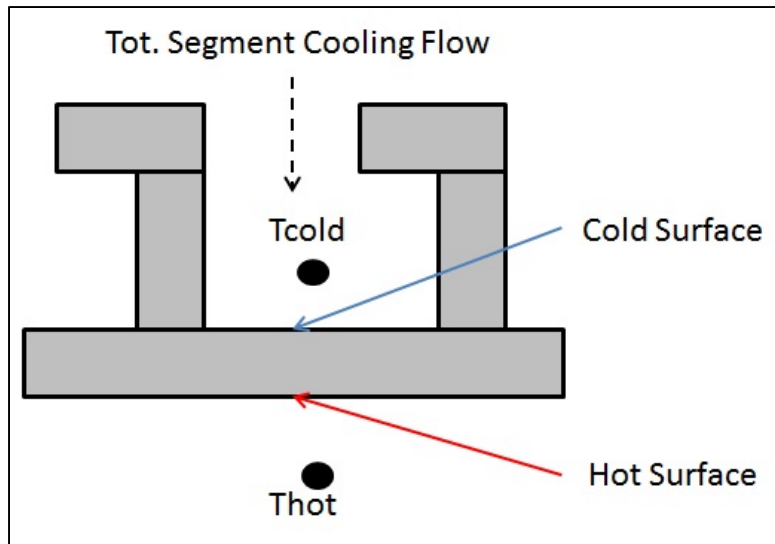


Figure 5.2: Assumption for the Cooling Correlations

The first objective of the correlation study is the creation of a simplified prediction model that includes hot gas and cooling air temperatures using the engine parameters in the current design process. In order to create a simplified prediction model, the correlation between the engine parameters and cooling flow will be calculated. Then, the engine parameters will be used to create a simplified predictions model. It should result in quicker cooling flow predictions.

The second objective of the correlation study is the creation of a simplified SS selection process using the simplified prediction model. The selection of a reference SS should be facilitated and the time of the design process should be reduced.

5.2 Creation of a Simplified Prediction Model

In this section, it will be explained how the simplified prediction model was created. First, the methodology that was used will be presented to explain the assumptions that were made. Second, the results of the correlation with cooling flow will be presented. Then, the options available to include T_{hot} and T_{cold} in the prediction model will be presented. Third, the

selection of a simplified prediction model will be presented. It will be explained how the models were created.

5.2.1 Methodology

The methodology used in the creation of the simplified prediction model is presented in Figure 5.3. First, the correlations between the engine parameters and segment cooling flow were assessed with $\alpha=5\%$. Since T_{cold} was not correlated, the correlation between $Thot$ - T_{cold} and cooling flow was computed to verify whether or not a regression model including $Thot$ and T_{cold} has a chance to be valid. Then, the engine parameters were used for the selection of a simplified prediction model.

Second, in the selection of a simplified prediction model, a standard model selection technique was used to study several models. Since no model was found valid with $\alpha=5\%$, the hypothesis that additional parameters could result in a valid model was made.

Third, the correlations with cooling flow and the selection of a simplified prediction model were studied with $\alpha=10\%$. One more parameter correlated with cooling flow was included in the prediction models. None of the models created with model selection were found valid. For this reason, it was decided to create simplified prediction models with $Thot$ and T_{cold} only. The two models were found valid with $\alpha=10\%$. The results that were used for validation assessment of the correlations and the regression model are presented in appendix II.

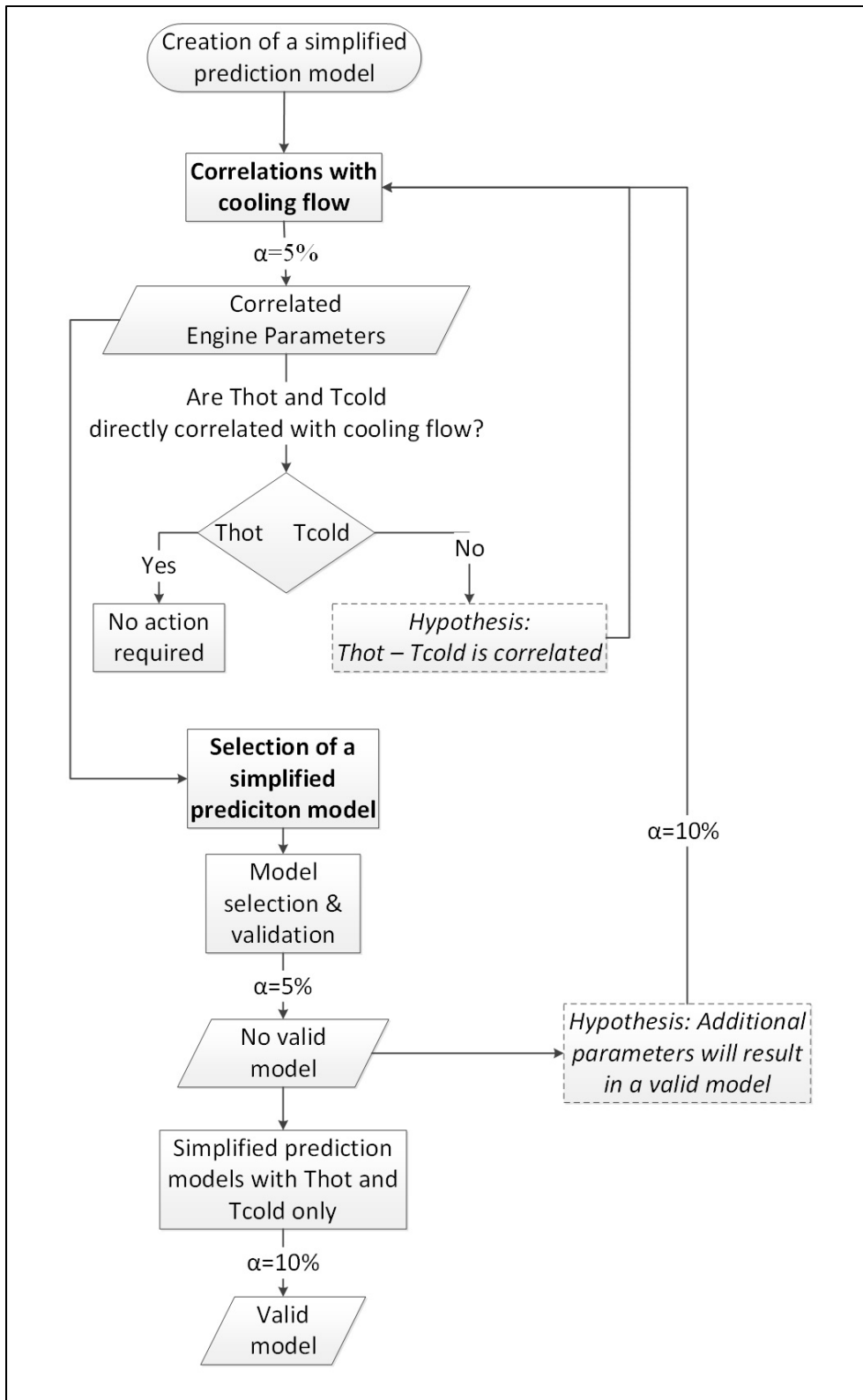


Figure 5.3: Methodology of the Correlation Study on Cooling Flow

5.2.2 Correlations with Cooling Flow

In the first step of the creation of simplified prediction model, the correlations between the engine parameters and cooling flow were calculated. The results are presented in Table 5.2. With $\alpha=5\%$, the average gas temperature $T_{\text{gas,avg}}$, the cooling effectiveness ε and the overall temperature distribution factor OTDF were found to be highly correlated with $R^2=64.4\%$ to $R^2=88.5\%$. A fourth parameter, the heat transfer coefficient of the hot surface H_{gas} , was found to be averagely correlated with $R^2=50.9\%$. With $\alpha=10\%$, the gaspath length also named length of the hot surface was also found to be correlated with cooling flow with a smaller $R^2=40.1\%$. The correlation study using $\alpha=5\%$ and $\alpha=10\%$ did not lead to the conclusion that the cooling air temperature $T_{\text{cool,source}}$, is correlated with cooling flow. In contrast with the other parameters, there is a probability of 76.1% to make the error concluding $T_{\text{cool,source}}$ is weakly correlated with cooling flow with $R^2=1.4\%$. Although $T_{\text{cool,source}}$ is not correlated, it was used to create a simplified prediction model. To justify why $T_{\text{cool,source}}$ was used, two options available to include both T_{hot} and T_{cold} will be presented.

Table 5.2: Correlations with Cooling Flow

Parameter	R^2 %	α %
$T_{\text{gas,avg}}$	88.5	5
Cooling Effectiveness, ε	84.8	5
OTDF	64.4	5
HTC _{gas}	50.9	5
Gaspath Length	40.1	10
$T_{\text{cool,source}}$	1.4	76.1

Sample size in the correlations $n=8$

Next, the first option to include T_{hot} and T_{cold} in the simplified prediction model is to use the cooling effectiveness ε . Equation 4.1 shows that the cooling effectiveness is function of $T_{\text{gas,peak}}$ and $T_{\text{coolant,in}}$. In Figure 5.4, $T_{\text{gas,peak}}$ and $T_{\text{coolant,in}}$ are the temperatures

surrounding the hot and the cold surfaces of the shroud segment. For this reason, $T_{gas,peak}$ and $T_{coolant,in}$ represent T_{hot} and T_{cold} . However $T_{gas,peak}$ and $T_{coolant,in}$ are not engine parameters of the current design process but function of the cooling effectiveness. As a result, the cooling effectiveness is used in the selection of a simplified prediction model.

$$\text{Cooling Effectiveness, } \varepsilon = \frac{T_{gas,peak} - T_{metal}}{T_{gas,peak} - T_{coolant,in}} \quad (4.1)$$

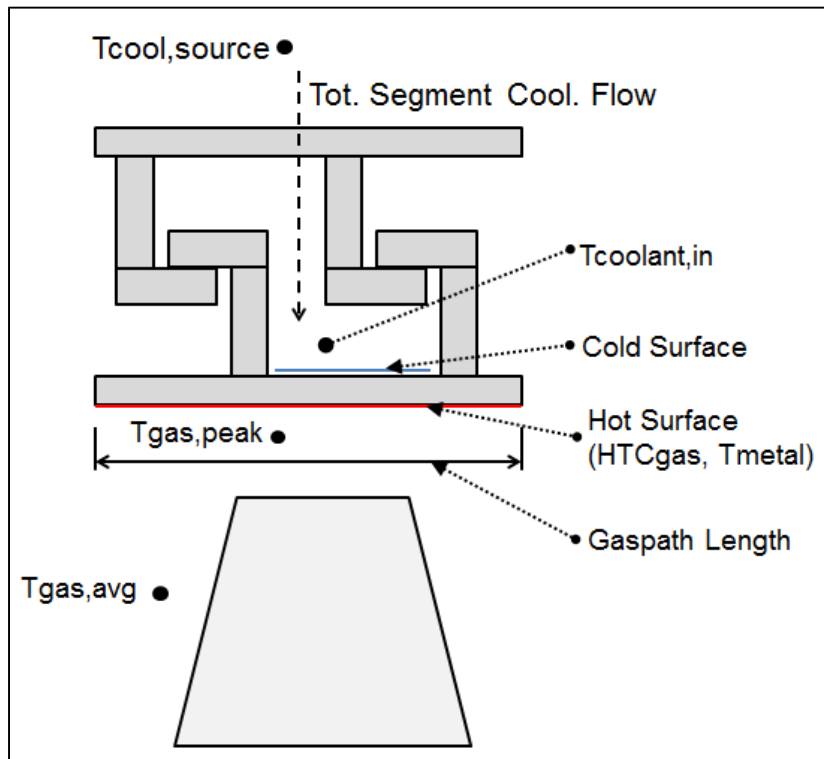


Figure 5.4: Parameters Correlated with Cooling Flow

The second option to include T_{hot} and T_{cold} in the simplified prediction model is to use $T_{gas,avg}$ and $T_{cool,source}$. In Figure 5.4, $T_{gas,avg}$ is the average temperature of the hot gas in the turbine stage and $T_{cool,source}$ is the temperature of the cooling air before it enters the turbine housing. In addition $T_{gas,avg}$ and $T_{cool,source}$ are not surrounding the hot and cold surfaces of the shroud segment therefore expected to be worse predictors than $T_{gas,peak}$ and $T_{coolant,in}$ in a simplified prediction model. Nevertheless, it is the only alternative to include

T_{hot} and T_{cold} in the simplified prediction model when ϵ is not. Since $T_{cool,source}$ was not correlated with cooling flow, the correlation between $T_{gas,avg}-T_{cool,source}$ and cooling flow was computed. In Table 5.3, $T_{gas,avg}-T_{cool,source}$ is highly correlated with cooling flow with $R^2=94.5\%$ and $\alpha=5\%$. As a result, a simplified prediction model that include $T_{gas,avg}$ and $T_{cool,source}$ has a chance to be valid.

Table 5.3: Correlation of $T_{hot}-T_{cold}$; $n=8$

Parameter	R^2 %	α %
$T_{gas,avg}-T_{cool,source}$	94.5	5

5.2.3 Selection of a Simplified Prediction Model

The second step consists in the creation of a linear regression equation similar to equation 4.2. The regression equation includes a combination of engine parameters correlated with cooling flow and $T_{cool,source}$. The standard procedure to create a regression equation is the model selection technique named best subset. Since the best subset failed to create a valid model with $\alpha=5\%$ and $\alpha=10\%$, additional regression equations were created using only hot gas and cooling air temperatures. In this section, it is explained why the best subset failed to create a valid regression equation and how the additional equations were created.

$$Tot\ Seg.\ Cooling\ Flow = \beta_1 + \beta_2 * Param. 1 + \dots + \beta_7 * Param. 6 \quad (4.2)$$

First, the best subset was used to create the regression equations A1 to A5 with a combination of the parameters marked with and 'X' in Table 5.4. Since the best subset does not tell whether a model is valid or not, α was observed for each equation. None of those models were found valid because $\alpha > 5\%$. The assumption that including additional parameters should result in a valid equation was made and $\alpha=10\%$ was used.

Table 5.4: Prediction Models with the Best Subset and $\alpha=5\%$; $n=8$

Model #	R_a^2 %	Tgas,avg	ε	OTDF	HTCgas	Gaspath Length	Tcool, source	α %
A1 to A5	-	X	X	X	X	N/A	X	>5

Second, the best subset including an additional parameter, the gaspath length, is presented in Table 5.5. The best and worse prediction models are B1 and B6 with $R_a^2=98.48\%$ and $R_a^2=86.62\%$. It was explained that the simplified prediction model should include Tgas,avg and Tcool,source or ε . The only models to meet this criterion are the models B1 to B4. The models B1, B3 and B4 include Tgas,avg and Tcool,source. On the other hand, the model B2 include Tgas,avg, Tcool,source and ε . However, B6 is the only valid model with $\alpha \leq 10\%$. As a result, the best subset failed to create a valid regression model. Additional models including only Thot and Tcold were created.

Table 5.5: Prediction Models with the Best Subset and $\alpha=10\%$; $n=8$

Model #	R_a^2 %	Tgas,avg	ε	OTDF	HTCgas	Gaspath Length	Tcool, source	α %
B1	98.48	X		X	X	X	X	72.7
B2	98.33	X	X	X	X	X	X	69.6
B3	95.92	X		X	X		X	30.1
B4	95.35	X				X	X	23.4
B5	94.46	X				X		14.2
B6	86.62	X						<10

Finally, the models including only Thot and Tcold are presented in Table 5.6. The first model C1 includes Tgas,avg and Tcool,source, two parameters correlated with cooling flow. The second model C2 includes Tgas,peak and Tcool,source. The two models were validated with $\alpha < 10\%$. In addition, the strength of the two models is similar with $R^2=96.0\%$ and 95.2% . However, Tgas,peak is the temperature surrounding the hot surface and is a function of

$T_{gas,avg}$ and OTDF, two engine parameters highly correlated with cooling flow. As a result C2 is more consistent with the current design process. Since C2 is more consistent with the current design process and C1 is not a much better model based on the value of R^2 , C2 was selected for the quick cooling flow predictions and the SS selection process.

Table 5.6: Prediction Models with Hot Gas and Cooling Air Temperatures; $n=8$

Model #	Regression Equation Total Segment Cooling Flow	R^2 %	α %
C1	$= \beta_1 + \beta_2 * T_{gas, avg} + \beta_3 * T_{cool, source}$	96.0	<10
C2	$= \beta_1 + \beta_2 * T_{gas, peak} + \beta_3 * T_{cool, source}$	95.2	<10

5.3 Accuracy of the Simplified Prediction Model

In this section, the simplified prediction model C2 will be presented. It will also be determined if the simplified prediction model can be used as a quick prediction tool with an estimation of its accuracy. An example will explain how prediction interval (PI) was used to assess the accuracy of the simplified prediction model. Second, the accuracy of the current design process and the simplified prediction model will be compared. In addition, the results presented in this section do not follow a standard statistical approach. Nevertheless, the results could be used as a basis in another research.

5.3.1 Prediction Interval of the Simplified Prediction Model

In order to assess the accuracy of the simplified prediction model, the first step consists in creating the 3D representation of the model, presented in Figure 5.5. The predicted and reference cooling flow are represented by a plane and dots. A total of 8 references were used to create this model. The predicted cooling flow is a function of the independent variables, $T_{gas,peak}$ and $T_{cool,source}$ that were converted into percentages. The minimum $T_{cool,source}$ and the maximum $T_{gas,peak}$ were defined as 0% and 100% respectively. To observe the overprediction and the residuals of the model, a cut at $T_{cool,source}=1.5\%$ was

made. This cut represents the predicted and reference cooling flow as a function of $T_{gas,peak}$ and a constant $T_{cool,source}$.

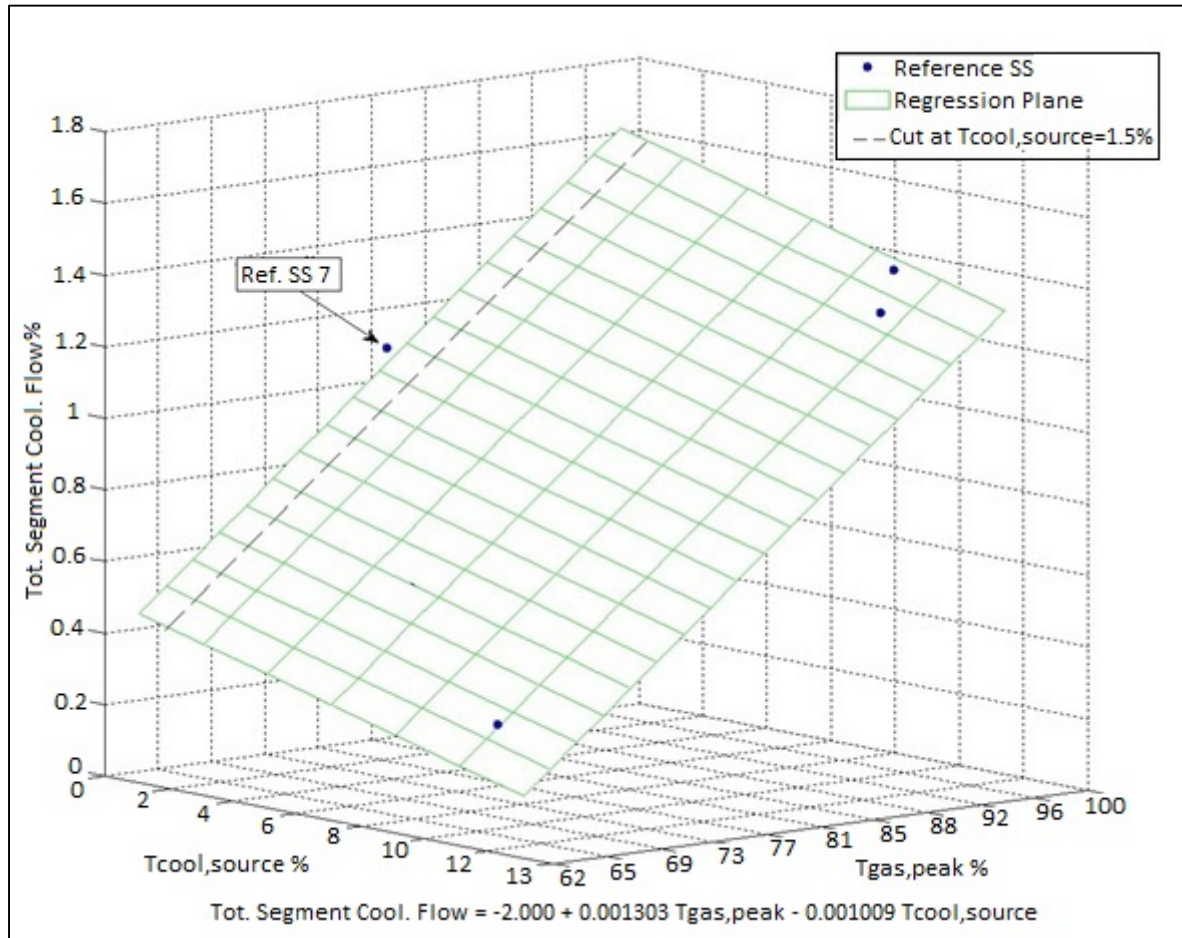


Figure 5.5: Simplified Prediction Model C2

The predicted cooling flow for a constant $T_{cool,source} = 1.5\%$ is presented in Figure 5.6. The predicted cooling flow is represented by a straight line and the 90% PI is represented by dotted lines. The reference cooling flow is represented by a red circle. A PI of 90% was used because the model was validated with $\alpha = 10\%$. That also means there is a probability of 90% that the predicted cooling flow will fall between the upper and lower limits of the prediction interval. In shroud segment cooling, it is better to overpredict than underpredict the cooling flow and reduce it later at the detail design phase if possible. As a result, only the difference between PI upper limit and the reference flow was used to assess the accuracy of the

simplified prediction model. The difference between the PI upper limit and the reference flow will be referred as the overprediction of the reference flow. For SS 7, the overprediction is 10%. The overprediction of SS 7 is small because the reference flow is above the predicted cooling flow and close to the PI upper limit. On the other hand, when the reference cooling flow is closer to the PI lower limit, the overprediction will be higher. Finally, there are 8 reference cooling flows that vary from 0.286 to 1.394. The overprediction for all the reference SSs will be presented next to estimate the accuracy of the simplified prediction model.

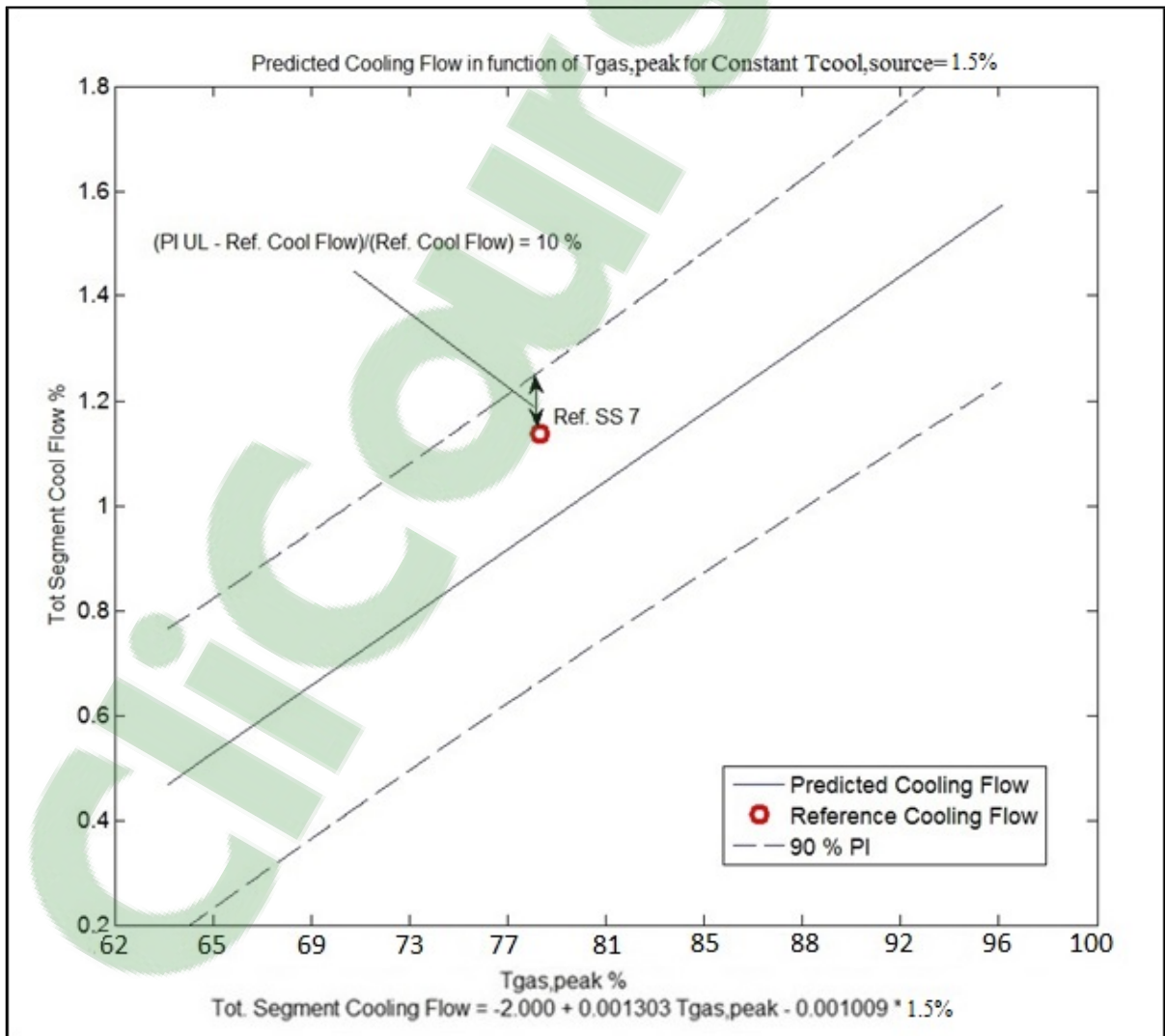


Figure 5.6: Overprediction for Reference Shroud Segment 7

The accuracy of the predictions for each of the reference SS is presented in Table 5.7. The values are presented from the smallest to the highest reference cooling flow from the first to the last row. The overprediction varies from 10% to 108%. That gives an average overprediction of 51%. As explained earlier, when the reference cooling flow is closer to the PI lower limit, the overprediction will be larger. However, the overprediction is also affected by the value of the reference cooling flow. For example, the overprediction is smaller for SS 8 than SS 3 because $63 < 108$ but the absolute overprediction is higher for SS 8 than SS 3 because $0.356 > 0.309$. That is explained by a smaller reference cooling flow for SS 3 where $0.286 < 0.564$. As a result, the model seems better at predicting higher cooling flows since the PI is not narrower when the predicted cooling flow is smaller. Finally, the average overprediction shows that the PI is too wide and suggests that the simplified prediction model is not accurate enough. In order to validate that the accuracy is insufficient, the simplified prediction model will be compared to the current design process.

Table 5.7: Accuracy of the Predictions

SS No.	Ref. Cool. Flow	PI UL	Overprediction	
			PI UL – Ref. Cool. Flow	%
3	0.286	0.595	0.309	108
5	0.330	0.523	0.193	59
2	0.418	0.839	0.421	101
8	0.564	0.920	0.356	63
7	1.136	1.255	0.119	10
4	1.198	1.559	0.361	30
1	1.297	1.569	0.272	21
6	1.394	1.657	0.263	19
<i>Average</i>			<i>0.287</i>	<i>51</i>

5.3.2 Comparison with the current design process

In order to compare the current design process and the simplified prediction model, the 2D representation of the simplified prediction model is presented in Figure 5.7. The independent variables, $T_{cool,source}$ and $T_{gas,peak}$ are represented by the horizontal and vertical axes. The diagonal lines represent the predicted cooling flow and the black dots represent the reference SSs numbered from 1 to 9. Shroud segment no.9 was not used to assess the accuracy of the model in the previous section because it did not qualify as a reference SS for the creation of the model. Nevertheless, SS 9 will be used to compare the accuracy of the model and the current design process because it is close to SS 8 in $T_{cool,source}$ and $T_{gas,peak}$. Furthermore, the cooling arrangement of the reference SSs is identified on the plot to show that the current design process uses the same cooling arrangement for the reference and the new SSs. Finally the five arrows (A, B, C, D and E) identify the SSs that were used to assess the accuracy of the current design process. For example, in C, SS 7 was used as a reference to predict the cooling flow of the SS 8. The predicted cooling flow of SS 8 was also calculated with the simplified prediction model. Finally, the predicted cooling flows were compared to the reference flow of SS 8. For a visual representation of this comparison, the simplified model will be presented in function of $T_{gas,peak}$ and a constant $T_{cool,source}=5.0\%$.

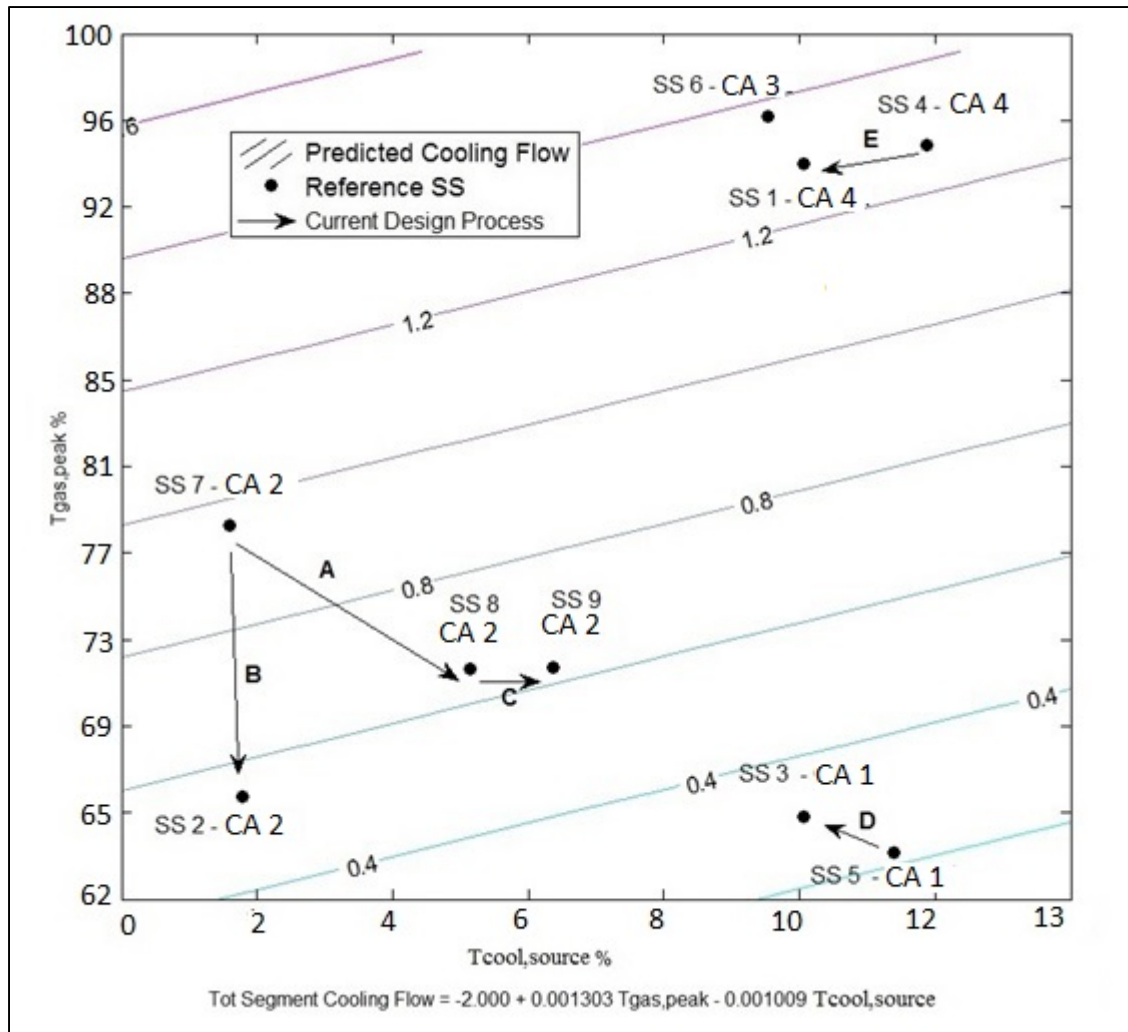


Figure 5.7: 2D Representation of the Simplified Prediction Model

The predicted cooling flow in function of $T_{gas,peak}$ and a constant $T_{cool,source}=5.0\%$ is presented in Figure 5.8. The straight line represents the prediction model. The 90% PI is represented by dotted lines. The reference and predicted flows of SS 8 are represented by the circles numbered from 1 to 4. All the cooling flows are computed for $T_{gas,peak}=71.7\%$. The simplified prediction model gives an average and a maximum cooling flow of 0.653 and 0.994. The current design process predicts a cooling flow of 0.508. Finally, the reference cooling flow for SS 8 is 0.564. It was explained that the accuracy of the simplified prediction model is assessed with the overprediction of the reference flow (0.994-0.564). Then, compared to the error of the current design process (0.564-0.508), the overprediction is larger

and the current design process is more accurate for SS8. The overprediction shows the largest error made by the simplified prediction model. The residual can also be used to assess the accuracy of the of the simplified prediction model. In a valid prediction model, the average of the residuals is zero. For this reason, the absolute value of the residual was calculated. For SS 8, the residual is equivalent to 0.653-0.564. If the residual is smaller than the error of the current design process, the average predicted cooling flow is more accurate. However, this does not take into account the PI. This is why the residual and the overprediction were compared to the error of the current design process in five test cases.

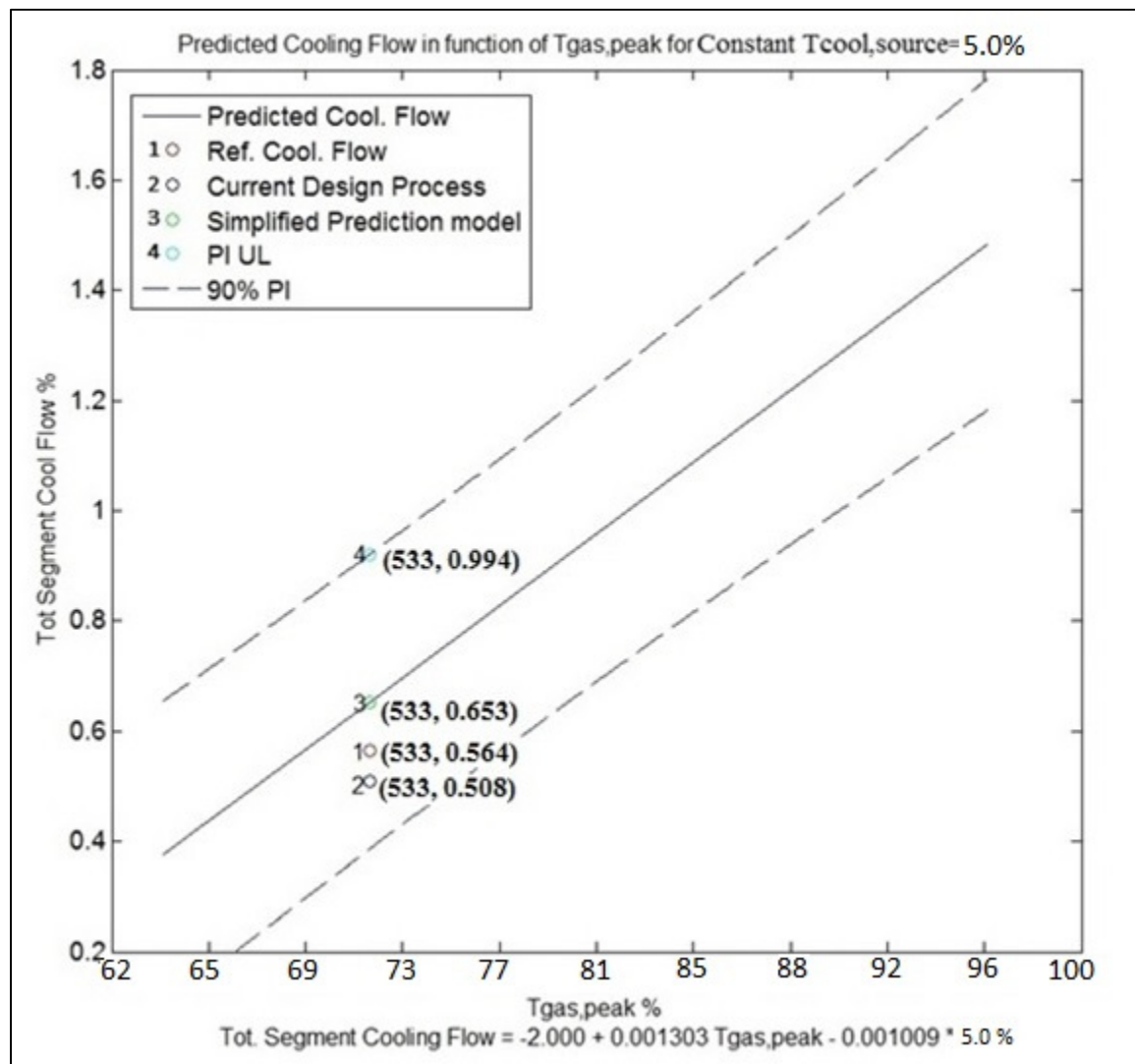


Figure 5.8: Accuracy Comparison for Reference Shroud Segment 8

The test cases A, B, C, D and E are presented in Table 5.8. In the five test cases, the error of the current design process, the absolute residual and the overprediction were divided by the reference cooling flow to have a logic comparison point. In the test case A, the absolute residual is 9% and the overprediction is 108%. In comparison, the error of the current design process is smaller with 0.02%. In all the test cases, the current design process is more accurate than the absolute residual. This proves that even without PI, the current design process is more accurate. In the test cases A to D, the current design process is more accurate than the overprediction. Even though the test case E show the same error for the current design process and the overprediction, the average error proves that the current design process is more accurate since $9\% < 64\%$. Finally, the average overprediction of the test cases (64%) is higher than average overprediction of the model (51%) because it does not take into account the more accurate overpredictions.

Table 5.8: Accuracy of Current and Simplified Predictions

Case	Ref. SS → New SS	Ref. Cool. Flow	Curr. Des. Process /Ref. %	Simplified Prediction Model	
				Abs. Residual /Ref. %	Overprediction /Ref. %
A	5 → 3	0.286	0.02	9	108
B	7 → 2	0.418	14	31	101
C	7 → 8	0.564	11	16	63
D	8 → 9	0.624	0.03	0.1	27
E	4 → 1	1.293	21	27	21
<i>Average</i>			<i>9</i>	<i>17</i>	<i>64</i>

5.3.3 Conclusions on the Accuracy

In conclusion, an average overprediction of 51% was calculated to show the low accuracy of the cooling flow predictions of the simplified prediction model. In order to prove that the simplified prediction model is not accurate enough, the error of the current design process was calculated for 5 test cases. It was compared with the overprediction and the absolute residual. The absolute residual confirmed the validity of the model. On the other hand, an average overprediction of 64%, higher than the average error of the current design process 9%, proved that the simplified prediction model is not accurate enough to be used as a quick prediction tool. Finally, the error of the current design process showed that the simplified prediction model is probably missing important effects.

The accuracy of the current design process was assessed. The selection of the reference SS also affects the accuracy in the current design process. For this reason, a simplified SS selection process was created. It will be presented in the next section.

5.4 Simplified Shroud Segment Selection Process

The simplified SS selection process is presented in Figure 5.9. It is similar to the current SS selection process. First, the reference and the new SSs must have the same cooling arrangement. Second, the 2D representation of the simplified prediction model is used to observe how distant two SSs are from one another in $T_{cool,source}$, $T_{gas,peak}$ and predicted cooling flow. For example, the horizontal, vertical and diagonal distances between the SSs 7 and 8 are calculated because they have the same cooling arrangement. Those distances are calculated for a second SS with the same cooling arrangement. The reference SS closer to the new SS is used in the predictions. Although this seems a promising approach, the simplified SS selection process does not prove that a closer reference SS provides the more accurate cooling flow predictions. This will be explained next with the comparison of the cooling flow predictions.

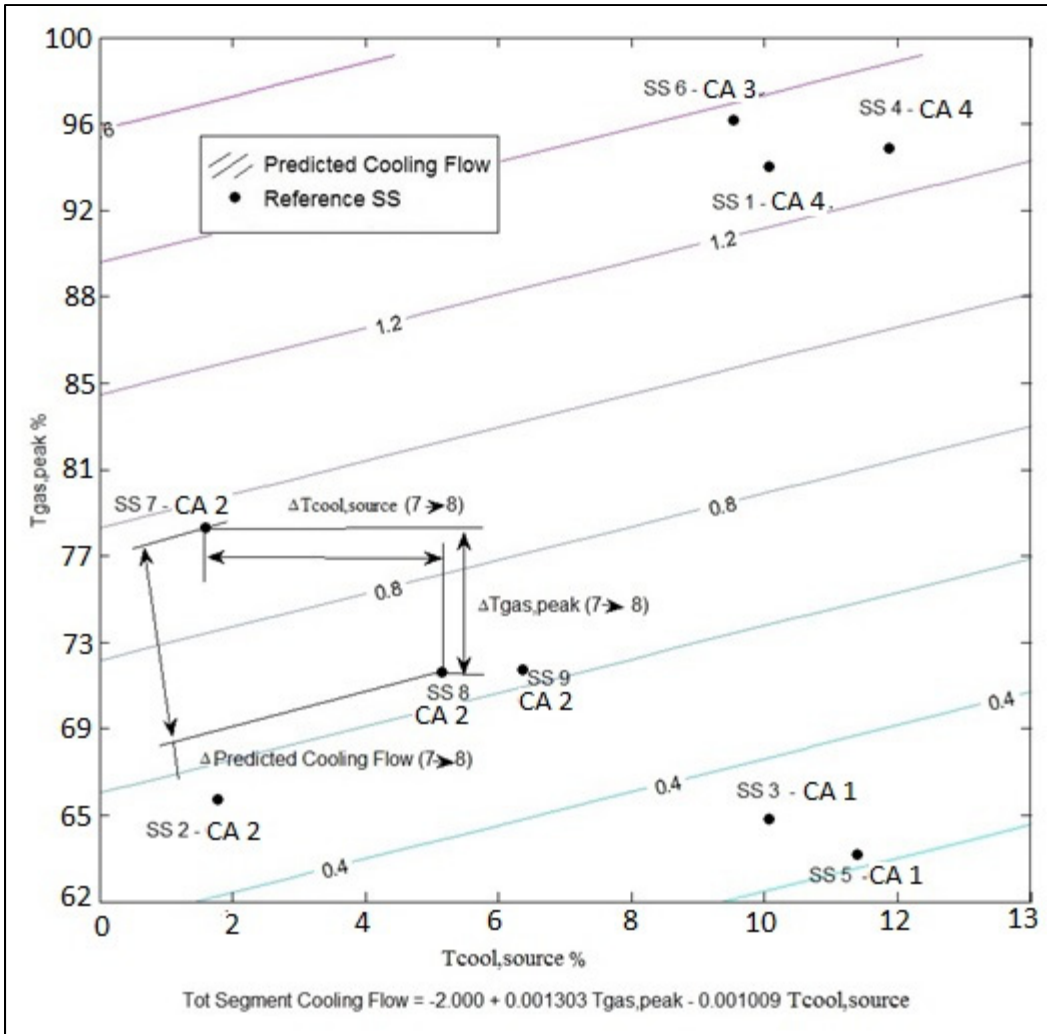


Figure 5.9: Shroud Segment Selection with the Simplified Prediction Model

The predicted cooling of various shroud segments is compared in three test cases in Table 5.9. In the first test case, the reference SSs 7 and 2 were used to predict the cooling flow of SS 8. Reference SS 7 is a better choice because the current design process error is smaller (11% < 21%). However, the simplified SS selection process would suggest that reference SS 2 is a better choice because it is closer in $T_{cool,source}$ (3.2 < 3.5), $T_{gas,peak}$ (5.7 < 6.5) and predicted cooling flow (0.307 > 0.107).

In the second test case, the reference SSs 7 and 8 were used to predict the cooling flow of reference SS 2. Reference SS 7 is a better choice with an error of 14%. However, the

simplified SS selection process does not prove that either of reference SS 7 and 8 are better. As a matter of fact, reference SS 7 is closer in $T_{cool,source}$ ($0.3 < 3.2$) but farther in $T_{gas,peak}$ ($12.1 > 5.7$) and predicted cooling flow ($0.414 < 0.107$).

In the third test case, the reference SSs 8 and 7 were used to predict the cooling flow of reference SS 9. Reference SS 8 is a better choice with an error of 0.031%. The simplified SS selection process is in agreement with this result since reference SS 8 is closer in $T_{cool,source}$, $T_{gas,peak}$ and predicted cooling flow.

Table 5.9: Engine Parameters Comparison in Shroud Segment Selection

Case	Ref. SS → New SS	Curr. Des. Process /Ref. %	$\Delta T_{cool,source}$	$\Delta T_{gas,peak}$	$\Delta Pred.Cool$ Flow
1	7→8	11	3.5	6.5	0.307
	2→8	21	3.2	5.7	0.107
2	7→2	14	0.3	12.1	0.414
	8→2	26	3.2	5.7	0.107
3	8→9	0.031	1.1	0.1	0.028
	7→9	14	4.6	6.3	0.625

In conclusion, the simplified SS selection process is inconclusive in terms of selecting the most appropriate reference SS. It is possible that when the reference SS is close enough, the simplified SS selection process is a good alternative to the current SS selection process. However, this was observed only in the third test case. To verify this, a distance limit should be defined. For example, only the reference SSs within $\pm 1.5\%$ in $T_{cool,source}$ and $T_{gas,peak}$ should be used. Since the reference and the new SSs must have the same cooling arrangement, additional reference SSs must be created to verify this hypothesis. The conclusions of the correlation study on shroud segment cooling flow will be presented next.

5.5 Conclusion

A correlation study on shroud segment cooling flow was conducted to minimize the number of engine parameters used in the current design process and to create a simplified SS selection process. The correlations between the engine parameters and cooling flow were calculated to create a simplified prediction model with T_{hot} and T_{cold} . Many prediction models were studied, but the standard model selection technique was inconclusive to find a valid prediction model. Then, a simplified prediction model using $T_{gas,peak}$ and $T_{cool,source}$ was created. This model was found valid and consisted with the current design process. In order to verify that this model could be used as a quick prediction tool and replace the current design process, its accuracy was assessed. With an average overprediction of 64% compared to an average error of 9% in the current design process, the simplified prediction model was found unacceptable for the cooling flow predictions. Finally, a simplified SS selection process was created. There was not enough evidence to show that a reference SS closer to new SS provides a more accurate cooling flow. As a result, the simplified SS selection process is not a good alternative to the current SS selection process.

Several aspects were not covered by the correlation study on shroud segment cooling flow. A good practice is to use a second sample for the validation of the model. That was not possible due to the small sample size. The sample size also affected the SS selection process. With additional data, it would be possible to study whether or not a small temperature range is an important criterion in SS selection. In addition, accuracy comparison of the current design process and the simplified prediction model showed that important effects might be missing. Non-linear prediction models could take into account those missing effects. Finally, the cooling flow is function of the cooling arrangement. Creating prediction models specific to the cooling technologies could result in more accurate cooling flow predictions.

CONCLUSION AND RECOMMENDATION

The parametric models, the new geometry and cooling flow correlations were created for the new design process for turbine housing and shroud segments. The following conclusions were explained in chapters 3 to 5.

1. Turbine housing (TH) and shroud segments (SS) parametric models and a user interface were created for the design module of the proposed design process. The parametric models and the user interface resulted in time saving of 50% and an increase in geometry accuracy of 56% compared to the existing design system. Finally, the parametric models were created to design cooled TH and SS. Additional work is necessary to verify if they are acceptable to design uncooled TH and SS.
2. New geometry correlations were created to minimize the number of parameters used to design TH and SS. With a total of 4 standardized dimensions, 5 hook and 1 rail correlations, the number of parameters was reduced from 50 to 36. As a result, the geometry correlations also resulted in time-saving compared to the existing design system. The correlations with thermal displacement for tip clearance were also computed to assess the risk of removing too many parameters from the parametric formulation. Nevertheless, when the proposed design process is completed, it should be verified whether or not the new geometry correlations affect the tip clearance, cooling flow and containment predictions.
3. A simplified prediction model was created with the new cooling flow correlations. Then, the model was used to create a simplified SS selection process that could contribute having quicker cooling flow predictions if additional work was done to find temperature range.

Considering the data structure, the static structure design module, the analysis and the optimization modules, it was estimated that the parametric models and the new correlations contribute about 30% in the creation of a new design process for turbine housing and shroud segments. In order to obtain a new design process, the following work must be completed.

1. Create an air system module necessary to complete the thermal and tip clearance modules.
2. Complete the static structures thermal module also necessary to complete the tip clearance module.
3. Complete and integrate the tip clearance module.
4. Create a containment module.
5. Create an optimizer capable of finding a balanced design (i.e. optimal tip clearance, cooling flow and containment thickness).

APPENDIX I

CORRELATIONS IN RISK ASSESSMENT

The correlation with static structure thermal displacement was calculated at two engine operating conditions TO and CR. A TO condition was used as a reference. When the parameters were also correlated at CR with the same α , they were used in risk assessment in chapter 3. For example, the parameters H1 and W13 are correlated at TO with $\alpha=10\%$. At CR, H1 and W12 are correlated with $\alpha=20\%$. For this reason, the level of risk of H1 and W13 was assigned in function of $\alpha=20\%$. In addition, H7 is correlated at TO with $\alpha=20\%$ but not at CR with $\alpha=20\%$. For this reason, no level of risk was assigned to this parameter.

Table A.1.1 - Correlation with thermal displacement TO

α	Parameters
10%	R1; R2; R3; R4; R5; H1; W12; W13
20%	R1; R2; R3; R4; R5; H1; W12; W13; H7; H8

Table A.1.2 - Correlation with thermal displacement CR

α	Parameters
10%	R1; R2; R3; R4; R5; W12
20%	R1; R2; R3; R4; R5; W12; H1; H6 ; H8; W13

APPENDIX II

VALIDITY ASSESSMENT IN COOLING FLOW CORRELATIONS AND REGRESSION EQUATIONS

The results presented in this appendix are:

1. A validation assessment of the correlations with cooling flow in Table A.2.1;
2. A validation assessment of 6 models found with the best subset in Table A.2.2.

Validation assessment is made with the P-value, the statistic used in the test of the correlation coefficient and the test of the regression coefficient. When $P\text{-value} \leq \alpha$, the null hypothesis is rejected in both tests. In that situation, $\rho \neq 0$ and $\beta \neq 0$. In chapter 4, when $\rho \neq 0$ and all the regression coefficients β are different than 0, it is concluded that there is a correlation and the regression equation is valid. When the correlation or the regression equation is not valid, the level of significance α is assumed to be equal to P-value to show the value of α at which it is concluded a correlation or a regression equation are valid. For example, in Table A.2.1, P-value for $T_{\text{cool,source}}$ is 0.761. Then α must be equal to 76.1% to conclude there is a correlation. On the other hand, the test of the regression coefficient must confirm that all the coefficients β_i are different than zero. As a result, the highest P-value is used to define the value of α at which it is concluded a regression equation is valid. The values in red in Table A.2.1 and A.2.2 show that $P\text{value} > \alpha$.

Table A.2.1 - Correlation with Cooling Flow (n=8; $\alpha=10\%$)

Parameter	P-value ≤ 0.10
$T_{\text{gas,avg}}$	$0.000 \leq 0.10$
OTDF	$0.017 \leq 0.10$
Cooling Effectiveness, ϵ	$0.001 \leq 0.10$
HTC_{gas}	$0.047 \leq 0.10$
Gaspath Length	$0.092 \leq 0.10$
$T_{\text{cool,source}}$	$0.761 > 0.10$

Table A 2.2 - Model Validation (n=8; $\alpha=10\%$)

Model	P-value $\leq \alpha$						
	β_1	β_2	β_3	β_4	β_5	β_6	β_7
$\beta_1 + \beta_2 * T_{gas,avg} +$ $\beta_3 * OTDF +$ $\beta_4 * HTC_{gas} +$ $\beta_5 * \text{Gaspath Length}$ $\beta_6 * T_{cool,source}$	0.727 > 0.10	0.014 \leq 0.10	0.111 > 0.10	0.086 \leq 0.10	0.133 > 0.10	0.065 \leq 0.10	-
$\beta_1 + \beta_2 * T_{gas,avg} +$ $\beta_3 * OTDF$ $\beta_4 * \epsilon +$ $\beta_5 * HTC_{gas} +$ $\beta_6 * \text{Gaspath Length}$ $\beta_7 * T_{cool,source}$	0.696 > 0.10	0.148 > 0.10	0.225 > 0.10	0.530 > 0.10	0.203 > 0.10	0.363 > 0.10	0.180 > 0.10
$\beta_1 + \beta_2 * T_{gas,avg} +$ $\beta_3 * OTDF +$ $\beta_4 * HTC_{gas} +$ $\beta_5 * T_{cool,source}$	0.301 > 0.10	0.007 \leq 0.10	0.171 > 0.10	0.151 > 0.10	0.050 \leq 0.10	-	-
$\beta_1 + \beta_2 * T_{gas,avg} +$ $\beta_3 * \text{Gaspath Length}$ $\beta_4 * T_{cool,source}$	0.097 \leq 0.10	0.002 \leq 0.10	0.230 > 0.10	0.234 > 0.10	-	-	-
$\beta_1 + \beta_2 * T_{gas,avg} +$ $\beta_3 * \text{Gaspath Length}$	0.142 > 0.10	0.000 \leq 0.10	0.027 \leq 0.10	-	-	-	-
$\beta_1 + \beta_2 * T_{gas,avg}$	0.001 \leq 0.10	0.000 \leq 0.10	-	-	-	-	-

LIST OF REFERENCES

- Bin, Xu, Chen Nan et Che Huajun. 2010. « An integrated method of multi-objective optimization for complex mechanical structure ». *Advances in Engineering Software*, vol. 41, n° 2, p. 277-285.
- Brophy, F., S. Mah and J. Turcotte. 2009. . « *Preliminary Multi-Disciplinary Optimization (PMDO) an Example at Engine Level* ». Lecture series on strategies for optimization and automated design of gas turbine engines, Vol. p.14. AVT-167.
- Chatterjee, Samprit, et Jeffrey S. Simonoff. 2013a. « Model Building ». In *Handbook of Regression Analysis*. p. 23-49. John Wiley & Sons, Inc. <http://dx.doi.org/10.1002/9781118532843.ch2>. Accessed September 27, 2014.
- Chatterjee, Samprit, et Jeffrey S. Simonoff. 2013b. « Multiple Linear Regression ». In *Handbook of Regression Analysis*. p. 1-21. John Wiley & Sons, Inc. <http://dx.doi.org/10.1002/9781118532843.ch1>. Accessed September 27, 2014.
- Hardee, Edwin, Kuang-Hua Chang, Jian Tu, Kyung K. Choi, Iulian Grindeanu et Xiaoming Yu. 1999. « A CAD-based design parameterization for shape optimization of elastic solids ». *Advances in Engineering Software*, vol. 30, n° 3, p. 185-199.
- Hennecke, D. K. 1985. « Active and Passive Tip Clearance Control. ». *VKI Lecture Series*, p. 34.
- Hicks, Charles Robert, et Kenneth V Turner. 1999. *Fundamental concepts in the design of experiments*. p. 40. Oxford University Press New York.
- SAS Institute Inc. 2013. JMP® 11 *Design of Experiments Guide*. Cary, NC: SAS Institute Inc. p..31-41
- Kreyszig, Erwin. 2010. « Mathematical Statistics ». In *Advanced Engineering Mathematics*. p. 1049-1062. John Wiley & Sons.
- Lattime, Scott B, et Bruce M Steinetz. 2004. « High-pressure-turbine clearance control systems: current practices and future directions ». *Journal of Propulsion and Power*, vol. 20, n° 2, p. 302-311.
- Lesik, Sally. 2009. « Simple Linear Regression ». In *Applied Statistical Inference with MINITAB®*. p. 177-180. CRC Press.
- Melcher, Kevin J, et J Kypuros. 2003. « Toward a fast-response active turbine tip clearance control ». In *International Symposium on Air Breathing Engines, Cleveland, Ohio*.

- Minitab Inc. (2007). *Minitab Statistical Software*, Release 15 for Windows, State College, Pennsylvania. Minitab® is a registered trademark of Minitab Inc.
- Ouellet, Yannick. 2013. « Conception préliminaire de disques de turbine axiale pour moteurs d'aéronefs ». École de technologie supérieure, 148 p.
- Panchenko, Y, K Patel, H Moustapha, M. J Dowhan, Stephen Mah et D Hall. 2002. « Preliminary Multi-Disciplinary Optimization in Turbomachinery Design ». In *Proceedings of RTO/AVT symposium on "Reduction of Military Vehicle Acquisition Time and Cost through Advanced Modelling and Virtual Simulation"*. (Paris, France) Vol. 57, p. 22. RTO-MP-089.
- General Electric Company. 1992. *Shroud cooling assembly for gas turbine engine*. US Patent 5169287. In *Google Patents*. <https://www.google.com/patents/US5169287>. Accessed August 09, 2015.
- Samareh, Jamshid A. 1999. « A survey of shape parameterization techniques ». In *NASA Conference Publication*. p. 333-344. Citeseer.
- Taeger, Dirk, et Sonja Kuhnt. 2014. « Tests in regression analysis » In *Statistical hypothesis testing with SAS and R*. p. 237-245. John Wiley & Sons.
- Zuckerman, N, et N Lior. 2006. « Jet impingement heat transfer: physics, correlations, and numerical modeling ». *Advances in heat transfer*, vol. 39, n° 06, p. 565-631.
- Zuckerman, Neil, et Noam Lior. 2005. « Impingement heat transfer: correlations and numerical modeling ». *Journal of heat transfer*, vol. 127, n° 5, p. 544-552.